IOSUD – „DUNAREA DE JOS" UNIVERSITY OF GALATI
Doctoral School of Mechanical and Industrial Engieneering

DOCTORAL THESIS

ABSTRACT

RESEARCH ON THE PROPERTIES OF LAYERS DEPOSITED BY WELDING WITH MULTI-ELEMENT ALLOYS

PhD Student
Eng. George SIMION

PhD Supervisor
Prof. dr. eng. Elena SCUTELNICU

PhD Co-Supervision
Prof. dr. eng. habil. Ionelia VOICULESCU

Series I 4: INDUSTRIAL ENGIENEERING No. 96
GALATI - 2024

IOSUD – DUNAREA DE JOS" UNIVERSITY OF GALATI
Doctoral School of Mechanical and Industrial Engieneering

DOCTORAL THESIS

ABSTRACT

RESEARCH ON THE PROPERTIES OF LAYERS DEPOSITED BY WELDING WITH MULTI-ELEMENT ALLOYS

PhD Student
Eng. George SIMION

Chair	Prof. dr. eng. DHC Cătălin FETECĂU
PhD Supervisor	Prof. dr. eng. Elena SCUTELNICU
PhD Co-Supervision	Prof. dr. eng. habil. Ionelia VOICULESCU
PhD Committee	Prof. dr. eng. Gheorghe OANCEA
	Prof. dr. eng. ec. Dumitru NEDELCU
	Prof. dr. eng. habil. Gabriel-Radu FRUMUȘANU

Series I 4: INDUSTRIAL ENGINEERING No. 96
GALATI - 2024

The PhD thesis series publicly defended in UDJG since October 1, 2013 are:

The fundamental field ENGINEERING SCIENCES

Series I 1: **Biotechnology**
Series I 2: **Computers and information technology**
Series I 3: **Electrical engineering**
Series I 4: **Industrial engineering**
Series I 5: **Materials engineering**
Series I 6: **Mechanical engineering**
Series I 7: **Food engineering**
Series I 8: **Systems engineering**
Series I 9: **Engineering and Management in Agriculture and Rural Development**

The fundamental field ECONOMIC SCIENCES

Series E 1: **Economy**
Series E 2: **Management**
Series E 3: **Marketing**
Series SSEF: **Science of sport and physical education**
Series SJ: **Justice**

The fundamental field HUMAN SCIENCES

Series U 1: **Philology - English**
Series U 2: **Philology - Romanian**
Series U 3: **History**
Series U 4: **Philology - French**

The fundamental field MATHEMATICS AND NATURAL SCIENCES

Serie C: **Chemistry**

The fundamental field BIOMEDICAL SCIENCES

Series M: **Medicine**
Series F: **Pharmacy**

ACKNOWLEDGMENTS

The writing of this doctoral thesis would not have been possible without the direct or indirect support and guidance of remarkable people, to whom I wish to express my special thanks and assure them of all my consideration, appreciation, and gratitude.

First of all, I express my deep gratitude to my scientific coordinator, Prof. dr. eng. Elena Scutelnicu, from the Faculty of Engineering of the "Dunarea de Jos" University of Galaţi, for her careful guidance, patience, and constant support throughout the university doctoral studies program. High academic standing, expertise, and valuable critical observations were essential, both for my professional development and for the making of this work, and for the publishing of the results of the scientific research. You masterfully guided me in the scientific formation, in doctoral preparation, through unconditional support in the elaboration of the articles and papers presented at national and international conferences and published, later, in magazines and volumes with an impact on the scientific world.

I would like to express my thanks, equally, to Prof. dr. eng. habil. Ionelia Voiculescu, from the National University of Science and Technology Politehnica Bucharest, for the scientific coordination and support given in the interpretation and processing of the experimental results. Together with Prof. dr. eng. Elena Scutelnicu, Prof. dr. eng. habil. Ionelia Voiculescu represented a professional landmark, supporting me in overcoming some obstacles that appeared in the scientific research program.

I feel very honored and I thank, on this occasion, to the members of the doctoral committee for accepting to be part of the committee for the public presentation of my doctoral thesis and, at the same time, I thank them for the careful analysis and professional evaluation of the results of the scientific research, presented in this work. I send sincere and warm thanks to the distinguished official referees - Prof. dr. eng. Gheorghe Oancea from Transilvania University in Braşov, Prof. dr. eng. ec. Dumitru Nedelcu from "Gheorghe Asachi" University in Iasi, Prof. dr. eng. habil. Gabriel-Radu Frumuşanu from the "Dunarea de Jos" University in Galati - for the comments made on the content and aspect of the work and for the useful information and advice I received, especially during the finalization of the thesis doctorate.

I would like to thank Prof. dr. eng. Julia Mîrza-Roşca, researcher and director of the Laboratory of Nanosciences and Nanomaterials of the University of Las Palmas de Gran Canaria, Spain, for the valuable observations and technical support that were of real use to me during the development of my doctoral thesis.

I would like to express my warm thanks to the members of the guidance committee, Prof. dr. eng. Cătălin Fetecău, Assoc. Prof. dr. eng. Carmen Cătălina Rusu, Assoc. Prof. dr. eng. Dan Cătălin Bîrsan, for the permanent support, for the observations and constructive discussions on the objectives of the doctoral thesis and the research methodology that allowed me to identify the best technical solutions in passing the obstacles appeared in investigating this topic of great interest for the industry.

Many thanks to Assoc. Prof. dr. eng. Octavian Mircea and Assist. Prof. dr. eng. Luigi-Renato Mistodie for the trust offered during the professional training period, for stimulating my interest in research, and for the support given in carrying out the experiments, to Prof. dr. eng. Costel Iulian Mocanu for the support given in determining the stress level, generated by the process of deposition by welding of the multi-element alloy, to Assist. Prof. dr. eng. Vasile Başliu, from the "Dunarea de Jos" University of Galati, and to Assist. Prof. dr. eng. Georgiana Chişiu, from the National University of Science and Technology Politehnica Bucharest, for the technical support provided in the preparation and investigation of the samples.

I am grateful to Eng. Liviu Bogdan, from Liberty Galati, who facilitated the sponsorship of my experimental activities, by providing metallic materials, to my colleagues and collaborators from the Manufacturing Engineering Department for the support and technical discussions that highlighted me new perspectives on the topic of research and stimulated me in completing the scientific research.

I express my thanks to the technical personnel, especially to Paul Mironov, who is passionated about metals welding, a true creator of beautiful art, who supported me in performing the samples and depositing layers of multi-element alloys on the steel substrate.

I would like to thank the management of "Dunarea de Jos" University of Galati and the management of the Doctoral School of Mechanical and Industrial Engineering for creating the mechanisms that allowed

me to carry out my research in good conditions, who financially supported the development of the infrastructure and my doctoral studies.

I am deeply grateful to my parents and family for their constant encouragement and unconditional support throughout my PhD studies.

The research methodology and the identification of the optimal technical solutions for solving an actual topic, with applications in strategic industrial fields, as well as the elaboration of the doctoral thesis, which I hope will significantly contribute to increasing the level of knowledge in the field of advanced materials development, have represented real challenges for my engineering career.

I assure of my deep appreciation and gratitude all those, previously nominated or not, who joined me in this adventure of knowledge. It was an honor for me to collaborate with exceptional researchers whose scientific results are recognized internationally, and I hope that the doctoral thesis will open new perspectives and research directions in the fields of manufacturing and development of advanced materials.

Galati, 2024

With gratitude,

Eng. George SIMION

CONTENT

Explanation: *The numbering of the equations, figures, and tables from the doctoral thesis is preserved in the summary of the doctoral thesis*

Introduction

The research and development of new materials play an essential role in the technological advancement and in increasing the quality of life. Just as the history of humanity is divided into periods, such as the Stone Age, Bronze Age or Iron Age, it can be considered that the development of new materials and the processes to obtain them have been the basis of the evolution of society. Each advance in the quality and diversity of materials has revealed significant innovations that have led to major advances in various fields, thus improving food science, health care and other branches that contribute to the people's state of comfort.

Starting with the 19th century, the materials science made remarkably and quickly progress. Steel, superalloys, plastics and ceramics have been developed and improved, and the last two decades a new category of materials – High Entropy Alloys (HEA) – has aroused the interest and the attention of researchers around the world. The particularity of these new materials is given by the chemical composition, in which at least four or five chemical elements are present, but no any of them is dominant chemical element.

The percentages of the main chemical elements in these High Entropy Alloys can be varied in different proportions; in addition, they can be micro-alloyed with other chemical elements, so the possible combinations are practically unlimited. The study of high entropy alloys is continuously advancing, focusing on the properties to be investigated, such as hardness, tensile strength, ductility, stability at high or low temperature, resistance to fatigue, wear and corrosion, many of them being superior to the those of the traditional alloys [1,2].

Despite the progress made, the current research and understanding of High Entropy Alloys is only the beginning of the exploration in the field of materials science. New information, observations, and results are constantly reported in the scientific articles whose main subject is the study of these new alloys. Structural phases have a significant influence on the mechanical properties of High Entropy Alloys. For instance, the face-centred cubic (FCC) structure generates lower strength and higher plasticity, while the body-centred cubic (BCC) structure determines higher strength, but less plasticity. The diversity of possible chemical compositions determines a considerable number of alloys that requires a deep analysis and attention. Changing the concentration of only one chemical element within the same alloys class can have a significant impact on the microstructure and properties of the alloy [3].

As the number of experiments focused on the study of High Entropy Alloys has increased, some researchers have suggested that entropy is not necessarily the main characteristic that gives unique properties to these materials. Consequently, alternative names such as multi-element alloys, multi-component alloys or compositionally complex alloys have been proposed. These alternative terms reflect better the compositional diversity and complexity of these alloys, suggesting that their exceptional properties are not due exclusively to high entropy, but also to complex interactions between the chemical elements [4].

Although a significant number of results obtained by researchers who have studied the multi-element alloys properties were promising, there is still a reluctance in transferring them from the research laboratories to industry. The main reason could be the high cost of fabrication,

generated both by the price of raw materials and the equipment and technology required for their manufacture. Thus, it is necessary to develop effective strategies to reduce the production costs, including the optimization of manufacturing processes, use of more economical alternative raw materials and innovation in processing technologies, in order to facilitate the large-scale use of multi-element alloys in industry.

Based on the current state analysis of development of multi-element alloys, it was identified a good opportunity to develop *an original and innovative method to obtain these special materials that could facilitate their large-scale use in the industrial applications*.

In this work, a new procedure for obtaining depositions of multi-element alloys from the AlCrFeNi system was designed, optimized and applied in the experimental tests. The motivation of choosing this type of alloys is supported by the superior mechanical properties - hardness, resistance to wear and corrosion – that recommend it for using in the industrial applications in which the improvement of the surface properties of common carbon steels is a requirement. This new technology is financially cost-effective and, in this way, the transfer of multi-element alloys from laboratory to the industrial area becomes affordable and efficient. The originality of this technology was recognized, the method being patented (patent no. 135988/29.03.2024) and rewarded with numerous medals, diplomas and trophies at the International Inventions Salons EUROINVENT (Iasi, 2023), UGAL INVENT (Galati, 2023), INVENTICA (Iasi 2024) and other scientific events.

The research directions followed in the experimental program to achieve the objectives of the PhD thesis are organized as follows:

- Development of an innovative process for obtaining multi-element alloys.
- Optimizing the welding deposition process, in order to obtain quality depositions of AlCrFeNi multi-element alloys on conventional steel substrate.
- Study of the multi-element alloys properties, deposited by TIG welding on carbon steel substrate, particularly the mechanical and metallurgical characterization of these alloys.
- Finite Element Analysis (FEA) and simulation of the welding deposition process, in order to investigate the thermal and mechanical effects generated during the welding process (temperature field, thermal cycles, stress level and displacements caused by the heat transfer). The method is an extremely useful tool in optimizing the parameters of the manufacturing process, such as the deposition process by welding of multi-element alloys.

In the first chapter of the thesis, it was developed the state-of-the-art in the field of multi-element alloys development. Aspects regarding their chemical composition and mechanical characteristics, as well as the main processes applied for obtaining cast or depositions of multi-element alloys have been investigated in detail. In the final of the chapter, there were presented and explained the motivation, objectives and directions of the research approached in the framework of the PhD thesis.

In the second chapter, the main equipment, methods and research methodology applied for achieving the expected results are presented. The numerical and experimental results were analysed, processed and interpreted in three university: the " Dunarea de Jos" University from Galaţi, the Polytechnic University of Bucharest and the University of Las Palmas de Gran Canaria.

The chapter 3 presents the theoretical concept of the new process for obtaining multi-element alloys from the AlCrFeNi system that was the basis of the research activity. The process consists in creating a beam of rods, with different compositions and/or diameters, and depositing it by melting, through the Tungsten Inert Gas (TIG) welding process, on the surface of a substrate material. The bundle can contain one or more aluminium, stainless steel and nickel-chromium alloy rods. The chemical composition of the multi-element alloy can be controlled by the diameter and number of rods used.

In the chapter 4, the experimental tests with the new method of obtaining multi-element alloy deposits are presented. It was necessary to optimize the welding parameters in order to obtain crack-free deposits. After preparing the samples, they were analysed from a chemical and mechanical point of view. The analysis of the chemical composition showed that the elements are uniformly distributed in the deposited material. The wear and corrosion resistance of the multi-element alloy deposited layers were also evaluated. In order to determine possible industrial applications of the new process for obtaining deposits with the multi-element alloy of the AlCrFeNi alloy class, the obtained results were compared with those of other researchers who investigated the mechanical characteristics of some traditional alloys currently used.

In the chapter 5, a model with finite elements was developed to simulate the depositing process of the multi-element alloy on S235 carbon steel substrate. The purpose of the modelling was to analyse the thermal effects (temperature filed and thermal cycles), as well as the stresses and displacements developed during the welding deposition process, due to the heat transfer.

In the chapter 6, there are presented and analysed in detail the results of the experimental validation of the numerical model developed for simulation of the process. An original device was designed and made in order to experimentally determine the temperature distribution, by thermocouples method, and the level of stresses by tensometry method.

In the chapter 7, the final conclusions related to the study of the multi-element layers deposited by TIG welding on carbon steel substrate, without or with subsequent remelting, are presented and discussed. Significant personal contributions to the knowledge improvement in the field of advanced materials development, such as the multi-element alloys, are described and explained in detail. Several directions for future research that definitely will open up new perspectives for further explorations and results which will arouse the interest of researchers and industry representatives are presented in the final of the chapte

CHAPTER 1

The current state of developement of multi-element alloys

1.1. Introduction

Since ancient times, the human civilization has made continuous efforts for discovering new metals and alloys, but also for the development of innovative materials that had an essential role in improving the quality of life by expanding the range of technical applications. Starting with the Bronze Age, the alloys have been traditionally developed according to the "basic chemical element" paradigm. Based on this elaboration method, one or two main chemical elements were chosen, such as copper in bronzes, iron in steels, aluminum in aluminum-based alloys, or nickel and chromium in superalloys. These chemical elements were mixed in predetermined proportions and by adding other alloying elements in lower percentages, materials with superior properties could be obtained [5].

In the last decades, due to the evolution and results reported in the field of materials development, a new category of alloys, namely High Entropy Alloys – HEA, began to draw the attention of researchers worldwide, [3,4,6–14]. These alloys are composed of at least four or five chemical elements with concentrations between 5 and 35%, without any of them being dominant. In addition to the main chemical elements, HEA alloys can be micro-alloyed with other elements, in concentrations lower than 5%, in order to improve the mechanical characteristics of the material.

The specific and distinctive composition of high entropy alloys gives them special mechanical properties, such as high strength and hardness, resistance to wear, corrosion, and to oxidation at high temperatures, and good structural stability. These special properties make high entropy alloys suitable materials for a wide range of industrial applications [15,16].

Due to the ability of high-entropy alloys to maintain their mechanical properties, both at low temperatures [17,18] and at high temperatures [19,20], the replacement of traditional alloys with HEA in industrial applications is as natural as possible.

1.2. Characterization of high entropy alloys

1.2.1. Chemical characterization of high entropy alloys

Traditionally, the pure metals and alloys used in industrial applications are based almost entirely on one main compound or element. The pure metallic materials, with a minimal degree of impurity, are used in the jewelry industry, in various applications in the electrical and optical fields, or in other specialized applications. The addition of alloying elements has the effect of improving the mechanical, physical, and chemical characteristics, and the materials obtained become extremely interesting and versatile for use, on a large scale, in industry. The metallurgists have explored the development of new alloys by combining several chemical elements in high and approximately equal proportions.

Two decades ago, two researchers groups have independently proposed the investigation of a new class of alloys which contain multiple chemical elements in approximately equiatomic concentrations. The teams were led by researchers Yeh J.W. and Cantor B. and published the first articles at the end of the year 2004 [21,22]. Jien-Wei Yeh and his team sustained an interesting theory related to these alloys, suggesting the hypothesis that the presence of multiple elements (five or more), in nearly equal proportions, would increase the configurational entropy sufficiently enough to overcome the tendency of intermetallic compounds formation that can have negative effects on the properties of the alloys.

They introduced a new and suggestive term for this class of materials that contain five or more chemical elements in relatively equal concentrations of 5%...35%, calling it high-entropy alloys. Other researchers have suggested alternative names, such as multi-component alloys, compositionally complex alloys, or multi-element alloys. Despite the fact that some researchers believe that entropy is not the main factor responsible for the structure and properties of these alloys, the term "high-entropy alloys" is likely to prevail [4].

Comparing to the conventional alloys, the high entropy alloys present specific characteristics, the difference being given by the existence of several chemical elements in approximately equimolar proportions, without the existence of a dominant chemical element. For this reason, comparing to the traditional alloys, specific effects, whose influence is much more pronounced, appear in the high-entropy alloys. Yeh J.W. investigated and identified these effects, with reference to the high entropy effect, the sluggish diffusion effect, the severe lattice distortion, and the cocktail effect.

1.2.2. Mechanical characterization of high entropy alloys

A review of the literature on high entropy alloys has revealed that their mechanical properties have been extensively studied, with particular focus on hardness [23–27], compressive strength [28–31], tensile strength [32–37], wear resistance [38–42], and fatigue resistance [43–47]. The findings indicate that these alloys have characteristics that could significantly broaden their range of industrial applications.

While some high-entropy alloys demonstrate superior mechanical properties in comparison with the traditional alloys at ambient temperature, the most notable advantage lies in their ability to mentain these properties under extreme temperature conditions, whether high or low.

1.3. Multi-element alloy manufacturing processes

1.3.1 Processes for obtaining multi-element alloys

The most common method for producing bulk multi-element alloys consists of melting the constituent chemical elements - whether in the form of powders, bars, rods, or profiles - in electric arc furnaces under a controlled atmosphere. [48–50]. The process involves the formation of an electric arc between a non-fusible electrode and the mixture of metals to be melted [51].

To enhance the homogeneity of the multi-element alloy, the resulting mixture undergoes several cycles of turning and remelting [52–54]. Researchers have observed that the most common defect developed by this manufacturing technique is the formation of heterogeneous structure, characterized by the segregation of chemical elements within the alloy, particularly when it includes elements with high density and high melting points, such as W, Ta, or Nb [55–

57]. In the scientific literature, alternative processes for obtaining bulk multi-element alloys have been identified, as follows:

- Sintering [27,30,58].
- Additive manufacturing [59,60],
- Bridgman solidification method [61–63],
- Induction melting [64–66],
- Mechanical alloying [67,68].

1.3.2. Multi-element alloy deposition processes

Comparing to the traditional materials, the production costs associated with multi-element alloys are considerably higher, primarily due to the complexity of the technological processes applied in producing the bulk products, the costs of raw materials, and the operational costs of processing facilities.

Given the high costs of producing multi-element alloys, researchers have increasingly focused on investigating cost-effective methods to enhance the quality and surface properties of traditional materials. These methods include the deposition of thin films as well as thicker layers [69–74]. The process of clading traditional steels with multi-element alloys offers a promising approach for transferring innovative material technologies from research into industrial applications. The literature presents several processes for depositing multi-element alloys onto substrate materials, typically being the carbon steel. Several methods used to obtain deposits with specialized properties, including those of medium and high entropy alloys, are presented bellow:

- Magnetron sputtering [75–79],
- LASER clading [80–83],
- Tungsten Inert Gas (TIG) welding clading [84,85],
- Sintering clading [86,87].

Due to the small thickness of the deposited layers, the deposition processes offer the advantage of rapid solidification in contrast to the methods employed for producing the bulk high-entropy alloys via melting in electric arc furnaces. According to certain studies, the rapid solidification is beneficial for high-entropy alloys, as it limits the phase transformations that occur during slow cooling, as well as the diffusion of elements and the formation of intermetallic compounds [69].

However, the methods mentioned above have certain drawbacks, including the limited thickness of the layers deposited by spraying, the use of complex and costly equipment, such as magnetrons and LASER systems, and the requirement for preparatory technological operations that include the powder mixture elaboration and previous procedures applied before melting it onto the substrate material. Additionally, the fabrication and handling of wires made from mixtures of various chemical elements require further operations included in the technological process. A synthesis of the current research in the field of high and medium-entropy alloys production indicates the need for developing new deposition procedures for achieving multi-element alloys. These procedures should be cost-effective and attractive for a broad range of industrial applications.

1.4. Conclusions

Based on the the state-of-the-art and detailed analysis of the scientific literature in terms of multi-element alloys development, the following conclusions can be drawn:

- High-entropy alloys are typically composed of at least four or five chemical elements, each of them being in concentration of 5% to 35%, and in equiatomic or approximately equiatomic proportions. No single element is dominant in the chemical composition.
- Certain high-entropy alloys exhibit outstanding mechanical properties at ambient temperature. Their most significant feature to be considered for the potential replacement of traditional alloys in applications industrial is their ability to maintain these properties under both high and low temperature conditions.
- The primary conventional processes for producing semi-finished products from high-entropy alloys include melting in electric arc furnaces under a controlled atmosphere and induction melting.
- The deposition of multi-element alloys onto conventional material substrates is typically achieved through methods such as magnetron sputtering, LASER plating, electrodeposition, and plasma spraying.
- To develop multi-element alloys that meet both quality and cost criteria, ongoing research is needed to develop innovative, efficient, and more cost-effective manufacturing technologies. Additionally, comprehensive interdisciplinary studies are essential to identify the most suitable industrial applications for these materials.

1.5. The motivation for choosing the topic and research directions

The motivation for choosing the theme, addressed in the doctoral thesis, is to increase the degree of knowledge in the following directions:

- development of procedures for producing multi-element alloys that meet quality standards and offer clear economic benefits to industry;
- development of new chemichal compositions recipes for obtaining multi-element alloys with medium entropy;
- investigation of the behavior and properties of multi-element alloys;
- identification and expanding of potential industrial applications.

The analysis of the state-of-the-art related to the on multi-element alloys research has revealed the opportunity to develop an innovative method for producing these advanced materials, facilitating the technology transfer from research to industrial applications. This work presents an innovative technology for the deposition of multi-element alloys from the AlCrFeNi system and investigates their properties to identify the most appropriate industrial applications. The selection of this alloy type is motivated by the outstanding properties - such as hardness, wear resistance, and corrosion resistance - which make it particularly suitable for improving the surface properties of conventional carbon steels. The novelty and originality of the method to achieve multi-element alloys, developed during the PhD program, have been patented, according to the patent no. 135988/29.03.2024. This invention has been awarded numerous medals, prizes, and trophies at invention exhibitions, including EUROINVENT (Iasi, 2023) and UGAL INVENT (Galati, 2023), INVENTICA (Iasi, 2024), as well as by the institution.

The research directions established for the development of the experimental program and achievement of the objectives of this PhD thesis are organized as follows:

- Development of an innovative procedure for developing multi-element alloys.

- Optimization of the welding deposition process to achieve high-quality depositions of the AlCrFeNi alloy class on a standard steel substrate.
- Investigation of the properties of multi-element alloys deposited by welding onto a carbon steel substrate, with focus on their mechanical and metallurgical characterization:
  - Macroscopic analysis of the samples to assess the quality, appearance, and height of the deposited layers. The aim of the investigation is to produce deposited layers free of visible defects, such as voids, cavities, or pores.
  - Microscopic analysis of the samples to examine the transition area and the uniformity of the fusion line, to evaluate the degree of homogeneity, and to determine the grain size of the deposited material. This analysis also aims to detect microscopic defects, such as cracks, pores, inclusions, and other discontinuities that could compromise the integrity of the deposited layer and the quality of the multi-element alloy.
  - Chemical composition analysis of the deposited layer to determine the base material's participation in the formation of the molten metal pool. This analysis will also establish the limit of the chemical elements diffusion from the deposited material to the substrate material and vice versa.
  - Investigation of the microhardness profile within the multi-element alloy, in order to determine the minimum thickness for which the deposited layer can be mechanically processed or can still have resistance to wear.
  - Assessment of wear and corrosion resistance of the deposited alloy to facilitate a comparative analysis with conventional materials, currently employed in industrial applications, with the aim of evaluating the potential of replacing them by multi-element alloys.
- Finite element modeling and simulation of the deposition welding process to analyze the thermal and mechanical effects generated by the welding process, including thermal field distribution, thermal cycles, stress levels, and displacements caused by the heat transfer. This approach serves as a critical tool for optimizing the parameters of the manufacturing process, particularly for the deposition welding of multi-element alloys with medium entropy.

CHAPTER 2

Research methodology, materials and equipment

2.1. The objectives of the PhD thesis and research methodology

The primary objectives of the doctoral thesis were to develop a novel procedure for the deposition of multi-element alloys and to examine the properties of layers deposited by TIG welding. To achieve these objectives, a research methodology was developed, as illustrated in Figure 2.1.

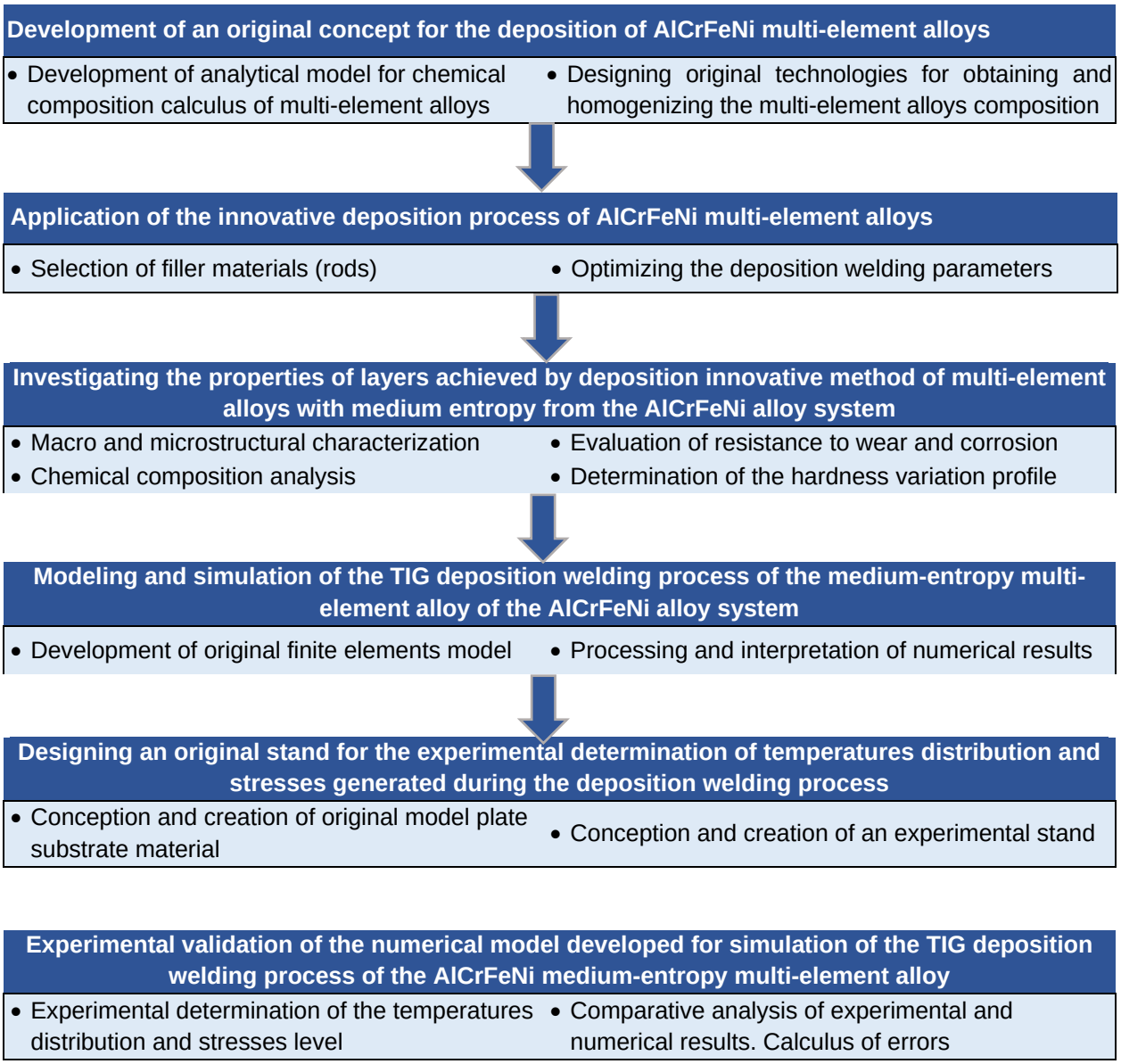

Fig. 2.1. The research methodology applied to achieve the objectives of the PhD thesis

2.2. Materials used in the experimental program

The substrate material employed in the experimental tests is the structural steel S235 (EN 10025 – 2), having the chemical composition and mechanical properties provided by the manufacturer, LIBERTY Galati, as detailed in Tables 2.1 and 2.2. For depositing the multi-element alloy from the AlCrFeNi system, plates with dimensions of 40x100x12 mm were cut, as Figure 2.2 shows. To prevent the potential inclusions, contamination of the molten pool with oxides, and the occurance of other defects generated during the deposition process, the surface of the plates was meticulously cleaned through polishing technique.

Table 2.1. Chemical composition of S235 substrate steel (manufacturer's certificate)

Material	C	Mn	Si	P	S	Al	Cu	Cr
S235	0.12	0.75	0.17	0.016	0.011	0.038	0.06	0.04
	Ni	**V**	**Mo**	**Ti**	**B**	**N**	**Fe**	**-**
	0.03	0.001	0.002	0.001	0.0002	0.0064	98.22	-

Table 2.2. Mechanical characteristics of S235 substrate steel (manufacturer's certificate)

Material	Tensile strenght σ_y [MPa]	Ultimate tensile strength σ_r [MPa]	Elongation [%]	Hardness Vikers [HV]
S235	320-350	440-450	32	155-190

For TIG (Tungsten Inert Gas) deposition welding of the multi-element alloy, performed in Ar protective atmosphere, a bundle of three rods with distinct chemical compositions was prepared, as follows: one aluminum rod ALTIG AL99.7 (EN ISO 18273: S Al 1450 (Al99.5Ti)), one stainless steel rod INTERROD 22 9 3 (EN ISO 14343-A: W 22 9 3 N L), and one Ni-Cr alloy rod NIROD 625 (EN ISO 18274-A: S Ni 6625 (NiCr22Mo9Nb)). The chemical composition of the rods mentioned above are detailed in Tables 2.3, 2.4, and 2.5.

Table 2.3. Chemical composition of ALTIG AL99.7 aluminum rod

Si	Mn	Cr	Cu	V	Ti	Al	B	Fe	Zn	Mg
0,06	<0,01	<0,17	<0,01	0,01	0,01	99,8	<0,01	0,09	<0,01	<0,01

Table 2.4. Chemical composition of INTERROD 22 9 3 stainless steel rod

C	Si	Mn	P	S	Cr	Ni	Mo	Cu	N
0,013	0,49	1,51	0,016	0,001	23,1	8,7	3,18	0,11	0,16

Tabel 2.5. Chemical composition of NIROD 625 Ni-Cr alloy rod

C	Si	Mn	P	S	Cr	Ni	Mo	Nb	Cu	Ti	Al	Co	Fe
0,06	0,1	0,02	0,003	0,001	22,2	64,4	8,8	3,68	0,01	0,19	0,1	0,01	0,3

2.3. Equipment used in the experimental program

2.3.1. Multi-process equipment for deposition welding and remelting

The technique employed for melting the rod beam to perform multi-element alloy deposits is the TIG (Tungsten Inert Gas) welding process, using a non-consumable electrode and Ar as shielding gas. The multi-process welding equipment, SAF-RO DIGIWAVE III 420, used for the deposition and remelting processes, is integrated into the research infrastructure of the Center for Advanced Research in Welding (SUDAV) from Faculty of Engineering, "Dunarea de Jos" University of Galati (UDJ Galati).

2.3.2. Equipment for structure analysis and microhardness measurement

To achieve a thin polished surface, Remet LS 1 equipment, which is part of the infrastructure at the *Centre for Advanced Research in Welding* (CC SUDAV), was used in the experimental program. A wet sanding procedure was applied, employing abrasive papers with 400, 600, 800, 1000, 1500, 2000, and 3000 grits and felt soaked in diamond powder.

The structure analysis of the deposited and remelted layers was conducted using optical microscopy and scanning electron microscopy (SEM) techniques, as illustrated in Figure 2.8. This analysis was carried out in the LAMET Laboratory of the *Department of Quality Engineering and Industrial Technologies* from the *Faculty of Industrial Engineering and Robotics, National University of Science and Technology Bucharest Polytechnic* (UNSTP Bucharest).

Fig. 2.8. Scanning electron microscope (LAMET Laboratory, UNSTP Bucharest)

Fig. 2.9. FALCON 500 Hardness Tester (CC SUDAV, UDJ Galati)

The profile of HV_{05} microhardness in the multi-element alloy layers was determined with FALCON 500 hardness testing equipment (see Fig. 2.9) and the results were collected and

processed with the IMPRESSIONS™ software program. This equipment and software are part of the research infrastructure at the *Centre for Advanced Research in Welding* (SUDAV), from *Faculty of Engineering, "Dunarea de Jos" University of Galati*.

2.3.3. Equipment for the analysis of wear and corrosion resistance

The tribological properties of the multi-element alloy deposited by welding onto the S235 steel substrate were assessed through wet abrasion tests which were conducted in the *Metrology Laboratory* of the *National University of Science and Technology Politehnica Bucharest*, utilizing the CSEM CALOWEAR equipment.

The corrosion resistance of the multi-element alloy layers was evaluated in the *Laboratory of Nanosciences and Nanomaterials* at the *University of Las Palmas de Gran Canaria* (ULPGC), Spain. This assessment involved specific tests using 3.5% sodium chloride (NaCl) solution and SP-150 potentiostat manufactured by Biologic, Seyssinet-Pariset, France.

2.3.4. Equipment for determining the temperature and stress values

To measure the temperature distribution, six K-type thermocouples and Lutron BMT-4208SD data acquisition system were employed. Stress measurements were performed with strain gauges of type 10/20 LY11. These sensors were applied to S235 steel plates with dimensions of 100x20x2 mm. The data collected by the Quantum X data acquisition system were subsequently analyzed with the "CatmanEasy-AP" software. The connection between the strain gauges and data acquisition system was established through data transmission cable and eight-port connectors.

2.4. Conclusions

This chapter outlines the principal materials, research methodologies, equipment, and devices employed in the development of the advanced research program within the doctoral study program. The experimental research was conducted in the following institutions:

- *Doctoral School of Mechanical and Industrial Engineering (SDIMI), "Dunarea de Jos" University, Galati (UDJ Galati);*
- *Centre for Advanced Research in Welding (CC SUDAV), "Dunarea de Jos" University, Galati (UDJ Galati);*
- *LAMET Laboratory and Metrology Laboratory, National University of Science and Technology Politehnica, Bucharest (UNSTP Bucharest);*
- *Laboratory of Nanosciences and Nanomaterials, University of Las Palmas de Gran Canaria, Spain (ULPGC).*

It is important to note that certain equipment, including that used for testing the resistance to wear and corrosion, measuring the temperature and stress, requires periodic calibration, in order to mitigate the measurement errors and to ensure the accuracy and validity of the research outcomes.

CHAPTER 3

Original procedure for obtaining multi-element alloys

The research conducted within the doctoral study program has materialized in the invention patent no. 135988/29.03.2024. This patent refers to an innovative method for developing multi-element alloys from the AlCrFeNi alloy system. The invention reveals elements of originality and technical advancements, and provides a cost-effective solution for fabricating deposited layers of AlCrFeNi multi-element alloys. The process, characterized by flexibility in achieving variable layer thickness and lack of constraints imposed by the technological process, is based on deposition welding technology with standardized filler materials, in Ar protective gas environment, without previous necessary preparatory technological operations [88].

3.2. Description of the procedure. Original elements. Case studies

One of the main objectives of the PhD thesis was to develop an original and advantageous economic method for producing deposited layers of multi-element alloys from the AlCrFeNi alloy system, with outstanding mechanical properties, significantly superior to the substrate properties. These layers, which can vary in thickness, are produced through a conventional deposition welding process (TIG), using standardized filler materials, without previous necessary preparatory technological operations.

Research into multi-element alloys of the AlCrFeNi class has demonstrated that these materials have remarkable mechanical strength, hardness, and wear resistance [31,87,89,90], making them well-suited for industrial applications, where special mechanical properties of surfaces are required.

3.2.1. New procedure for obtaining the multi-element alloys from the AlCrFeNi system

The manufacturing process consists of melting a bundle of rods with varying chemical compositions and diameters, by TIG welding method, to obtain deposits of multi-element alloys with controlled chemical composition on traditional carbon steel substrate. The atomic percentages of the chemical elements incorporated into the multi-element alloy can be adjusted based on the mechanical properties required in the industrial applications. Additionally, the multi-element alloy can be microalloyed with elements such as C, Nb, Mn, Mo, Ta, W, etc., which have the role to improve the alloys' properties. The bundle of rods is positioned in the electric arc zone developed between the non-consumable W electrode and the material substrate. To ensure uniform coverage of the substrate, the deposited layers are partially overlapped, each layer extending approximately 30-60% on the width of the previous deposit. The welding deposition process is conducted in Ar shielding gas atmosphere. To improve the chemical homogenization and enhance the mechanical properties of the deposited alloy, a remelting procedure is performed

by TIG welding process, without additional filler materials, on transverse, longitudinal, or combined direction, relative to the initial deposition welding direction. The process is schematically presented in Figure 3.1, where 1 represents the W electrode, 2 is the shielding gas (Ar), 3 indicates the deposited multi-element alloy, 4 is the rod bundle, and 5 signifies the steel substrate (base material).

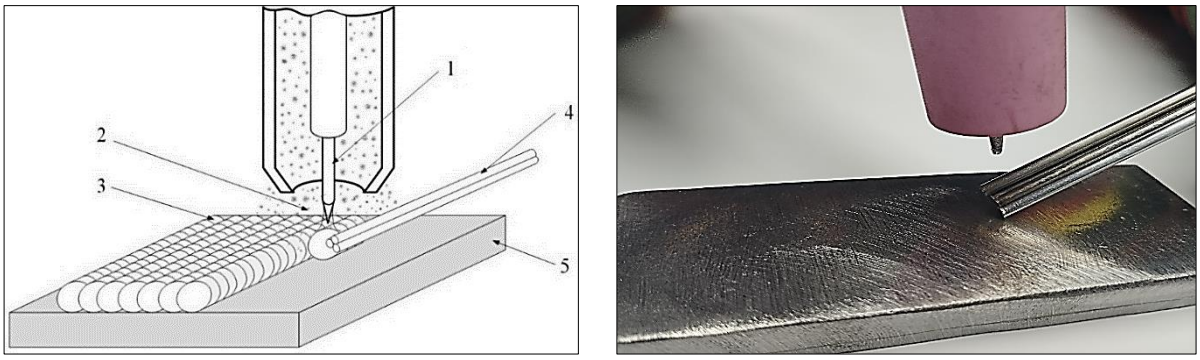

Fig. 3.1. Obtaining multi-element alloys by TIG welding deposition process

3.2.2. Depositions of AlCrFeNi multi-element alloys – Case studies

The chemical composition of the multi-element alloy is meticulously controlled by selecting the chemical composition, number, and diameter of the rods that form the bundle that has the role of filler material. The AlCrFeNi multi-element alloys, with varying chemical compositions, achieved by melting the bundle of rods through the TIG deposition welding, is exemplified by the case studies 1 and 2, selected from the 4 cases described in the PhD thesis.

Case study 1: The bundle of wires comprises aluminum, stainless steel, and NiCr alloy rods, all of them having identical diameters (2 mm). By weighing the rods and based on the chemical composition certificates, provided by the manufacturer, the chemical composition and the atomic ratio of the new multi-element alloy can be determined by analytical method. Finally, the AlCr0.7FeNiMo0.1 alloy, obtained by deposition welding, is presented in detail in Table 3.2.

Tabel 3.2. Chemical composition of the medium-entropy multi-element alloy AlCr0.7FeNiMo0.1

Chem. elem.	C	Mn	Si	S	P	Cr	Fe	Ni	Mo	Nb	Al	N
m [g]	0.03	0.37	0.3	0.01	0.01	10.92	16.66	17.42	3	0.88	8.47	0.02
wt [%]	0.056	0.633	0.509	0.019	0.021	18.793	28.68	29.995	5.157	1.514	14.581	0.042
at [%]	0.23	0.57	0.9	0.03	0.01	17.88	25.4	24.9	2.66	0.55	26.73	0.15

Where: m is mass, wt – weight ratio, at – atomic ratio

Case study 2: In this case, the objective was to mitigate the risk of cracking in the welded material by decreasing the aluminum concentration below 7%, by using an aluminum rod with a smaller diameter. The bundle of rods with different diameters consists of one aluminum rod with diameter of 1.6 mm, one stainless steel rod with diameter of 2.4 mm, and one NiCr alloy rod with

diameter of 2.4 mm. This configuration results in the Al0.5Cr0.7FeNiMo0.1 alloy, with the chemical composition detailed in Table 3.3.

Tabel 3.3. Chemical composition of the medium-entropy multi-element alloy Al0.5Cr0.7FeNiMo0.1

Chem. elem.	C	Mn	Si	S	P	Cr	Fe	Ni	Mo	Nb	Al	N
m [g]	0.05	0.53	0.43	0.02	0.02	15.71	23.98	25.09	4.31	1.27	5.43	0.04
wt [%]	0.061	0.688	0.544	0.021	0.023	20.446	31.196	32.641	5.612	1.647	7.065	0.046
at [%]	0.27	0.67	1.05	0,03	0.01	20.99	29.82	29.33	3.12	0.65	13.98	0.17

3.3. Conclusions

The investigations conducted in this chapter, which are the main subject of the invention patent no. 135988/29.03.2024, have led to several significant conclusions in terms of developing new materials appropriate for industrial applications that require specific properties:

- Multi-element alloys from the AlCrFeNi system can be produced applying this innovative method that involves the use of aluminum, stainless steel, and Ni-Cr alloy rods.
- The innovative technique presented in this chapter - melting of bundle of rods by TIG deposition welding - enables the production of high-quality multi-element alloy coatings, leading to substantial improvements in surface quality.
- The chemical composition of multi-element alloys, fabricated through this new patented method, can be precisely controlled by selecting the appropriate rods, number, and diameters of the rods.
- The multi-element alloys will comprise also additional microalloying elements from the composition of selected rods - such as Nb, Mn, Mo, Ta, W etc. - confirming the beneficial effects on the conventional alloys properties already reported in the literature.
- Based on standard welding technique and available common filler materials, the novel procedure for producing multi-element alloy depositions is a cost-effective solution that facilitates the technology transfer from the research laboratory to industry.

CHAPTER 4

Experimental research on the properties of AlCr0.7FeNiMo0.1 medium-entropy multi-element alloy made by TIG deposition welding

4.1. Implementation of the experimental program

4.1.1. Rods selection for developing the filler material

In the experimental phase of the doctoral studies program, the depositions of AlCrFeNi multi-element alloy on S235 steel substrate were performed by melting a bundle of three rods with distinct chemical composition (Fig. 4.1). The simultaneous melting of three rods in common molten pool, created by TIG welding, results in formation of multi-element alloy with particular chemical composition. In this work, the welding rods bundle, each of rods having diameter of 2.4 mm, comprises one ALTIG AL99.7 aluminum rod, one INTERROD 22 9 3 stainless steel rod, and one Ni-Cr NIROD 625 rod.

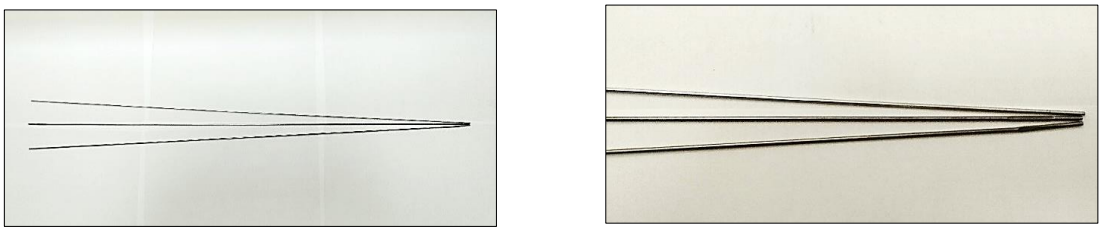

Fig. 4.1. Bundle of welding rods

Prior to melting and deposition onto the substrate, the rods, each of them having the diameter of 2.4 mm, were weighed. The results indicated an average mass of 12.2 g for the ALTIG AL99.7 aluminum rod, 36.17 g for the NIROD 625 Ni-Cr alloy rod, and 35.26 g for the INTERROD 22 9 3 stainless steel rod. Based on these measurements and on the chemical composition certificates, provided by the rods manufacturer, the composition of the AlCr0.7FeNiMo0.1 microallyed with Nb, Mn, Si, Ti, Cu, C, and Co was determined by analytical calculus (Table 4.1).

Table 4.1. AlCr0.7FeNiMo0.1 alloy's chemical composition determined by analytical calculus

Chem. elem.	C	Mn	Si	S	P	Cr	Fe	Ni	Mo	Nb	Al	N	Co	Cu	Ti
m [g]	0.01	0.54	0.21	0.00	0.01	16.14	22.33	26.36	4.31	1.33	12.24	0.06	0.004	0.04	0.07
wt [%]	0.008	0.641	0.254	0.001	0.009	19.3	26.7	31.51	5.155	1.592	14.631	0.067	0.004	0.046	0.082
at [%]	0.03	0.58	0.45	0.001	0.004	18.37	23.37	26.18	2.66	0.85	26.84	0.24	0.004	0.04	0.08

4.1.2. Preliminary studies to determine the optimal process parameters

4.1.2.1. Experimental determination of the primary welding parameters

After setting the primary welding parameters – I_s=220A, U_a=15V, v_s=10.8 cm/min - successive welding beads were made on the 40x100x12 mm steel plates. The properties of the distinct samples have been analyzed (Fig. 4.3): sample (a) on which the AlCrFeNi alloy was initially deposited (Fig. 4.3a), and samples (b), (c), (d) on which the initially deposited material was remelted by TIG technique without the filler material. This method aimed to enhance the chemical homogeneity and to improve the mechanical properties of the deposited multi-element alloy. The remelting operations were conducted on three orientations: longitudinally (Fig. 4.3b), transversely (Fig. 4.3c), and in combined (longitudinal and transverse) way (Fig. 4.3d), relative to the initial deposition direction.

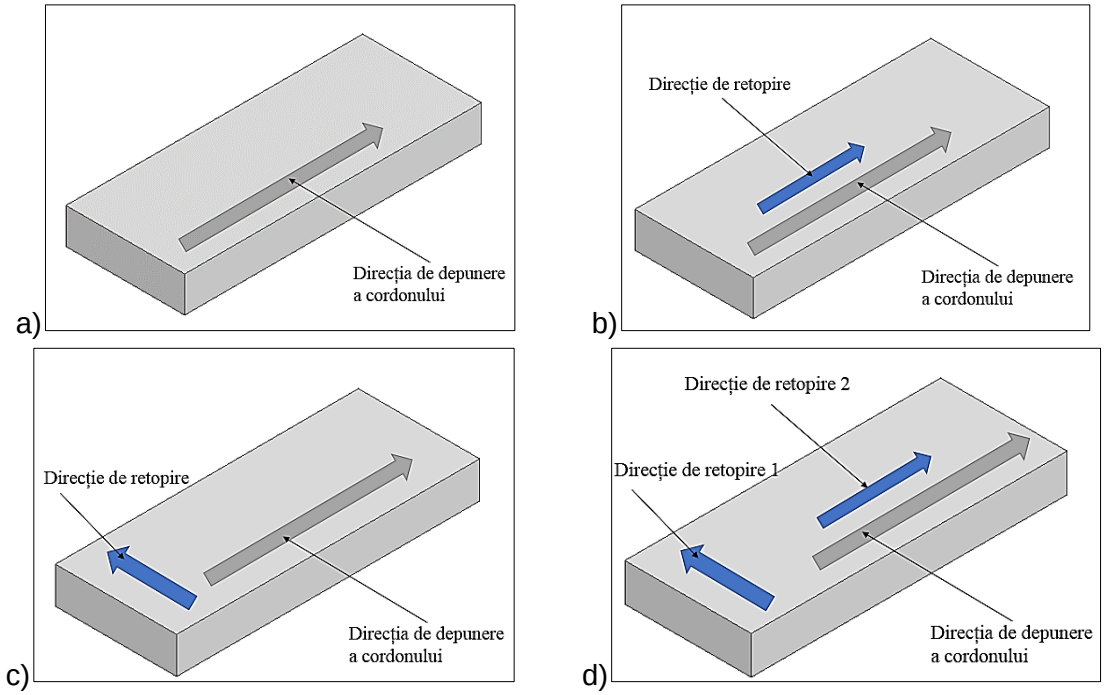

Fig. 4.3. Directions of deposition (a) and remelting (b, c, d) of the AlCrFeNi multi-element alloy

4.1.3. Welding parameters for obtaining the AlCr0.7FeNiMo0.1 alloy

Following the experimental tests, the samples were subjected to non-destructive testing (NDT) in order to determine the welding parameters and the interpass temperature which are critical factors in achieving high-quality deposits. The optimal parameters identified are as follows:

- *Currentul de sudare (I_s): 220A* that ensures effective control of the welding pool and satisfactory geometry of the deposited layers.
- *Interpass Temperature (T): 300°C* that is optimal to produce crack-free depositions.

Based on repeated experimental tests and taking into consideration the influence of the welding parameters and of the interpass temperature, the final deposition layers were performed on S235 steel plates with dimensions of 12x40x100 mm (Fig. 4.8). Complete coverage (100%) was achieved after five successive depositions, each of them overlapping approximately 50% on the previous deposit width.

The primary parameters for both the deposition and remelting processes, carried out longitudinally, transversely, and in combined way, relative to the initial deposition direction, are presented in Tables 4.4 to 4.7. The parameters are defined as previously described, where D_g represents the gas flow and t_g the pre-gas/post-gas time.

Fig. 4.8. Non-destructive testing of samples accepted for investigation of AlCr0.7FeNiMo0.1 multi-element alloy properties

Table 4.4. Optimal welding parameters of deposition process

Process	**I_s [A]**	**U_a [V]**	**v_s [cm/min]**	**D_g [l/min]**	**t_g [s]**	**Heat Input [J/cm]**
Deposition	220	18	17	18	1/6	8385

Table 4.5. Optimal welding parameters of deposition longitudinal remelting processes

Process	**I_s [A]**	**U_a [V]**	**v_s [cm/min]**	**D_g [l/min]**	**t_g [s]**	**Heat Input [J/cm]**
Deposition	220	18	13	18	1/6	10966
Longitudinal remelting	220	15	20	18	1/6	5940

Table 4.6. Optimal welding parameters of deposition transversal remelting processes

Process	**I_s [A]**	**U_a [V]**	**v_s [cm/min]**	**D_g [l/min]**	**t_g [s]**	**Heat Input [J/cm]**
Deposition	220	18	18	18	1/6	7920
Transversal remelting	220	16	40	18	1/6	3168

Table 4.7. Optimal welding parameters of deposition combined remelting processes

Process	I_s [A]	U_a [V]	v_s [cm/min]	D_g [l/min]	t_g [s]	Heat Input [J/cm]
Deposition	220	18	15	18	1/6	9504
Transversal remelting	220	15	35	18	1/6	3394
Longitudinal remelting	220	18	30	18	1/6	4752

4.2. Analysis of the properties of multi-element alloy layers

4.2.2. Codification of technologies applied for deposition welding

For easy identification of samples in the chemical, metallurgical, and mechanical study, the samples' codes have been established in a suggestive manner for each technological variant:

- 1D - samples with AlCr0.7FeNiMo0.1 deposited layers without remelting;
- 1L - samples with AlCr0.7FeNiMo0.1 deposited layers and longitudinal remelting;
- 1T - samples with AlCr0.7FeNiMo0.1 deposited layers and transverse remelting;
- 1C - samples with AlCr0.7FeNiMo0.1 deposited layers and combined remelting.

4.2.3. Analysis of the structure and chemical composition of the multi-element alloy

Following the chemical etching with Nital 4% reagent, the S235 steel substrate, onto which successive material layers were deposited, was emphasized. These layers were deposited by melting the bundle of rods that have distinct chemical compositions. Melting simultaneously the rods in common molten pool by TIG welding method, a medium-entropy multi-element alloy was achieved.

Figure 4.10 presents the macrostructure of AlCr0.7FeNiMo0.1 multi-element alloy deposited on the steel substrate. After mechanical processing, the thickness of the deposited layer remained approximately 2.5 mm. It is evident that the deposited material has appropriately adhered to the S235 steel substrate. Visual inspection confirmed that the connection between the materials is adequate, and no cracks, pores, voids, gaps, or other defects have been observed.

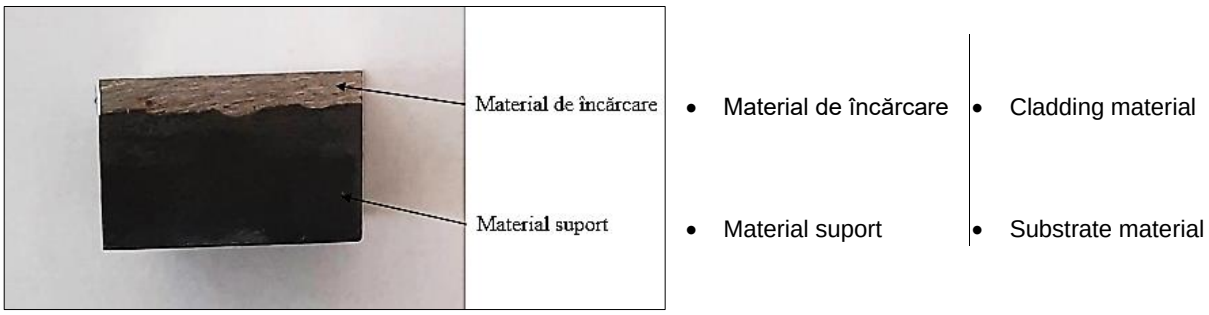

Fig. 4.10. Cross-section in the specimen taken from the deposition area

4.2.3.1. Microscopic and chemical analysis of the multi-element alloy obtained by deposition welding and subsequent longitudinal remelting (sample 1L)

The microscopic examination of the S235 steel substrate revealed a structure consisted of elongated ferrite grains and pearlite (Fig. 4.11a). In the heat-affected zone (HAZ) within the base material, there is a noticeable alteration in the geometry of the ferrite grains, which transform from elongated shape into formations with irregular grain boundaries. Among these ferrite formations, a relatively uniform dispersion of pearlite is observed (Fig. 4.11b). The transition region, marked by the fusion line between the two materials, is continuous and free of imperfections. A slight increase in grain size is evident near the fusion line, as shown in figure 4.11c. Figure 4.11d provides a detailed view on the fusion line area, positioned at the intersection between two successive deposited layers.

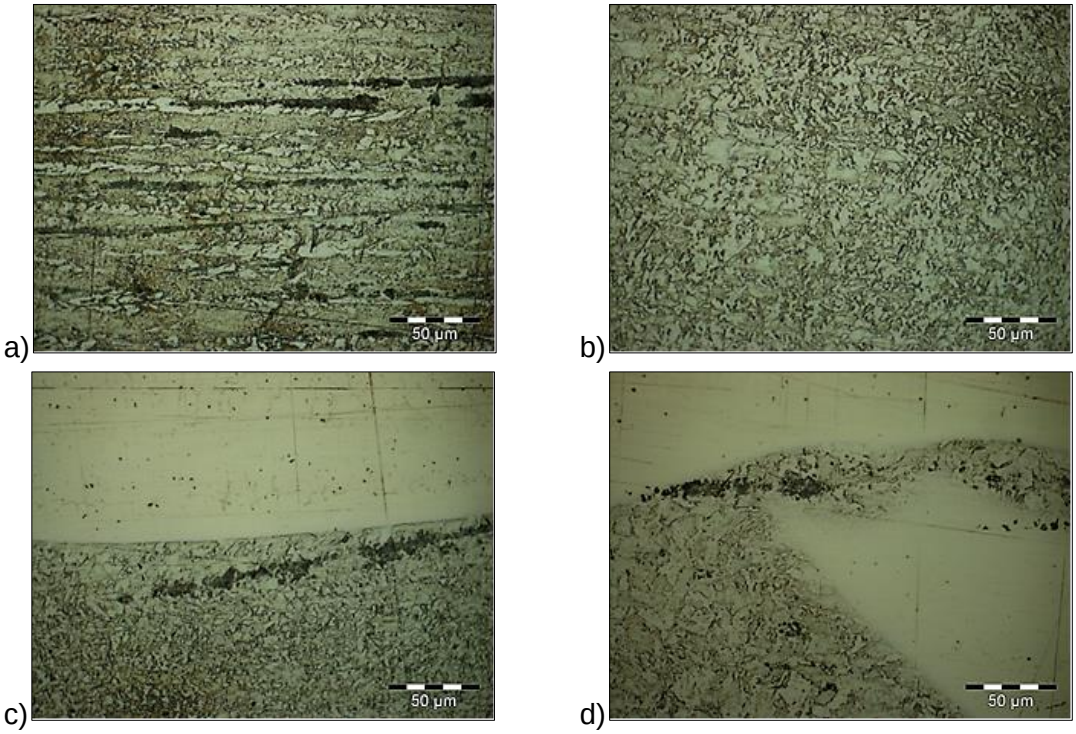

Fig. 4.11. Microstructure of sample 1L (deposition welding and longitudinal remelting): a) base material; b) Heat Affected Zone; c) fusion line between the deposited layer and the base material; d) fusion line between two successive depositions

The chemical composition of the deposited layer was determined by employing the scanning electron microscopy (SEM). A micro-zone with five grains, located in the sample 1L that was achieved by depositing the AlCr0.7FeNiMo0.1 multi-element alloy, followed by subsequent remelting on longitudinal direction, was analyzed (Fig. 4.12). The image revealed elongated grains aligned with the thermal flow, containing precipitates of intermetallic compounds.

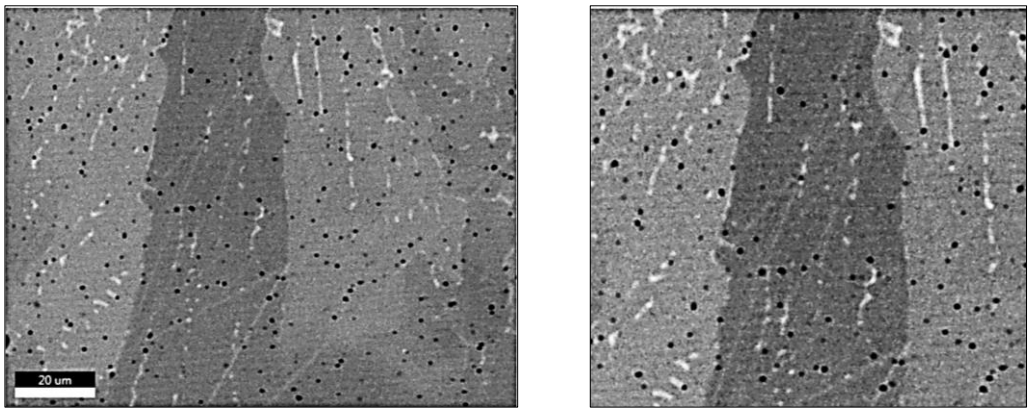

Fig. 4.12. SEM analysis of the chemical composition (sample 1L)

The chemical composition of the AlCr0.7FeNiMo0.1 multi-element alloy in the layer deposited and subsequently remelted in the longitudinal direction was determined through spectral analysis. The following chemical elements were identified (Fig. 4.13): Fe at 59.09 wt% (55.46 at%), Ni at 17.94 wt% (16.02 at%), Cr 13.15 wt% (13.26 at%), Al at 7.07 wt% (13.74 at%), Mo at 1.85 wt% (1.01 at%), and Nb at 0.9 wt% (0.51 at%). Other microalloying elements present in the rods used for the TIG deposition welding - C, Mn, Si, Co, Cu, and Ti - were found to be in concentrations too low to be detected by the energy dispersive X-ray spectroscopy (EDS).

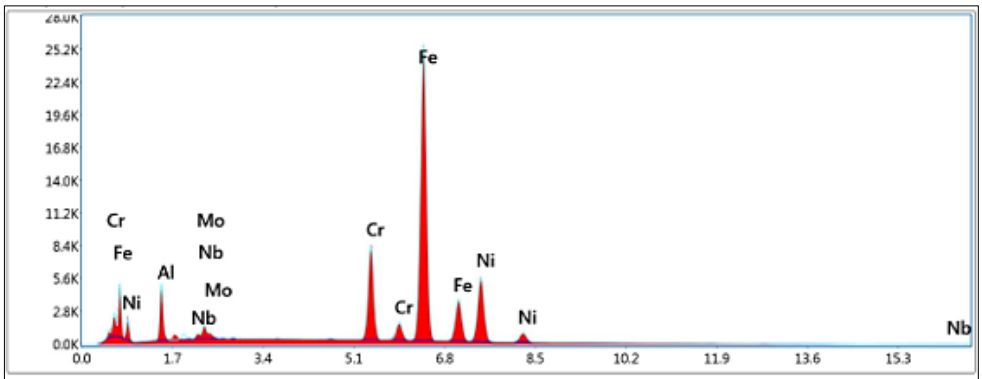

Element	Weight %	Atomic %	Net Int.	Error %	Kratio	Z	A	F
AlK	7.07	13.74	139.48	8.65	0.0219	1.1187	0.2765	1.0017
NbL	0.90	0.51	15.33	9.46	0.0059	0.9044	0.7230	1.0012
MoL	1.85	1.01	33.46	8.36	0.0128	0.8954	0.7723	1.0015
CrK	13.15	13.26	395.38	2.04	0.1388	0.9914	0.9764	1.0907
FeK	59.09	55.46	1356.96	1.69	0.5756	0.9902	0.9603	1.0244
NiK	17.94	16.02	311.58	2.82	0.1600	1.0052	0.8813	1.0067

Fig. 4.13. Spectral analysis in the multi-element alloy obtained by deposition welding and longitudinal remelting (sample 1L)

In the same micro-zone, a distribution map of the chemical elements was generated, revealing good chemical homogeneity. The results indicated that the alloying elements - Fe, Ni, Cr, Al, Mo, and Nb - are uniformly distributed throughout the multi-element alloy, demonstrating an adequate homogeneity level (Fig. 4.14).

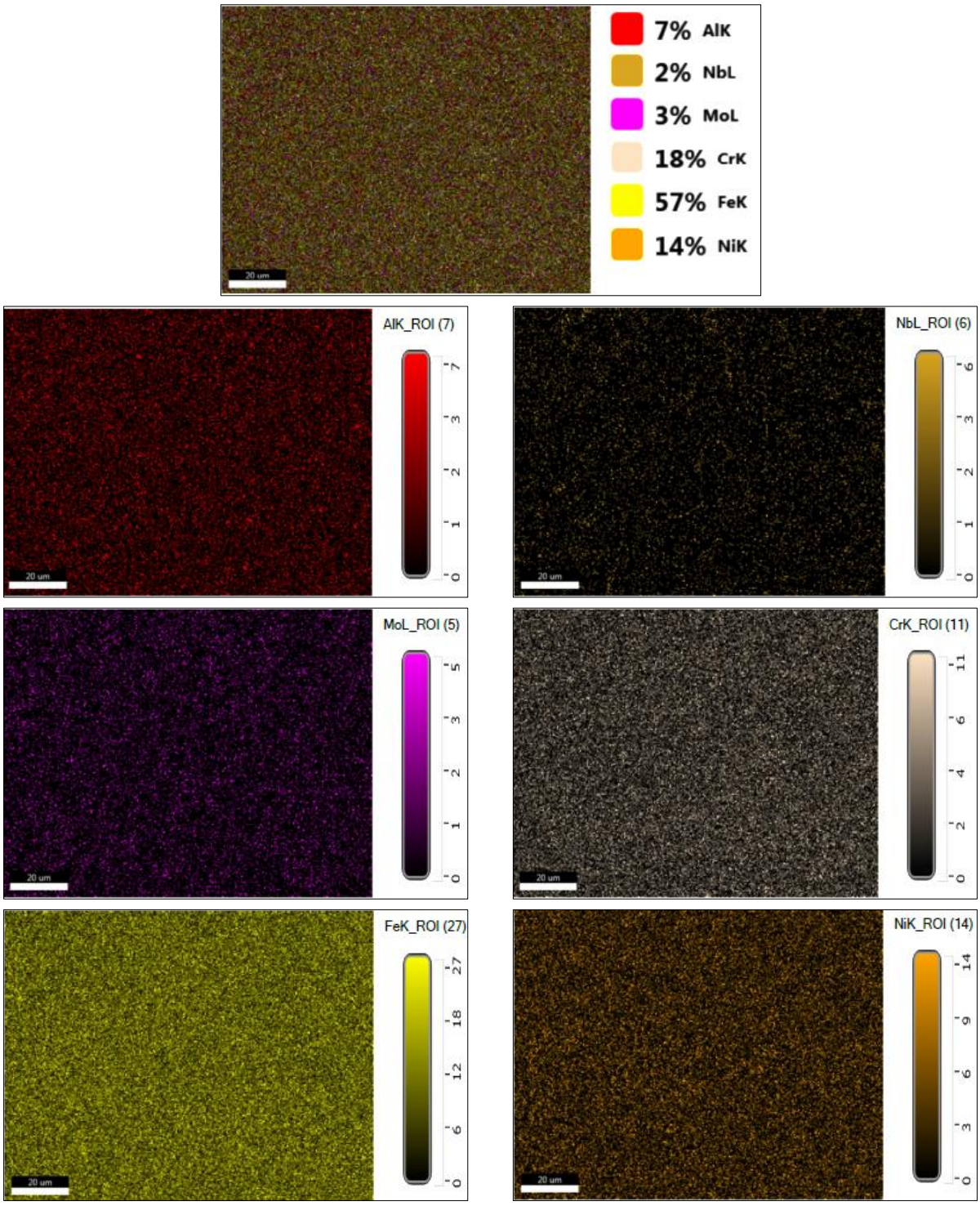

Fig. 4.14. Elemental distribution in the multi-element alloy obtained by deposition welding and longitudinal remelting (sample 1L)

In the deposited layer, small, white, filamentous compounds were identified (Fig. 4.15). Their development, attributed to the slow diffusion process, is a common phenomenon in multi-element alloys. These compounds exhibit an acicular morphology with thicknesses less than 1 µm and lengths approximately 5 µm, and with high Nb content ranging from 7 to 12%.

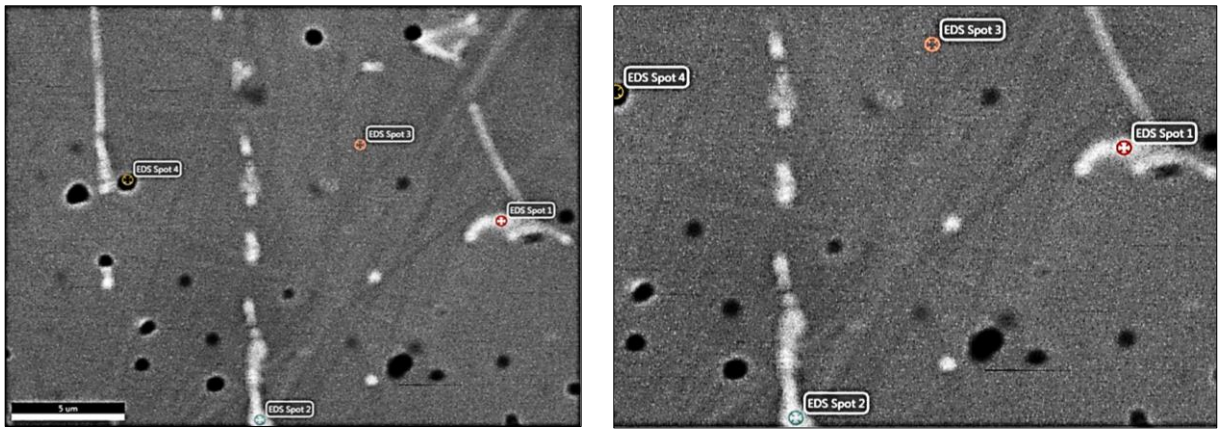

Fig. 4.15. Inter-metallic filiform compounds with high Nb content precipitated in the matrix of the multi-element alloy obtained by deposition welding and longitudinal remelting (sample 1L)

4.2.3.2. Microscopic and chemical analysis of the multi-element alloy obtained by deposition welding and transverse remelting (sample 1T)

Figure 4.32 illustrates the microstructure within the layer deposited by welding and subsequently remelted in the transverse direction (1T), highlighting specific points (Spot 1, Spot 2, Spot 3) selected for the chemical composition analysis. The primary chemical elements identified through SEM analysis are Fe (59.93–61.18 wt%; 55.54–56.95 at%), Ni (17.39–18.20 wt%; 15.4–16.04 at%), Cr (12.49–12.56 wt%; 12.49–12.52 at%), and Al (6.45–6.91 wt%; 12.42–13.26 at%). In addition to these elements, Mn (0.84–0.91 wt%; 0.79–0.76 at%), Si (0.74–0.77 wt%; 0.81–0.86 at%), and Nb (0.78–0.82 wt%; 0.44–0.46 at%) were also detected, with results comparable with the chemical analysis results of other samples.

Figure 4.36 displays the micro-zone within the multi-element alloy where the distribution maps for the principal alloying elements were generated. Upon examining the microstructure of the multi-element alloy produced through deposition welding, followed by the transverse remelting, an accumulation of white-colored compounds at the grain boundaries is observed. The distribution maps reveal a uniform dispersion of alloying elements such as Ni, Cr, Co, Fe, and Mn, whereas Al exhibits both uniform distribution and localized accumulation, leading to the formation of aluminum nitride (AlN) compounds.

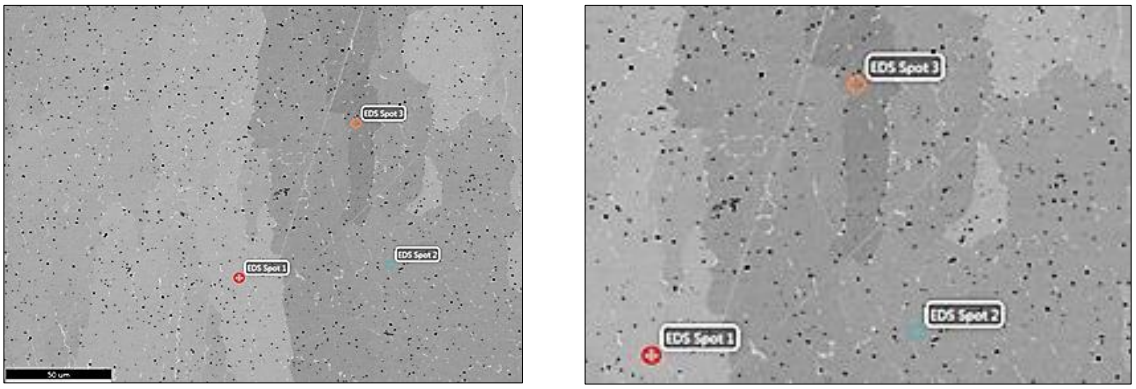

Fig. 4.32. Microstructure of the multi-element alloy obtained by deposition welding and transverse remelting (sample 1T)

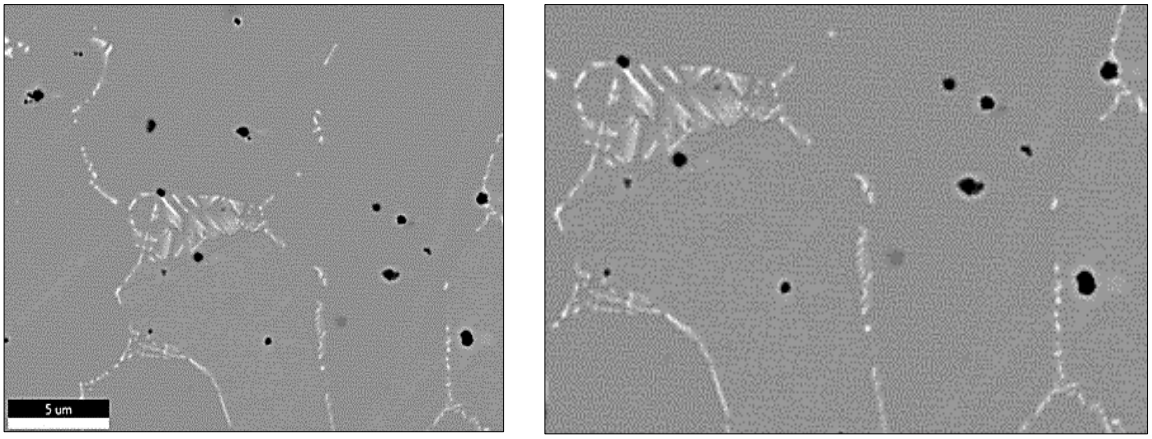

Fig. 4.36. Micro-zone located in the multi-element alloy obtained by deposition welding and transverse remelting (sample 1T)

The chemical elements Nb and Mo play a significant role in the formation of compounds identified at the grain boundaries. The presence of Nb and Mo compounds at these boundaries in the multi-element alloy offers certain advantages, as these elements are known to enhance the strength, hardness, and corrosion resistance of conventional metallic materials.

Figure 4.45 illustrates the microstructure of a section within the heat-affected zone of sample 1T, along with the locations where the chemical composition was determined. The fusion line (LF) distinctly separates the multi-element alloy layer (top area) from the underlying unalloyed steel substrate (bottom area).

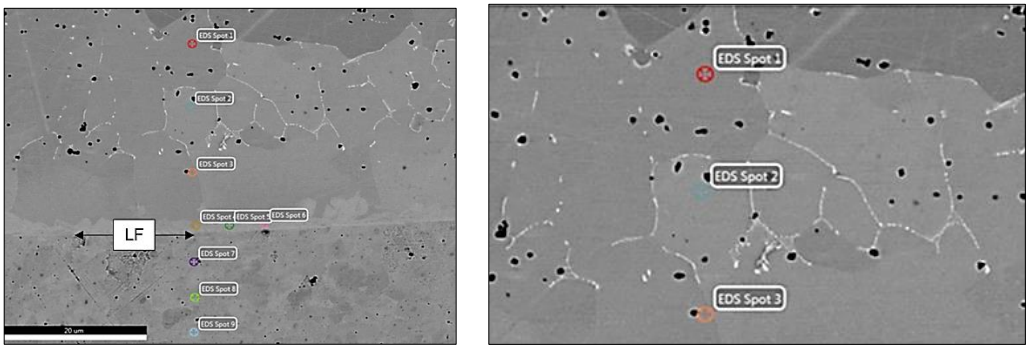

Fig. 4.45. Microstructure of Heat Affected Zone of sample 1T

4.2.3.3. Microscopic and chemical analysis of the multi-element alloy obtained by deposition welding and combined remelting (sample 1C)

Figure 4.57 presents the microstructure of the multi-element alloy obtained through deposition welding and combined remelting (sample 1C), along with the location of the chemical analysis area. The image reveals the presence of Al-rich compounds within the grain structure and also Nb and Mo-rich intermetallic compounds arranged along the grain boundaries. The chemical analysis of the area designated as Full Area 1 (Figure 4.58) indicates that the composition of the multi-element alloy is predominantly composed of Fe (58.97wt%), with typical alloying elements Si, Mn, and Nb dissolved within it.

The principal alloying elements of the multi-element alloy, produced through deposition welding, followed by combined remelting, are Ni (17.34wt%), Cr (11.04wt%), and Al (8.35wt%). In conventional alloys, Nb is typically added to stabilize the microstructure and to reduce susceptibility to intergranular corrosion. Although Mo was detected in the elemental distribution maps, it could not be quantified by the EDAX sensor due to the similar spectral of Nb.

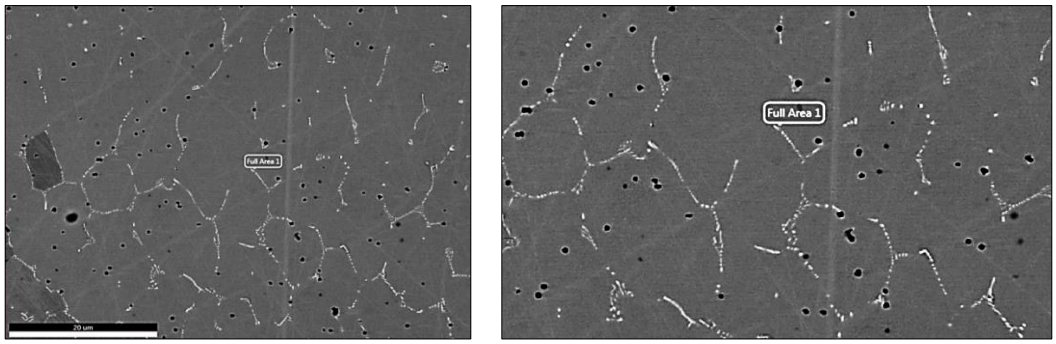

Fig. 4.57. Microstructure of the multi-element alloy obtained by deposition welding and combined remelting (sample 1C)

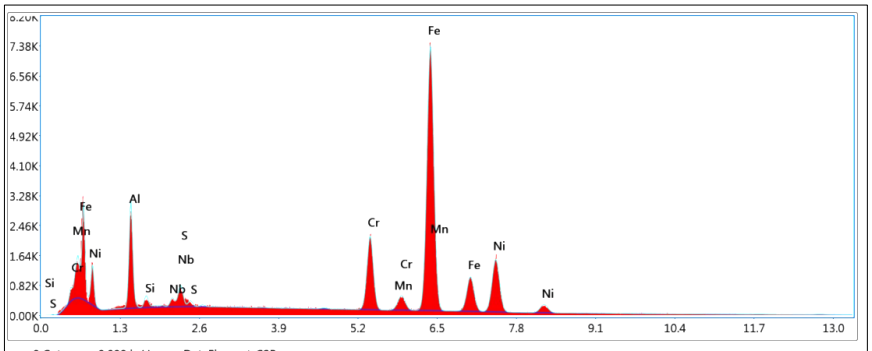

Smart Quant Results

Element	Weight %	Atomic %	Net Int.	Error %	Kratio	Z	A	F
AlK	8.35	15.69	240.58	8.15	0.0349	1.1231	0.3712	1.0016
SiK	0.75	1.36	27.75	12.93	0.0040	1.1494	0.4613	1.0028
NbL	1.11	0.60	22.48	20.24	0.0078	0.8910	0.7866	1.0010
S K	1.22	1.94	50.66	6.61	0.0095	1.1287	0.6836	1.0070
CrK	11.04	10.77	286.03	2.88	0.1173	0.9858	0.9849	1.0940
MnK	1.21	1.12	27.09	13.99	0.0125	0.9662	0.9897	1.0808
FeK	58.97	53.55	1111.13	2.07	0.5796	0.9828	0.9775	1.0230
NiK	17.34	14.98	238.31	3.47	0.1601	0.9956	0.9216	1.0064

Fig. 4.58. Results of spectral analysis in the multi-element alloy obtained by deposition welding and combined remelting (sample 1C)

4.3.3.4. Microscopic and chemical analysis of the multi-element alloy obtained by deposition welding without remelting (sample 1D)

Figure 4.72 provides an image from the central area of the 1D sample within the layer deposited by TIG welding, indicating the region selected for the chemical element analysis. The chemical analysis of this region, labeled Full Area 1 (Figure 4.73), reveals that the concentration of alloying elements in the multi-element alloy align with the ranges observed in the analyses of samples 1T, 1L, and 1C. Notably, there is a slight decrease in the Fe concentration from 59wt%

(observed in the remelted samples) to 54wt% in the non-remelted sample. This decrease may be attributed to a slight increase in the contribution of the base metal during the remelting process of the deposited layers.

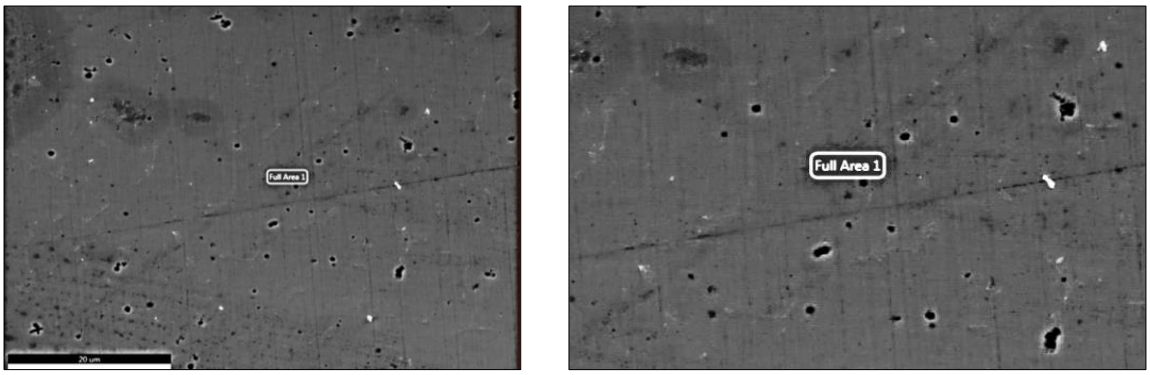

Fig. 4.72. Microstructure in the central area of the layer deposited by TIG welding without remelting (sample 1D)

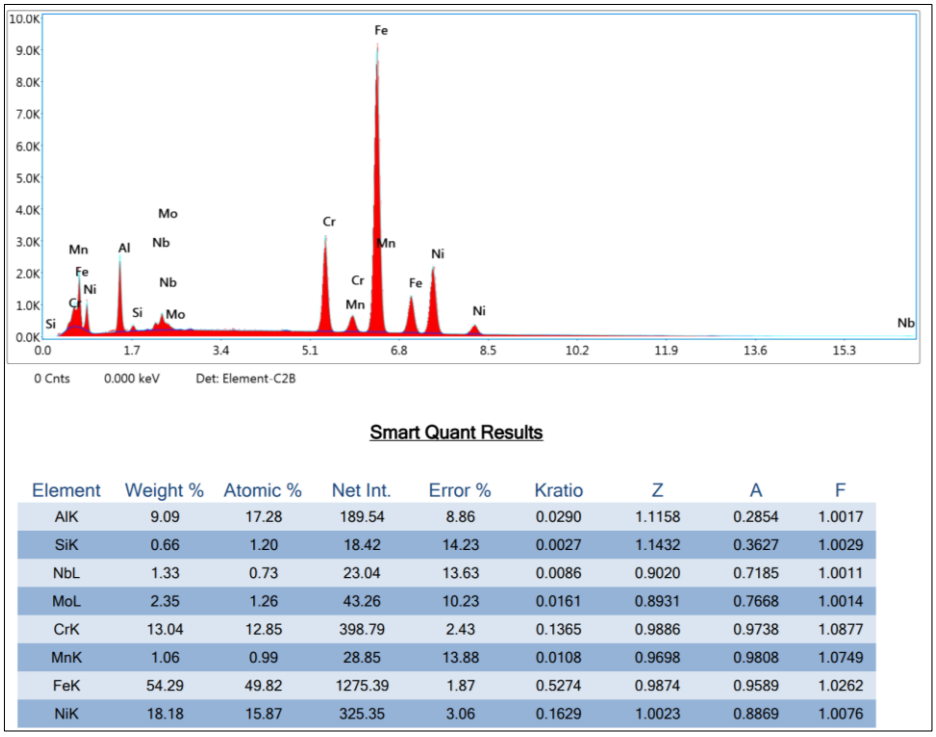

Smart Quant Results

Element	Weight %	Atomic %	Net Int.	Error %	Kratio	Z	A	F
AlK	9.09	17.28	189.54	8.86	0.0290	1.1158	0.2854	1.0017
SiK	0.66	1.20	18.42	14.23	0.0027	1.1432	0.3627	1.0029
NbL	1.33	0.73	23.04	13.63	0.0086	0.9020	0.7185	1.0011
MoL	2.35	1.26	43.26	10.23	0.0161	0.8931	0.7668	1.0014
CrK	13.04	12.85	398.79	2.43	0.1365	0.9886	0.9738	1.0877
MnK	1.06	0.99	28.85	13.88	0.0108	0.9698	0.9808	1.0749
FeK	54.29	49.82	1275.39	1.87	0.5274	0.9874	0.9589	1.0262
NiK	18.18	15.87	325.35	3.06	0.1629	1.0023	0.8869	1.0076

Fig. 4.73. Results of spectral analysis in the layer deposited by TIG welding without remelting (sample 1D)

4.3.3.5. Dilution of the multi-element alloy with the S235 steel substrate material

The chemical analyses of the multi-element alloys deposited using by four technological variants on samples 1L, 1T, 1C, and 1D indicate an increase in the Fe concentration from 26wt% (the estimated Fe percentage for the alloy derived from the bundle of rods) to 59wt%, and a decrease in the concentrations of the other elements: Ni from 31wt% to 18wt%, Cr from 19wt% to 12wt%, Al from 14wt% to 7wt%, Mo from 5wt% to 2wt%, and Nb from 1.6wt% to 1wt% (Table

4.9). These variations in concentration are attributed to the participation of the S235 steel substrate to the formation of the molten pool, the participation coefficient being around 45%.

This participation percentage of the base material to the the weld and to the final composition of the AlCr0.7FeNiMo0.1 alloy layer is in line with the findings reported by other researchers who have studied disimilar material clading by TIG welding process [85,91,92]. It can be concluded that the use of rod of AlCr0.7FeNiMo0.1 multi-element alloy developed for TIG deposition welding would lead to a result comparable to that obtained by melting and depositing a bundle of rods with different chemical compositions. Conclusively, the inovative process for producing AlCrFeNi depositions by welding, developed through this doctoral research, offers the advantage of enabling clading by TIG welding process, without the need of developing prior rods through other fabrication methods.

Table 4.9. Dilution of AlCr0.7FeNiMo0.1 alloy with S235 steel substrate material

Material	C wt[%]	Mn wt[%]	Si wt[%]	Cr wt[%]	Fe wt[%]	Ni wt[%]	Mo wt[%]	Nb wt[%]	Al wt[%]	Co wt[%]	Cu wt[%]	Ti wt[%]
S235 steel	0.12	0.75	0.17	0.04	98.22	0.03	0.02	-	0.038	-	0.06	0.001
AlCr0.7FeNiMo0.1	0.008	0.641	0.254	19.3	26.7	31.51	5.155	1.592	14.631	0.004	0.046	0.082
Sample 1L	**-**	**-**	**-**	**13.15**	**59.09**	**17.94**	**1.85**	**0.9**	**7.07**	**-**	**-**	**-**
Sample 1T	**-**	**-**	**-**	**12.53**	**60.56**	**17.8**	**-**	**0.8**	**6.68**	**-**	**-**	**-**
Sample 1C	**-**	**-**	**-**	**11.04**	**58.97**	**17.34**	**-**	**1.1**	**8.35**	**-**	**-**	**-**
Sample 1D	**-**	**-**	**-**	**13.04**	**54.29**	**18.18**	**2.35**	**1.33**	**9.09**	**-**	**-**	**-**

4.2.4. Determination of the hardness profile in the multi-element alloy

A significant increase in hardness, approximately 3.5 times, was observed, the average value rising from 165 HV0.5 in the base material to 570 $HV_{0.5}$ in the deposited layers. The lowest average hardness was measured in the layer without remelting (558 $HV_{0.5}$), while the highest value was obtained in the layer which was subsequently subjected to combined remelting, showing an approximate 5% increase in comparison with the non-remelted sample. Similar hardness values, ranging between 500 and 600 HV, have also been reported by other researchers who have investigated alloys that belong to the AlCrFeNi system [93,94].

Table 4.13. Results of hardness testing in the substrate material and multi-element alloy layers

Material	Hardness $HV_{0,5}$	Average Hardness	Standard deviation	Coefficient of variation
S235 Steel	158; 166; 163; 170; 168	164.82	4.83	2.93
Sample 1D	539; 542; 573; 564; 574	558.42	16.62	2.98
Sample 1T	571; 560; 571; 554; 578	566.77	9.69	1.71
Sample 1L	581; 573; 567; 565; 588	574.77	9.78	1.7
Depunere 1C	570; 599; 564; 598; 563	578.88	18.29	3.16

4.2.5. Determination of the wear resistance of the multi-element alloy

The results of the wear testing are presented in Tables 4.15-4.18:

- for the deposition without subsequent remelting, an average wear coefficient of k=6.95·10^{-7}[mm^3/Nm] was recorded (Table 4.15);
- the deposition with subsequent longitudinal remelting (Table 4.16) exhibited improved wear resistance, the average wear coefficient being 5.17·10^{-7}[mm^3/Nm];
- the deposition with subsequent transverse remelting (Table 4.17) showed increased wear resistance, the average wear coefficient being 4.18·10^{-7}[mm^3/Nm];
- the multi-element alloy produced by deposition welding with combined remelting (Table 4.18) exhibited the highest wear resistance, around 2.7 times greater than the alloy non-remelted, the average wear coefficient being 2.59·10^{-7}[mm^3/Nm].

The wear resistance testing demonstrated superior performance of the multi-element alloys that was subjected to subsequent remelting. This technological process can be associated with heat treatment, which enhances the surface quality, influencing positively the properties such as grain refinement, pore remove, defects mitigation, good chemical homogeneity, and lower internal stresses in the deposited multi-element alloy [95–98].

Table 4.15. Results of the wear testing in the multi-element alloy deposited layers (sample 1D)

No. crt.	Friction length [mm]	Load force F_N [N]	Wear coefficient k [mm^3/Nm]	Volume of wear material V [mm^3]	Wear intensity	Depth wear layer [mm]
1	214956.28	0.19	2.5412E-07	0.010378672	7.50316E-08	0.016128504
2	214956.28	0.202	1.13583E-06	0.018544912	1.00296E-07	0.021559346
Average	**214956.3**	**0.196**	**6.95E-07**	**0.014462**	**8.77E-08**	**0.018844**

Table 4.16. Results of the wear testing in the multi-element alloy layers (sample 1L)

No. crt.	Friction length [mm]	Load force F_N [N]	Wear coefficient k [mm^3/Nm]	Volume of wear material V [mm^3]	Wear intensity	Depth wear layer [mm]
1	214956.28	0.183	6.60189E-07	0.025969864	1.18688E-07	0.025512795
2	214956.28	0.207	3.73504E-07	0.016619431	9.4947E-08	0.020409449
Average	**214956.3**	**0.195**	**5.17E-07**	**0.021295**	**1.07E-07**	**0.022961**

Table 4.17. Results of the wear testing in the multi-element alloy layers (sample 1T)

No. crt.	Friction length [mm]	Load force F_N [N]	Wear coefficient k [mm^3/Nm]	Volume of wear material V [mm^3]	Wear intensity	Depth wear layer [mm]
1	214956.28	0.22	5.49157E-07	0.025969864	1.18688E-07	0.025512795
2	214956.28	0.278	2.85919E-07	0.017085913	9.62703E-08	0.020693898
Average	**214956.3**	**0.249**	**4.18E-07**	**0.021528**	**1.07E-07**	**0.023103**

Table 4.18. Results of the wear testing in the multi-element alloy layers (sample 1C)

No. crt.	Friction length [mm]	Load force F_N [N]	Wear coefficient k [mm^3/Nm]	Volume of used material V [mm^3]	Wear intensity	Depth worn layer [mm]
1	214956.28	0.193	1.51905E-07	0.006302023	5.84673E-08	0.012567913
2	214956.28	0.165	3.66275E-07	0.012990948	8.39447E-08	0.018044449
Average	**214956.3**	**0.179**	**2.59E-07**	**0.009646**	**7.12E-08**	**0.015306**

The comparative analysis of the wear resistance results in case of traditional alloys layers, reported by the researchers worldwide [99–105], indicates that the data achieved in this doctoral research are comparable or even higher to the existing alternatives. Furthermore, the deposition welding technology, applied for melting the bundle of aluminum, stainless steel, and nickel-chromium rods, with the aim to obtain the AlCr0.7FeNiMo0.1 alloy, offers significant advantages. These advantages refer to the low cost of equipment (TIG welding) and the chemical composition, which does not contain rare metals and needs a reduced Ni-Cr superalloy percentage. The good wear resistance of the AlCr0.7FeNiMo0.1 deposited alloy can be attributed to the presence of aluminum in the alloy's chemical composition, that contributes to the hardening and to increased strength of multi-element alloys, as it was found in the scientific literature.

4.2.6. Determination of the corrosion resistance of the multi-element alloy

In the experimental part, focused on determining and analyzing the corrosion resistance of the multi-element alloy produced by deposition welding, all samples, with and without subsequent remelting of the deposited layers, the electrochemical measurements were conducted in accordance with the ASTM G 102-89:2010 standard [106]. The linear polarization testing was employed to identify the direct relationship between the applied polarization and the current response at the corrosion potential (E_{corr}). The potential range varied from -0.25V to 1V relative to E_{corr}, with a sweep rate set at 1.66 mV/s. The current passing through the electrode was continuously monitored during the experiments. Additionally, the electrochemical impedance spectroscopy (EIS) testing was performed by recording simple sine waves across a frequency range from 0.1 to 105 Hz, in accordance with ISO 16773-1-4:2016 [107]. The analysis of the resulted spectra facilitated the establishment of a correlation between the chemical and physical characteristics of the developed alloys and the evolution of the electrochemical process [108].

Figure 4.99 presents the open circuit potential (OCP) diagrams for all samples (1C, 1D, 1T, 1L), which had multi-element alloy layers deposited under various technological conditions. These samples were immersed in 3.5% NaCl solution for 24 hours. The OCP diagrams illustrate the material tendency to corrosion phenomenon. A shift in potential (E) toward more positive values indicates the formation of a passive film, suggesting an enhanced corrosion resistance.For the 1D sample, which was deposited without subsequent remelting, the potential abruptly shifted from -0.2 mV to -0.5 mV, indicating the material inability to form a protective passive layer. Conversely, for the 1C sample, the potential moved from -0.3 mV to -0.1 mV, with a noticeable increase after approximately 4 hours, reflecting favorable behavior against the corrosion process. The 1T sample reached a steady state after about 5 hours, with the potential increasing after 10 hours due to passive film formation. For the sample1L, the potential decreased from -0.1 mV to -0.2 mV with minor fluctuations, showing a tendency towards positive values after 24 hours.

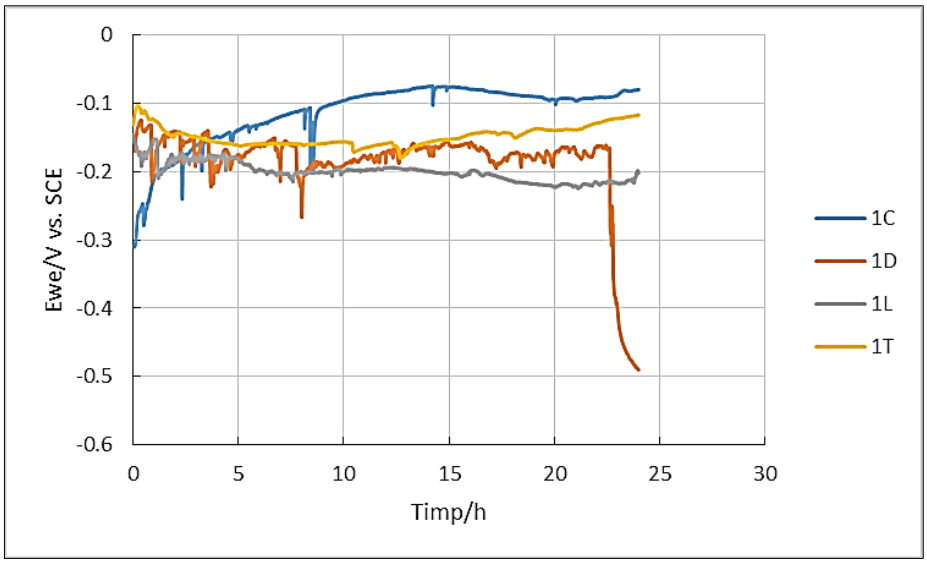

Fig. 4.99. OCP diagrams plotted for the multi-element alloy achieved by deposition welding, with or without subsequent remelting (3.5% NaCl solution, imsersion time 24 h)

The configuration of the polarization curve offers valuable information on the electrochemical behavior of the alloy. Figure 4.100 presents the polarization curves for the samples with multi-element alloy deposited layers. These curves are plotted based on the Stern and Geary equation, reflecting that the difference between the applied potential and the open circuit potential is correlated with the logarithm of the current measured during the electrochemical reaction [109].

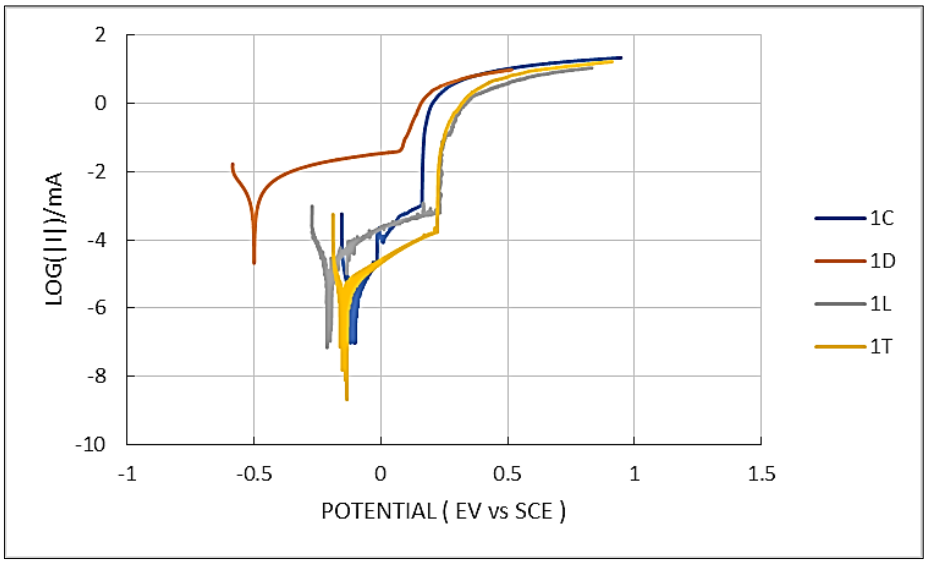

Fig. 4.100. Linear polarization curves of the samples 1C, 1D, 1L, 1T achieved by different technological variants

The anodic and cathodic Tafel slopes (*βa* and *βc*) for all samples were determined by the analysis of potentiodynamic curves. These curves were generated using the EC-Lab® v-9.55 software over a ±250 mV range relative to the open circuit potential (OCP). The corrosion testing results are summarized in Table 4.19. The parameters have been defined as follows: *βa* is the

anodic Tafel slope, *βc* represents the cathodic Tafel slope, E_{corr} the corrosion potential, I_{corr} indicates the corrosion current density, and V_{corr} refers to the corrosion rate.

When the calculated anodic slope *βa* exceeds significantly the cathodic slope *βc*, as it is noticed for the samples 1T, 1L, and 1C, it suggests that the material exhibits a tendency toward passivation. This phenomenon is characterized by the formation of protective surface layer that mitigates or inhibits the corrosion process. Conversely, if this condition is not met, as it is case of the sample 1D, the material is considered more susceptible to the corrosion phenomenon [110].

Tabel 4.19. Electrochemical corrosion testing results for the samples 1D, 1T, 1L, 1C

Sample	β_a [mV/dec]	β_c [mV/dec]	E_{corr} [mV]	I_{corr} [μA/cm^2]	V_{corr} [mm/year]
1D	109.6	86.5	-499.764	1.096	0.0213
1T	66.1	29.4	-148.176	0.001	0.019 E-03
1L	103.6	58.2	-203.802	0.012	0.234 E-03
1C	66.2	33.7	-110.468	0.002	0.039 E-03

A comparative analysis of the corrosion testing results of the AlCr0.7FeNiMo0.1 deposited layers with the findings reported in the literature by other researchers who studied various materials under similar conditions [111–114] highlights the advantages of the innovative procedure developed in the doctoral program.

Briefly, the results presented and discussed in this work indicate that the multi-element alloy AlCr0.7FeNiMo0.1, deposited without subsequent remelting, exhibits higher corrosion resistance compared to carbon steels. Furthermore, the multi-element layers deposited by welding, followed by subsequent remelting, demonstrated enhanced corrosion resistance comparing to stainless steels.

4.2.7. Industrial applications

The analysis and interpretation of the results regarding the properties of the layers deposited by TIG welding revealed that the multi-element alloy, AlCr0.7FeNiMo0.1 layers, subjected or not to subsequent remelting, exhibits a hardness of 550-600 $HV_{0.5}$. Additionally, the corrosion resistance of the deposited and remelted layers exceeds the resitence to corrosion of of stainless steels, and the wear resistance is comparable or even superior to certain materials which are currently employed in industrial applications designed to enhance the wear resistance of various metalic components. Therefore, the AlCr0.7FeNiMo0.1 multi-element alloy is characterized by both high corrosion resistance and wear resistance, making it highly suitable for applications in industrial sectors where components must perform well under demanding operating conditions in corrosive and/or abrasive environments. Such applications include:

- *Machine Building Industry:* Components of production equipment (molds, dies)
- *Chemical Industry:* Equipment for chemical processing (tanks, containers, parts for handling chemical substances);
- *Energy Production Industry:* Turbine blades;
- *Oil and Gas Industry:* Valves, pumps, and drilling tools
- *Naval Industry:* Naval propellers, offshore structures, metal components exposed to the marine environment;
- *Mining Industry:* Components of mining machinery and equipment;
- *Pulp and Paper Industry:* Components for manufacturing systems, blades, rollers.

4.3. Conclusions

The investigation and characterization of multi-element layers deposited by welding, followed or not by subsequent remelting, have revealed significant and valuable information in terms of development of materials with outstanding properties, such as high or medium entropy alloys. The following information is the key conclusions regarding the properties of these alloys:

- The medium entropy alloy AlCr0.7FeNiMo0.1 can be produced using an original and innovative procedure, which involves melting a bundle of rods - comprising three rods with a diameter of 2.4 mm and distinct chemical compositions (Al ALTIG AL99.7, stainless steel INTERROD 22 9 3, and nickel-chromium alloy NIROD 625) - by TIG welding process.
- To prevent the crack formation during the solidification of the AlCr0.7FeNiMo0.1 multi-element alloy, the inter-pass temperature must be maintained at 300°C, as it was experimentally determined.
- The metallurgical compatibility between the S235 steel substrate and the AlCr0.7FeNiMo0.1 multi-element alloy is approproiate, demonstrated by the absence of defects at the alloy-substrate interface and confirmed through the macroscopic analysis.
- The spectral analysis has demonstrated that the chemical elements of the AlCr0.7FeNiMo0.1 multi-element alloy are uniformly distributed within the deposited layer on the substrate material.
- Compounds rich in Nb and Mo were observed at the grain boundaries of the multi-element alloy deposited layers, having a positive impact on the mechanical strength, hardness, and corrosion resistance of the alloys.
- The remelting process determines higher participation of the substrate material to weld formation and, implicitly, a greater influence on the final chemical composition of the deposited layer, also demonstrated by the increase in the concentration of Fe from 54wt% to 59wt%.
- The participation of the base material to the chemical composition of the deposited metal is approximately 45%, a value that is in line with the findings reported by other researchers who studied the cladding by TIG welding process;
- The average micro-hardness of the multi-element alloys, achieved by all technologies, is 570 $HV_{0.5}$. The lowest hardness value was recorded for the alloy without subsequent remelting (558 $HV_{0.5}$), while the highest, with approximate increase of 5%, was observed in the alloy subjected to combined remelting. This increase in hardness can be attributed to the homogenization phenomenon and grain refinement, resulting from both longitudinal and transverse remelting.
- Tribological studies revealed that the multi-element alloy exhibited the lowest wear resistance in the absence of subsequent remelting (sample 1D), and the highest wear resistance (2.7 times greater than that of sample 1D) was achieved in the alloy subjected to combined remelting (sample 1C).
- The wear resistance of the AlCr0.7FeNiMo0.1 deposited layers is comparable or either superior to that of the traditional materials used in the wear resistant coatings.
- Subsequent remelting by TIG welding, without addition of filler material, enhances the corrosion resistance of the multi-element alloy deposited layers.
- The corrosion testing indicated that the corrosion resistance of the layer deposited without remelting, immersed in a 3.5% NaCl solution, is superior comparing to the unalloyed and low-alloy carbon steels, while the deposited and remelted alloys exhibit corrosion resistance superior to that of stainless steels.

- The wear and corrosion tests conducted on the AlCr0.7FeNiMo0.1 multi-element alloy layers demonstrated that these alloys have superior resistance to wear and to corrosion in comparision to the stainless steels.
- Studies on hardness, wear resistance, and corrosion resistance have demonstrated the critical importance of remelting the deposited layers, highlighting the positive impact on these properties. Therefore, the remelting process should be considered a key factor when deposition welding technologies are designed to achieve multi-element alloys.
- The innovative process developed for producing the AlCr0.7FeNiMo0.1 multi-element alloy is not only technically viable, but also economically advantageous, due to the low cost of the TIG welding equipment and the lack of expensive metals, such as cobalt,.

CHAPTER 5

Modeling and simulation of TIG deposition welding process of AlCr0.7FeNiMo0.1 medium-entropy multi-element alloy

5.2. Modelling and simulation of the TIG deposition welding process of the multi-element alloy AlCr0.7FeNiMo0.1

To analyze the temperature distribution and stress levels, a numerical model was developed in order to simulate the TIG deposition welding process of the AlCr0.7FeNiMo0.1 multi-element alloy on S235 steel substrate. The process parameters used as input data for the numerical model were identical with those used in the experimental program. The model simulated the deposition of the five weld beads on S235 steel sheet with dimensions of 100x40x12mm. Each of the four samples – deposition without remelting (1D), deposition with longitudinal remelting (1L), deposition with transverse remelting (1T), and deposition with combined remelting (1C) - was subjected to assessment of the thermal (temperature distribution) and mechanical (equivalent stresses, displacements) modifications.

The mesh of the geometric model comprises 129,488 nodes and 83,460 tetrahedral elements. This configuration enables precise simulation of the effects of the welding process, providing valuable information for evaluating the thermomechanical behavior of the investigated materials. The application of precise and well-calibrated model enhances the accuracy of simulation and analysis of the deposition and remelting processes, thereby contributing significantly to the advancement of knowledge in the development of materials with special properties and their performance under industrial conditions.

5.2.1. Multi-element alloy deposition by TIG welding without subsequent remelting

The model developed to simulate the TIG deposition welding process, without subsequent remelting, is depicted in Figure 5.2. This model includes a graphical representation of the geometry of the S235 steel plate and the weld beads deposited using the AlCr0.7FeNiMo0.1 multi-element alloy. The process parameters, which were used as input data for the simulation, are consistent with those employed in the experimental program. Additional input data include the dimensions of the heat source, detailed in Table 5.2, which define the geometry of the heat source, determine the amount of heat conducted into the base material, and play a crucial role in the thermal, mechanical, and metallurgical changes experienced by the materials during the welding process under the influence of the electric arc. The heat source is considered a volumetric semi-ellipsoid source, according to the Goldak model. The configuration of the heat source is illustrated in Figure 5.3, where c_f represents the front length, c_r the rear length, a the width, and b the depth of the source. The dimensions of the heat welding source are presented in Table 5.2.

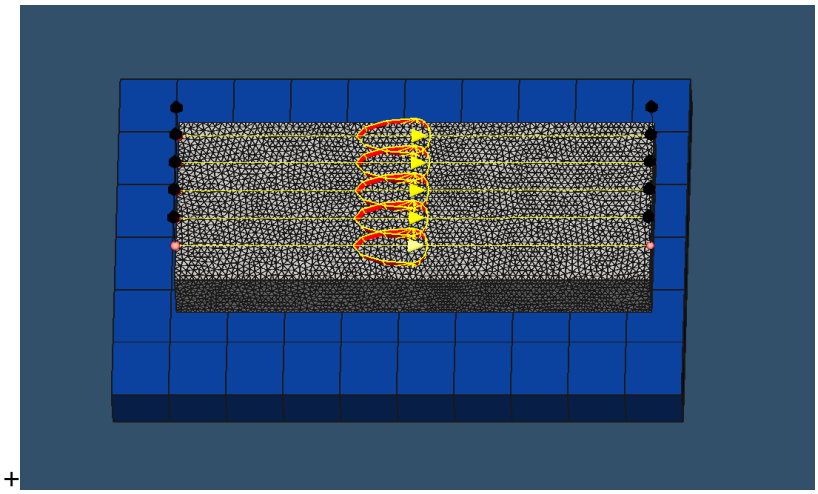

Fig. 5.2. The geometric model developed for simulating the TIG deposition welding process without subsequent remelting of multi-element alloy layers

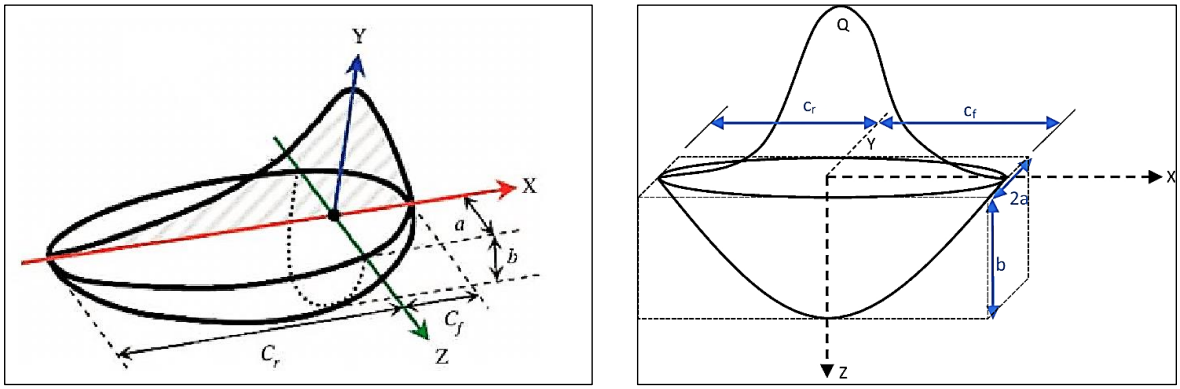

Fig. 5.3. The heat source model used to simulate the TIG deposition welding process of multi-element alloys [115,116]

Tabel 5.2. Dimensions of the heat source used to simulate the TIG deposition welding process without subsequent remelting

Process	Dimensions of the heat source			
	c_f [mm]	c_r [mm]	a [mm]	b [mm]
Deposition	3.12	12.5	4.45	9.27

5.2.1.1. Temperature distribution predicted by simulation of TIG deposition welding without subsequent remelting

Figure 5.4 illustrates the temperature distribution resulting from the conduction heat transfer during the TIG deposition welding process of the multi-element alloy layers. The maximum temperature within the molten metal pool is observed to range between 1700 and 1800°C, which aligns with values reported in other scientific articles focused on welding simulation. Accurate prediction and analysis of the temperature distribution are crucial, as the heating and cooling cycles induce expansion and contraction within the metalic structure. These thermal fluctuations can lead to the development of residual stresses, which may subsequently cause deformations, displacements, or even cracking of the welded joints.

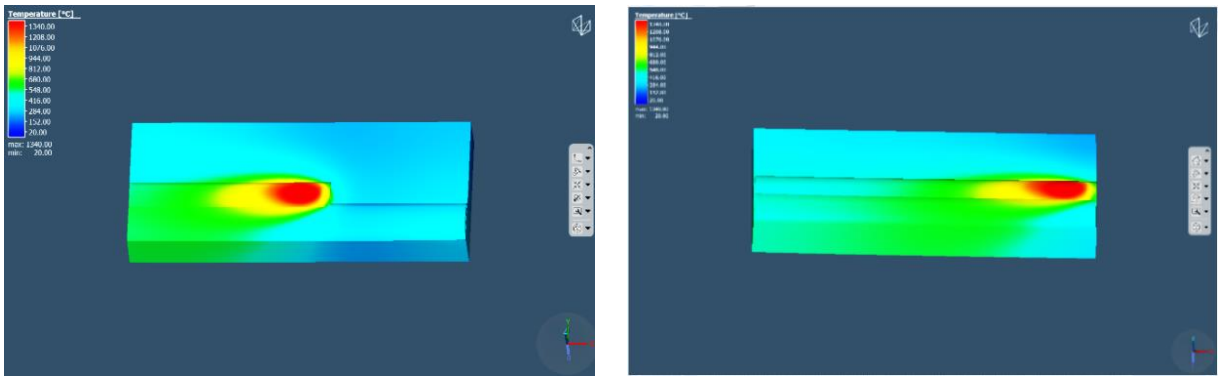

Fig. 5.4. Temperature distribution predicted by simulation of TIG deposition welding of multi-element alloy without subsequent remelting

5.2.1.2. Stress field distribution predicted by simulation of TIG deposition welding without subsequent remelting

The analysis of the distribution of equivalent Von Mises stresses and the prediction of the maximum values offer critical insights on the mechanical performance of welded structures and, on the other hand, can be a useful tool for assessing their structural integrity. Figure 5.5 depicts the distribution of the Von Mises equivalent stress field generated during the TIG deposition welding of multi-element alloy beads. Numerical results indicate that the maximum stress levels reach approximately 700MPa in the multi-element alloy and 350MPa in the S235 steel plate. These values are significantly lower than the tensile strength of both materials, suggesting adequate mechanical performance and good behaviour under operational conditions.

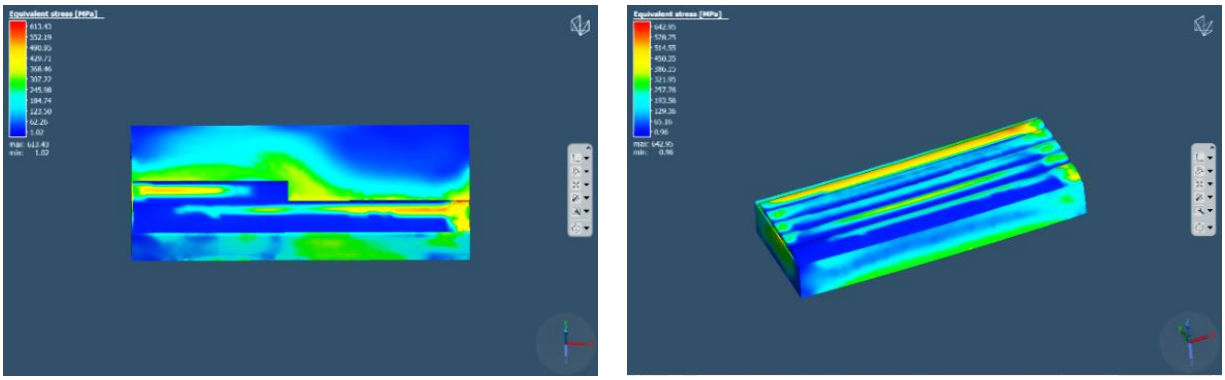

Fig. 5.5. Von Mises equivalent stress field predicted by simulation of TIG deposition welding of multi-element alloy without subsequent remelting

5.2.2. Multi-element alloy deposition by TIG welding with longitudinal remelting

The model developed for simulating the TIG deposition welding process of the multi-element alloy layers, followed by longitudinal remelting, is illustrated in Figure 5.11. The parameters of the deposition welding and remelting processes are identical to those applied in the experimental part. The dimensions of the heat source, introduced as input data in the numerical model, are determined by the process parameters values, as shown in Table 5.4.

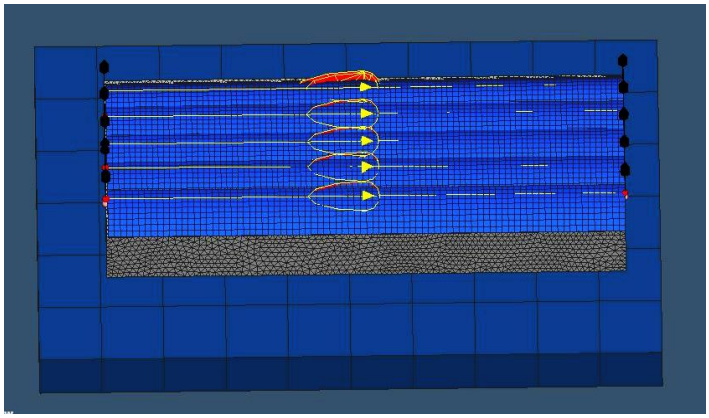

Fig. 5.11. The geometric model developed for simulating the TIG deposition welding process with subsequent longitudinal remelting of multi-element alloy layers

Tabel 5.4. Dimensions of the heat source used to simulate the TIG deposition welding process with subsequent longitudinal remelting

Process	Dimensions of the heat source			
	c_f [mm]	c_r [mm]	a [mm]	b [mm]
Deposition	2.74	10.95	3.67	7.65
Longitudinal remelting	2.77	11.09	3.74	7.8

5.2.2.1. Temperature distribution predicted by simulation of TIG deposition welding with subsequent longitudinal remelting

From the analysis of the temperature distribution (Fig. 5.12), generated during the deposition welding and remelting processes of the multi-element alloys layers, it was found that the maximum temperature recorded in the molten metal pool reaches values between 1650 and 1800°C. Although the heat input applied during remelting is lower than that applied in the deposition welding phase, a continuous increase in the temperature of the steel substrate was noticed. This phenomenon can be explained by the cumulation of the thermal effects, generated in the two processes, being determined by the introduction, through the subsequent remelting process, of additional amount of heat in the sample.

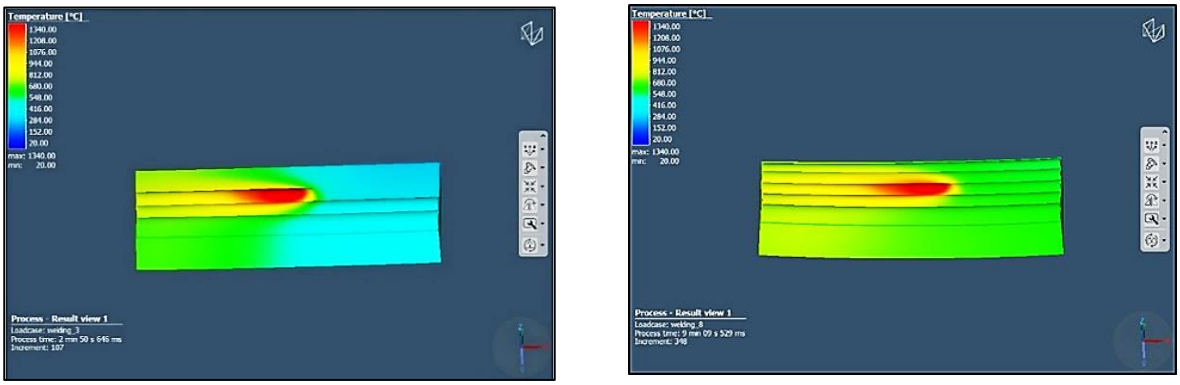

Fig. 5.12. Temperature distribution predicted by simulation of TIG deposition welding of multi-element alloy with subsequent longitudinal remelting

5.2.2.2. Stress field distribution predicted by simulation of TIG deposition welding with subsequent longitudinal remelting

The distribution of the Von Mises equivalent stress field, generated during the deposition welding and subsequent longitudinal remelting of the five multi-element alloy beads, is depicted in Figure 5.13. The maximum stress values observed in the multi-element alloy reach 700MPa during the deposition welding phase and increase up to 900MPa during the remelting phase. This increase in stress, compared to the deposition welding without subsequent remelting, is attributed to the prolonged exposure to high temperatures and the uneven heating of the substrate material. This uneven heat distribution, generated during the deposition welding and remelting processes, results in stress concentration in specific regions of the plate, thereby the maximum stress level increasing within the entire metalic structure.

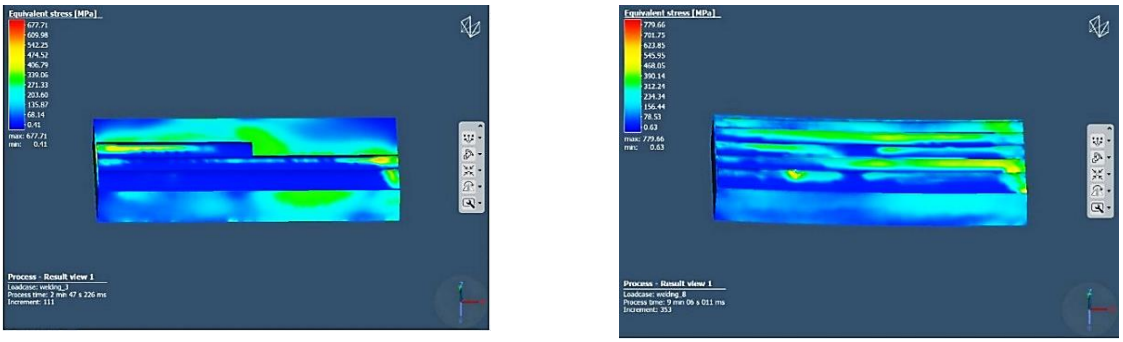

Fig. 5.13. Von Mises equivalent stress field predicted by simulation of TIG deposition welding of multi-element alloy with subsequent longitudinal remelting

5.2.3. Multi-element alloy deposition by TIG welding with transverse remelting

Figure 5.18 presents the geometric model developed to simulate the deposition welding process of the multi-element alloy, followed by subsequently remelting on the transverse direction. This model simulates five weld-deposited beads along with 16 transverse remelting paths. The process parameters for both deposition welding and remelting, introduced as input data in the numerical model, are identical with those employed in the experimental program.

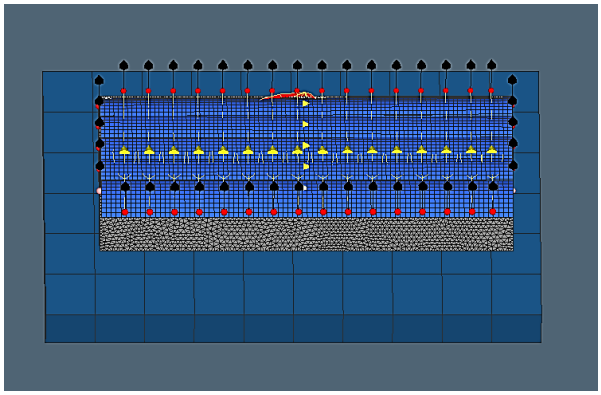

Fig. 5.18. The geometric model developed for simulating the TIG deposition welding process with subsequent transverse remelting of multi-element alloy layers

The dimensions of the heat source, determined experimentally, are summarized in Table 5.6. The modelling of simulation conditions is crucial for generating relevant and realistic output data. Proper modeling of the heat source and the spatial heat distribution significantly influences the accuracy of the simulation process and, consequently, the reliability of the numerical results obtained. These results must be critically analyzed because the decisions regarding the optimal welding technologies are based on the outcomes achieved.

Tabel 5.6. Dimensions of the heat source used to simulate the TIG deposition welding process with subsequent transverse remelting

Process	Dimensions of the heat source			
	c_f [mm]	c_r [mm]	a [mm]	b [mm]
Deposition	3.06	12.25	4.32	9.01
Transverse remelting	2.27	9.07	2.73	5.7

5.2.3.1. Temperature distribution predicted by simulation of TIG deposition welding with subsequent transverse remelting

The analysis of the temperature distribution (Fig. 5.19), obtained from the simulation of the deposition welding process of the five weld beads, followed by their transverse remelting along 16 paths, revealed that the maximum temperature in the molten metal pool reaches 1600-1700 °C. This temperature is slightly lower than in the previous technology version, due to the reduced heat input applied during deposition welding (around 30%) and remelting (approximately 50%). Similarly to the simulation of longitudinal remelting, an increase in the temperature is observed during the second phase of the manufacturing process. This increase is attributed to the cumulative thermal effects generated by both the deposition welding and remelting processes.

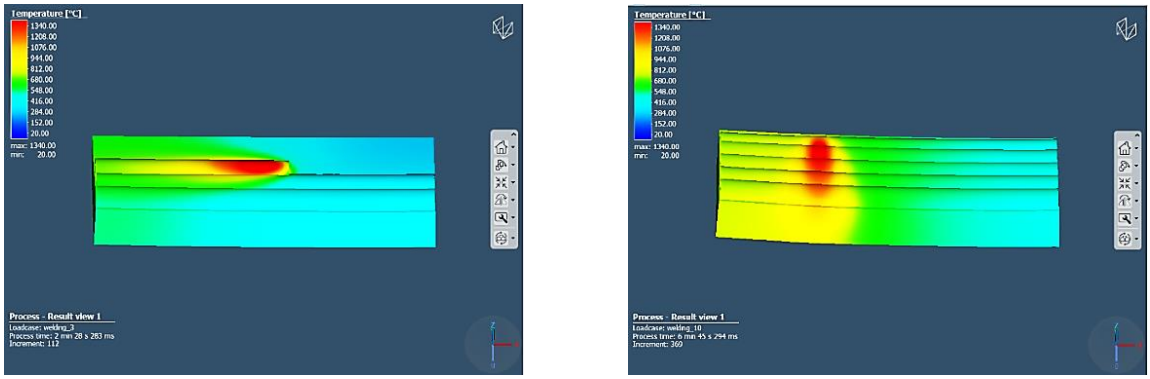

Fig. 5.19. Temperature distribution predicted by simulation of TIG deposition welding of multi-element alloy with subsequent transverse remelting

5.2.3.2. Stress field distribution predicted by simulation of TIG deposition welding with subsequent transverse remelting

Figure 5.20 illustrates the distribution of the Von Mises equivalent stress field developed during the deposition and transverse remelting processes. The results reinforce the significant impact of primary welding parameters on the thermo-mechanical changes observed in the base material. A slight reduction in the Von Mises stress level is noticed compared to the previous technological variant, attributed to the lower heat input values used during welding. In the multi-

element alloy, maximum stress values reach up to 650MPa during deposition and 700MPa during transverse remelting. The experimental tests of multi-element alloy deposition welding and transverse remelting, revealed a more pronounced non-uniform heating of the steel plate, compared to the longitudinal remelting process - a phenomenon corroborated by the simulation results. Although this uneven heating might suggest higher stress levels, the primary welding parameters play a crucial role, significantly influencing the thermo-mechanical effects generated in the base material. Consequently, welding with approximately 30-50% lower heat input led to 25% Von Mises equivalent stresses lower.

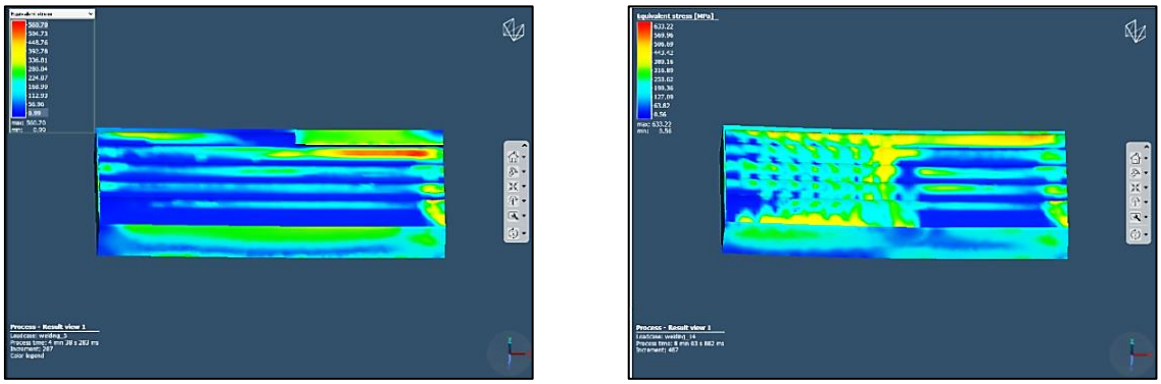

Fig. 5.20. Von Mises equivalent stress field predicted by simulation of TIG deposition welding of multi-element alloy with subsequent transverse remelting

5.2.4. Multi-element alloy deposition by TIG welding with combined remelting

Figure 5.25 illustrates the model developed for simulating the deposition process of the multi-element alloy by TIG welding, incorporating combined remelting without filler material. This model includes the simulation of the five deposited multi-element alloy beads, along with 16 transverse remelting paths, followed by 5 longitudinal remelting paths. The process parameters for deposition and combined remelting used in this simulation are consistent with those applied in the experimental program. The dimensions of the heat sources, which were introduced as input data in the finite element model, are detailed in Table 5.8.

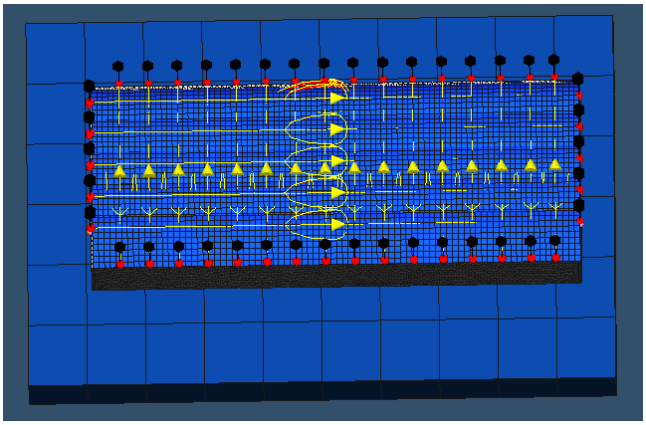

Fig. 5.25. The geometric model developed for simulating the TIG deposition welding process with subsequent combined remelting of multi-element alloy layers

Tabel 5.8. Dimensions of the heat source used to simulate the TIG deposition welding process with subsequent combined remelting

Proces	Dimensions of the heat source			
	c_f [mm]	c_r [mm]	a [mm]	b [mm]
Deposition	3.27	13.07	4.74	9.87
Transverse remelting	2.32	9.26	2.83	5.9
Longitudinal remelting	2.57	10.3	3.35	6.98

5.2.4.1. Temperature distribution predicted by simulation of TIG deposition welding with subsequent combined remelting

Figure 5.26 presents the temperature distribution from the simulation of the deposition of the five multi-element alloy beads, followed by combined remelting phase. The maximum temperature in the molten metal pool reaches values between 1700°C and 1800°C, which is closely aligned with the temperatures observed in other technologies variants involving transverse or longitudinal remelting.

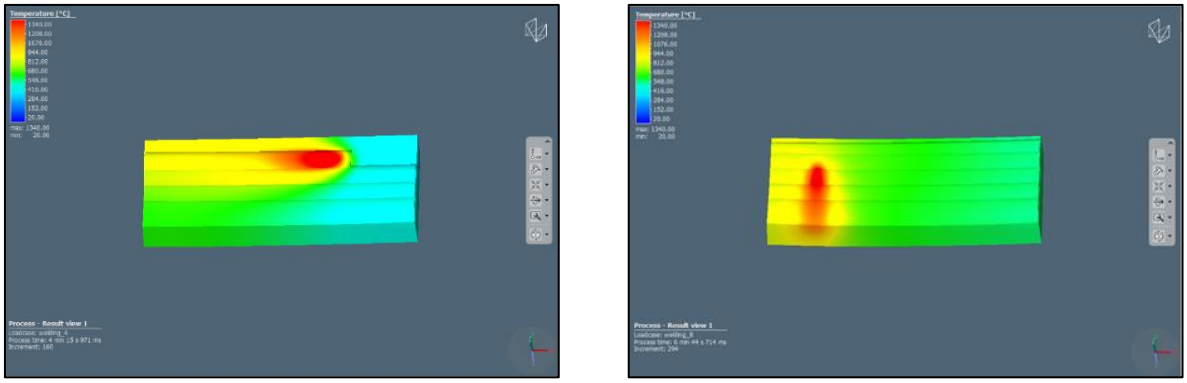

Fig. 5.26. Temperature distribution predicted by simulation of TIG deposition welding of multi-element alloy with subsequent combined remelting

5.2.4.2. Stress field distribution predicted by simulation of TIG deposition welding with subsequent combined remelting

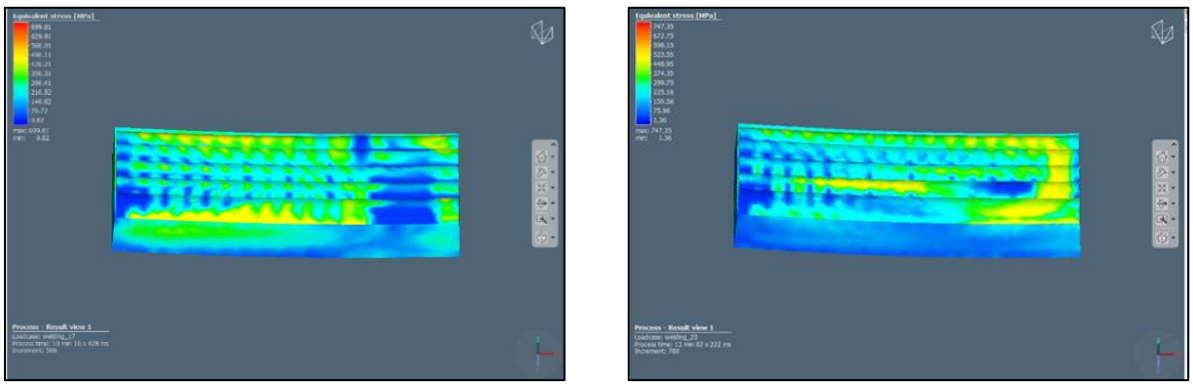

Fig. 5.27. Von Mises equivalent stress field predicted by simulation of TIG deposition welding of multi-element alloy with subsequent combined remelting

Figure 5.27 illustrates the distribution of the Von Mises equivalent stress field generated during the deposition and combined remelting process. Notably, the equivalent stresses achieved during this process were the highest recorded among all the investigated variants, reaching up to 930MPa in the deposited alloy, due to the increased amount of heat introduced in the materials.

5.3. Conclusions

Based on the results analysis and discussion regarding the simulation of the TIG deposition welding process of the multi-element alloy AlCr0.7FeNiMo0.1, both with and without subsequent remelting, the following important conclusions can be drawn:

- The maximum temperature achieved in the molten metal pool ranges between 1650 and 1800°C, aligning with values reported in the literature for fusion welding of ferrous alloys.
- During TIG deposition welding of the multi-element alloy without subsequent remelting, the maximum stress values are 700MPa in the alloy and 300-350MPa in the S235 steel plate.
- In case of deposition welding of the multi-element alloy, followed by longitudinal remelting, the maximum equivalent Von Mises stresses reach 700MPa during the deposition phase and increase to 900MPa during the remelting phase.
- The results from the simulation of the alloy deposition process, followed by transverse remelting, highlight the significant influence of the heat input on stress level. Specifically, a lower heat input causes reduced Von Mises equivalent stress values in the multi-element alloy, predicting 650MPa during deposition welding and up to 700MPa during remelting.
- Prolonged exposure to high temperatures, as observed in the deposition followed by combined remelting (both transverse and longitudinal), lead to the highest equivalent Von Mises stresses, reaching up to 930MPa.

CHAPTER 6

Experimental validation of numerical model developed for simulation of TIG deposition welding of AlCr0,7FeNiMo0,1 medium entropy multi-element alloy

6.1. Experimental program for numerical model validation

6.1.1. Designing and making the stand for the measurement of temperature values and stress level

Due to the potential deterioration of the thermocouples and strain gauges during the TIG deposition welding and remelting of multi-element alloys on S235 steel substrate plates measuring 100x40x12 mm, a special experimental setup was developed to accurately determine the thermo-mechanical changes (thermal cycles and stresses) determined by the welding process. A monolithic support plate with extended arms to minimize the influence of the electric arc on the stress distribution and to facilitate the positioning of strain gauges was designed.

Figure 6.5 illustrates the experimental stand, designed and made in the CC SUDAV, that was employed to measure temperature and stress during the multi-element alloy deposition by TIG welding. The stand was equipped with data acquisition devices, including the QantumX and Lutron BMT 4208SD, as well as four strain gauges and six thermocouples. These instruments were used to collect the experimental data, which were subsequently processed, analyzed, and compared with the numerical simulation results.

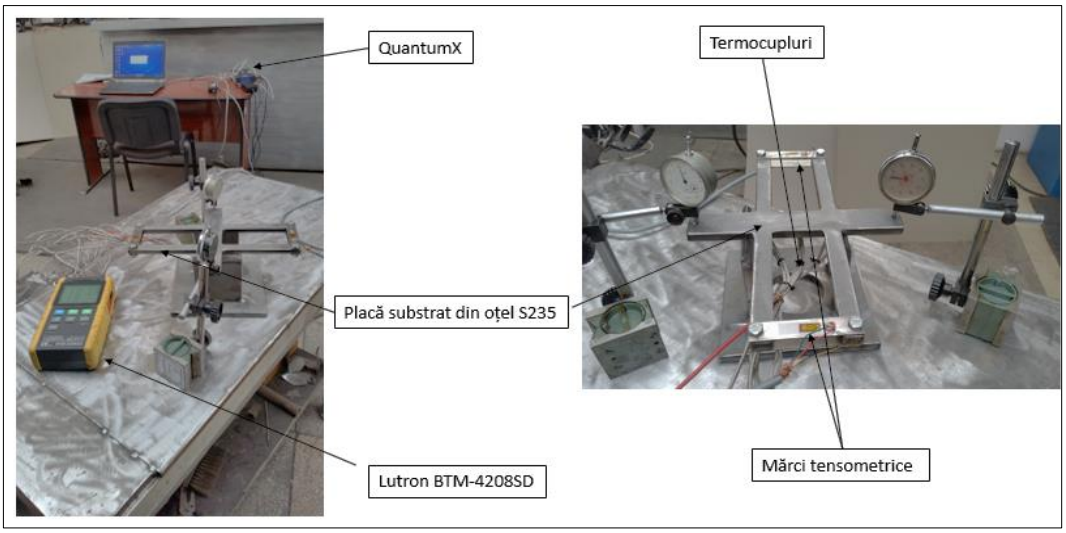

Fig. 6.5. Stand for measuring the temperature values and stress level developed during the TIG deposition welding process

6.1.2. Characterization of the materials used in the experimental program

Weld beads of multi-element alloy AlCr0.7FeNiMo0.1 were deposited by TIG welding process on 12 mm thick S235 steel plate. The chemical composition and mechanical properties of the base material and the deposited multi-element alloy are presented in Tables 6.1 and 6.2 and the process parameters are shown in Table 5.3. To mitigate the risk of cracking, the temperature between successive passes was maintained at 300°C, similarly to the conditions used in the experimental part.

Table 6.1. Chemical compositions of S235 steel and deposited AlCr0.7FeNiMo0.1 alloy

Material	C [%]	Mn [%]	Si [%]	Cr [%]	Fe [%]	Ni [%]	Mo [%]	Nb [%]	Al [%]	Co [%]	Cu [%]	Ti [%]
S235	0.12	0.75	0.17	0.04	98.22	0.03	0,02	-	0.038	-	0.06	0.001
AlCr0.7FeNiMo0.1	0.01	0.64	0.25	19.3	26.7	31.5	5.16	1.59	14.63	0.01	0.05	0.08

Table 6.2. Mechanical characteristics of S235 steel and deposited AlCr0.7FeNiMo0.1alloy

Material	Ultimate tensile strength σ_r [MPa]	Elongation [%]	Vikers hardness [HV]
S235	440-450	32	155-190
AlCr0.7FeNiMo0.1	1400-2100	0-40	500-800

6.1.3. TIG deposition welding process parameters

The welding current is the primary parameter set on the control panel of the SAF-RO DIGIWAVE III 420 welding source. The parameter value was 220A, identical with the value set in the experimental program, designed for the characterization of deposits made with the multi-element alloy AlCr0.7FeNiMo0.1. The welding parameters, either recorded or computed, for each deposited bead, are shown in Table 6.3.

Table 6.3. Parameters of the TIG deposition welding process of AlCr0.7FeNiMo0.1 medium-entropy multi-element alloy

Deposited bead	I_s [A]	U_a [V]	v_s [cm/min]	Heat input [kJ/cm]
1	220	21	25	6.7
2	220	21	26	6.4
3	220	22	26	6.7
4	220	22	23	7.6
5	220	21	27	6.2

6.2. Finite element modeling of the temperature field and stress level

6.2.1. Development and discretization of the geometric model

The geometric model was designed and developed using the MSC APEX software, while the deposition process by TIG welding was simulated with the Simufact Welding program. For simulating the deposition of the multi-element alloy onto the surface of the S235 steel plate, a semi-ellipsoidal heat source was assumed for all five weld beads. The geometric model, including the finite element mesh, is illustrated in Figure 6.6.

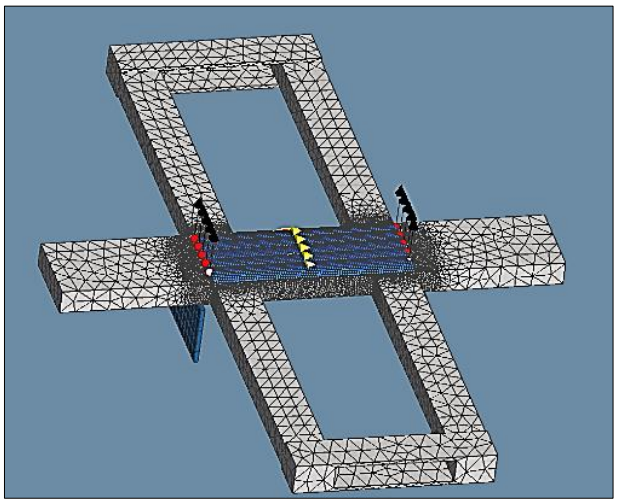

Fig. 6.6. Geometric model developed for simulation of TIG deposition welding process of multi-element alloy

To accurately simulate the deposition process by TIG welding and minimize the potential errors that may occure in the numerical model, the geometry and dimensions of the sheet, used as substrate for depositing the medium-entropy multi-element alloy AlCr0.7FeNiMo0.1, have been maintained identical to those employed in the experimental program.

6.2.2. Finite element analysis of the temperature distribution

Figure 6.7 shows the temperature distribution, developed during the deposition process by TIG welding, for each of the five deposited layers. Also, it can be observed the geometry of the molten metal pool, in liquid state, whose temperature exceeds the melting point of the deposited multi-element alloy.

Based on the analysis of numerical results achieved from the thermal analysis, it was found that the maximum temperature reached in the welding pool is in the range of 1650...1750°C, values that match the numerical results in terms of simulation of the welding process of ferrous alloys, which have been reported in numerous articles published in journals with high impact in the scientific world.

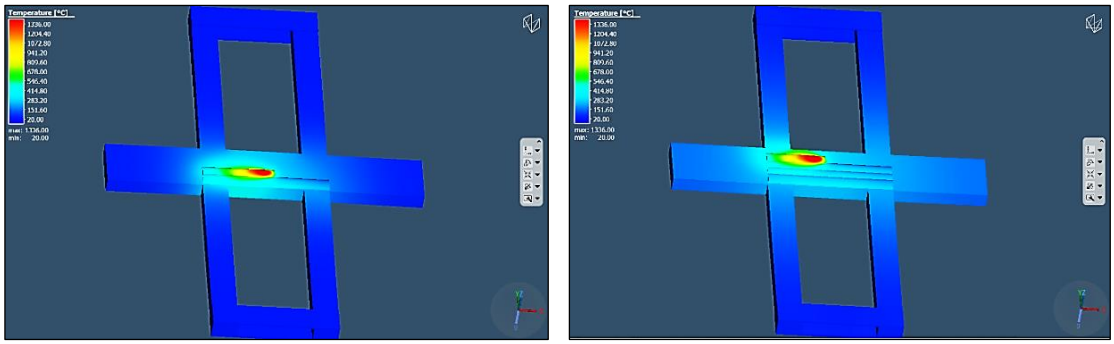

Fig. 6.7. Temperature distribution predicted by simulation of TIG deposition welding of multi-element alloys layers (the interpass temperature between two successive depositions is 300°C)

6.2.3. Finite element analysis of the Von Mises equivalent stress level

The distribution of the Von Mises equivalent stress field developed during the TIG deposition welding process for each of the five weld beads is depicted in Figure 6.9. The maximum stress values recorded in the multi-element alloy AlCr0.7FeNiMo0.1 (witch has a tensile strength range of 1400 to 2100 MPa.) reach up to 700 MPa. The maximum stress values within the S235 steel substrate, which has a tensile strength of 440-450 MPa, are limited to 350 MPa.

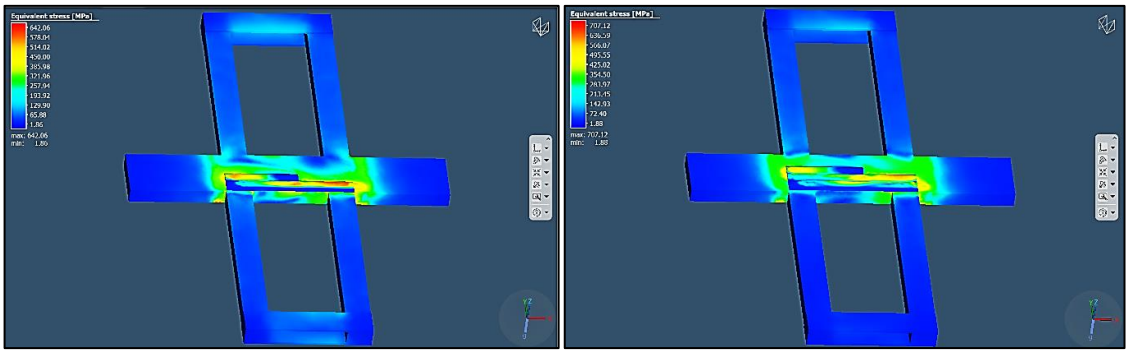

Fig. 6.9. Von Mises equivalent stress field predicted by simulation of TIG deposition welding of multi-element alloys layers

A notable variation in stress values is observed, being strongly influenced by the stage of the welding process. Specifically, when a new weld bead is deposited, a decrease in the stress level within the previously deposited beads is noticed. This decrease can be attributed to the effects induced by the successive depositions, the process being similar to a heat treatment.

6.3. Validation of the numerical model. Calculus of errors

To validate the numerical model developed for finite element analysis of the heat transfer and stress level developed during the TIG deposition welding process, both numerical results obtained by the finite element method and experimental results acquired through thermocouples and strain gauges methods were graphically processed and comparatively analysed. The experimental stress data were gathered from the strain gauge measurements, whose position was similarly located as in the experimental setup described in the previous chapters. Due to

interference from the electric current, data from four out of six thermocouples (1, 3, 4, and 6) were successfully collected and processed. Figures 6.10 and 6.11 present the experimental (red chart) and numerical (blue chart) variations in temperature and stress levels.

The thermal cycles, depicted in Figure 5.12, illustrate the temperature variation in the reference points where the thermocouples were positioned. Each point recorded the temperature variation, corresponding to the heating and cooling cycles, developed during the deposition of the five weld beads. To calculate the errors associated with the developed numerical model, the equation (6.1) can be applied, providing an straightforward and rapid analytical calculation.

$$e = \frac{\sum_{i=1}^{n} \left| \frac{T_{exp_n} - T_{sim_n}}{T_{exp_n}} \cdot 100 \right|}{n} \tag{6.1}$$

where: T_{exp} represents the temperature measured by the experimental method; T_{sim} - temperature resulting from the finite element analysis; n – the reference time interval.

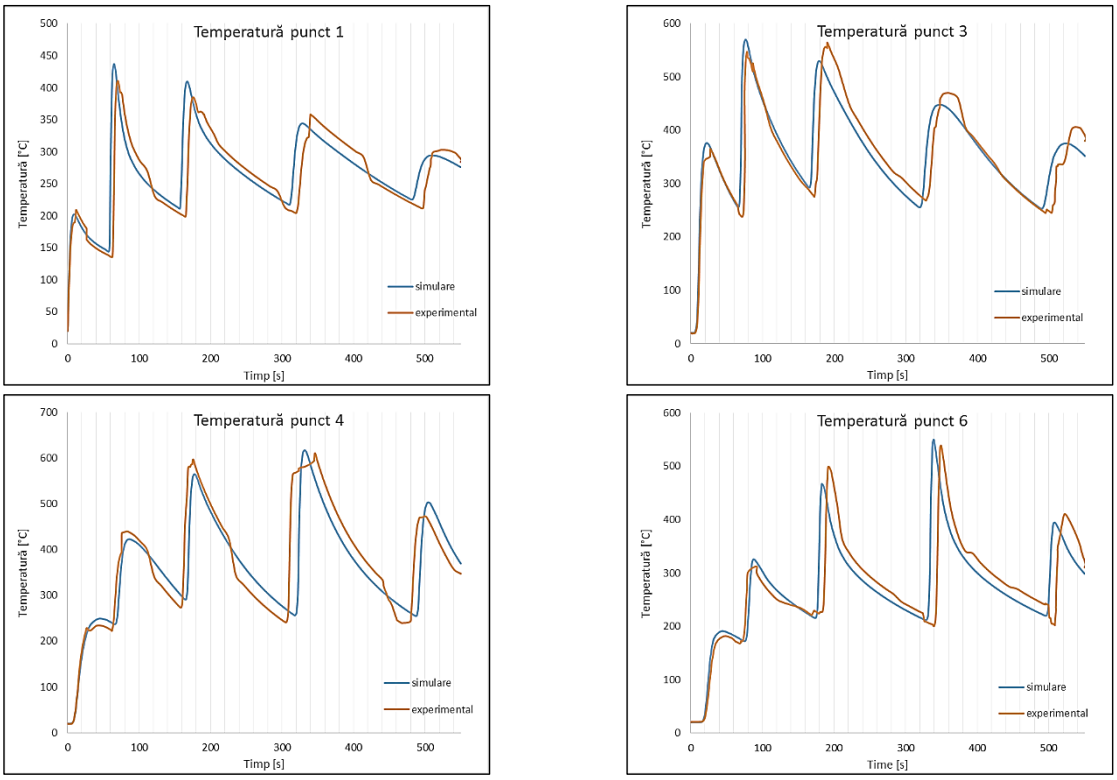

Fig. 5.12. Thermal cycles determined by FEM and experimentally by the thermocouples mesurement method

The reference points correspond to the locations where the thermocouples (1, 3, 4, 6) were positioned during the experimental program. The resulting errors were found to be within the range of 4.18% to 5.62% (4.53% in the spot 1, 4.72% in the spot 3, 5.62% in the spot 4, and 4.18% in the spot 6). These values are comparable to the findings of other researchers who have developed and experimentally validated numerical models for simulating various welding processes [117–120]. The graphs that describe the stress variation in the reference points, obtained both experimentally and numerical modeling, are presented in Figure 6.11. The strain gauges were mounted in mirrored pairs in the spots 1-2 and 3-4, the correlation between these

positions being evident in the charts from Figure 6.11. Specifically, when the stress is tensile stress in a certain spot, compressive stress is recorded in the corresponding mirrored spot.

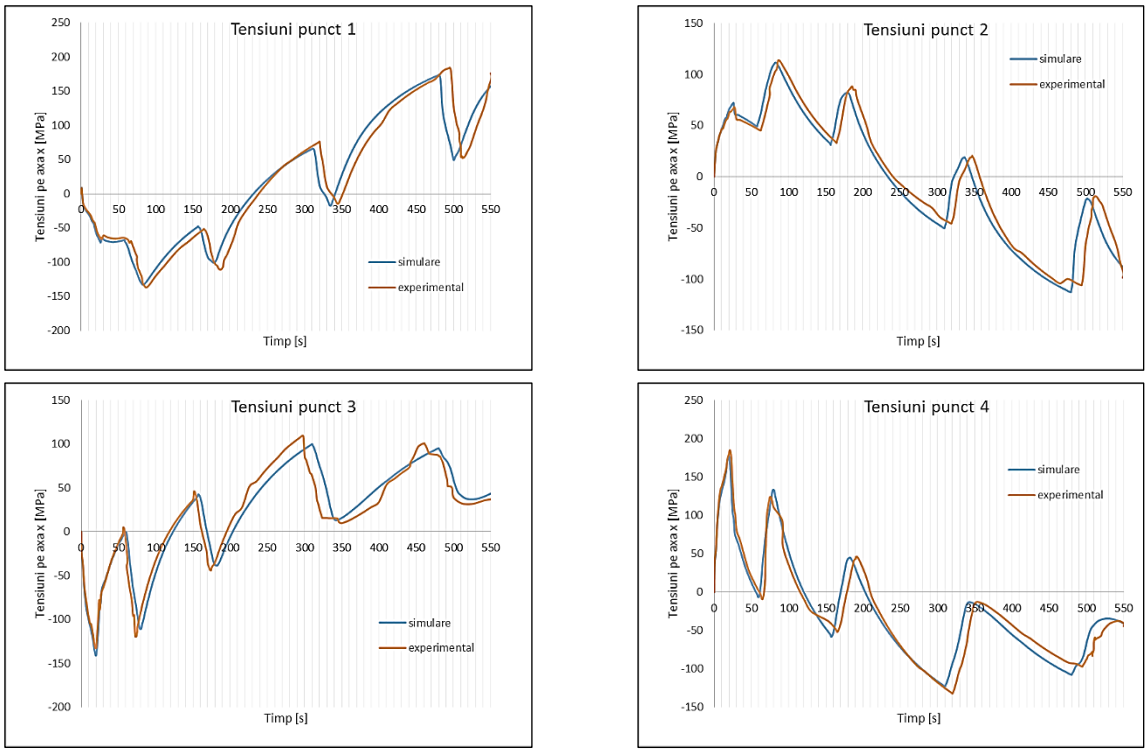

Fig. 6.11. Stress level vs. time determined by FEM and experimentally by the strain gauge mesurement method

6.4. Conclusions

Based on the results achieved by experimental testing and finite element analysis of the TIG deposition welding of the AlCr0.7FeNiMo0.1 medium-entropy alloy, the following important conclusions can be draw:

- The maximum temperature reached in the welding pool ranged from 1650°C to 1750°C, which are in line with the values reported in the literature for fusion welding of ferrous alloys.
- The model developed for simulation of the AlCr0.7FeNiMo0.1 alloy deposition on S235 steel substrate was experimentally validated by measuring the temperature with thermocouples and the stress level with strain gauges, using an original experimental stand designed and made in the *Centre for Advanced Research in Welding* (SUDAV).
- The comparative analysis of the experimental and numerical values of temperature and stress level revealed minor errors in the range of 4-6% which demonstrates the viability and accuracy of the numerical model that could be effectively applied to other materials and welding regimes.

CHAPTER 7

Final conclusions, personal contributions and future research directions

7.1. Final conclusions

7.1.1. Development of multi-element alloys

Over the past two decades, a novel category of alloys has emerged, capturing significant attention from researchers worldwide. These materials, named high-entropy alloys, consist of at least four or five chemical elements, distributed in equiatomic or near-equiatomic proportions, with no single element playing a dominant role. While the term "high entropy" is commonly used to describe these alloys, some scientists argue that the entropy is not the primary factor contributing to their unique properties. Consequently, alternative names such as multi-component alloys, multi-element alloys, or compositionally complex alloys have been proposed. Due to their distinctive properties and potential applications, high-entropy alloys have become a focal point in materials research, particularly regarding their behavior under operational conditions. The research on these new materials has concentrated on clarifying the mechanisms related to their structural and functional behavior and on optimizing their chemical composition with the aim to achieve enhanced performance that make them appropriate for various environmental conditions.

Improving the mechanical properties or achieving similar properties at reduced costs can offer significant advantages for integrating the multi-element alloys into industrial applications. However, despite the substantial progress in the research and development of these alloys, the technology transfer from the research laboratory to industrial applications remains a challenge. A possible explanation is related to the current manufacturing processes for these alloys that are not yet suitable for large-scale industrial implementation. Therefore, continuing the research focused on developing and optimizing new manufacturing technologies that would facilitate the efficient and economical production of these advanced materials is essential.

7.1.2. Original procedure for obtaining multi-element alloys by TIG welding

Based on the state-of-the-art in terms of multi-element alloys development, it was identified the need to continue the research, particularly in developing a novel process for manufacturing these alloys and facilitating the technology transfer from research to industry and expanding the applicability range, too. In the pursuit of this goal, an original and innovative method for AlCrFeNi multi-element alloys deposition by welding was developed in the framework of the doctoral research program. The selection of this alloy type was motivated by its remarkable mechanical properties, including hardness, resistance to wear and corrosion, which are critical for industrial applications where the quality of steel surfaces needs to be improved. The originality of the process for producing these multi-element alloys, developed during the doctoral program, has been recognized through the invention patent no. 135988/29.03.2024. This innovation has

been awarded with numerous medals, awards, and trophies at various invention exhibitions, including EUROINVENT (Iasi, 2023), UGAL INVENT (Galati, 2023), INVENTICA (Iasi, 2024), and other scientific events:

- The novel method for welding deposition of multi-element alloys on conventional steel substrate consists of melting a bundle of rods with distinct chemical compositions by TIG welding process in inert shielding gas (Ar) environment.
- This innovative approach enables the control of the chemical composition of multi-element alloys by selecting the appropriate rods, as well as their number and diameters.
- The resulting multi-element alloys incorporate also micro-alloying elements present in the rods, such as carbon (C), niobium (Nb), manganese (Mn), molybdenum (Mo), tantalum (Ta), tungsten (W) etc. As in the case of traditional alloys, The micro-alloying elements have an importnat role, in obtaining specific mechanical and chemical properties.
- For the AlCrFeNi alloys, produced through this patented process, aluminum rods, stainless steel, and Ni-Cr alloy were chosen to be melted by fusion welding in a common welding pool. By adjusting the number and the diameter of rods, the chemical composition of the multi-element alloy can be controlled, as well as the risk of cracking and improvement of properties such as resistance to wearand corrosion, plasticity.
- This innovative deposition method represents a cost-effective economic solution, facilitating the transition of technology from research laboratory to more industrial sectors. Employing a well-established welding process and standardized filler materials, this technique provides affordable and efficient solution for developing multi-element alloys and broadening the industrial applicability.

Based on this innovative concept and method applied for achieving depositions of multi-element alloys by welding, a comprehensive experimental program was conducted to optimize the process parameters. The key findings resulted from the experiments are described below:

- The AlCr0.7FeNiMo0.1 multi-element alloy can be successfully produced by melting a bundle of rods with a diameter of 2.4 mm. This bundle comprises one Al ALTIG AL99.7 rod, one INTERROD 22 9 3 stainless steel rod, and one Ni-Cr NIROD 625 alloy rod.
- The welding current, a critical parameter that has a strong influence on the penetration and geometry of the welding pool, was maintained constant at 220A value. This value was found to be optimal for all technology variants applied to obtain depositions of AlCr0.7FeNiMo0.1multi-element alloys.
- Preliminary results indicated that the cracking risk can be prevented by maintaining the interpass temperature of 300°C during the deposition of AlCr0.7FeNiMo0.1 alloy. This temperature was identified as optimal for minimizing the residual stress level and for reducing the cracking risk.

7.1.3. Characterization of AlCr0.7FeNiMo0.1 medium-entropy multi-element alloy deposited by TIG welding

Following the experimental determination of optimal welding parameters, a complex study of the properties of AlCr0.7FeNiMo0.1 medium entropy alloy, performed by four distinct technology variants – deposition welding without subsequent remelting (1D); deposition welding followed by longitudinal remelting (1L); deposition welding followed by transverse remelting (1T); and deposition welding followed by combined remelting (both transverse and longitudinal) – was developed and applied. These investigations provided critical insights into the field of advanced materials science that are summarized below:

- The macroscopic examination of samples made by four different deposition methods revealed the lack of defects, indicating that the optimal welding conditions have ensured metallurgical compatibility between the AlCr0.7FeNiMo0.1 multi-element alloy and the S235 steel substrate.
- Scanning Electron Microscopy (SEM) analysis of the multi-element alloy layers, deposited by TIG welding, with or without subsequent remelting, demonstrated a uniform distribution of the main chemical elements - Al, Fe, Ni, and Cr - across the deposited layers. This uniform distribution confirms the feasibility and high quality of the deposition welding process.
- The formation of niobium (Nb) and molybdenum (Mo)-rich compounds at the grain boundaries within the multi-element alloy enhances the tensile strength, hardness, and corrosion resistance, similarly to the effects observed in traditional alloys.
- The chemical composition of the multi-element alloy is influenced by the substrate material that participates with approximately 45% to the composition of layer, being in line with the results reported in other studies focused on TIG deposition welding of dissimilar materials.
- The remelting process significantly affects the final chemical composition of the multi-element alloy. Energy Dispersive Spectroscopy (EDS) analysis revealed an increase in iron (Fe) concentration from 54% to 59% in layers that were subsequently subjected to remelting by TIG welding without filler metal.
- The average hardness of the AlCr0.7FeNiMo0.1 medium-entropy multi-element alloy, deposited by four different technology variants, was 570 $HV_{0.5}$.
- The tribological testing of the AlCr0.7FeNiMo0.1 alloy indicated that it exhibits superior wear resistance compared to traditional material coatings. This exceptional tribological performance demonstrates the potential suitability of the alloy for a wide range of industrial applications.
- The lowest wear resistance was observed in the alloy deposited by welding without subsequent remelting. Conversely, the alloy subjected to deposition welding, followed by combined remelting, demonstrated the highest wear resistance, approximately 2.7 times greater than that of the non-remelted alloy.
- The corrosion testing of the AlCr0.7FeNiMo0.1 multi-element alloy, achieved by TIG welding, revealed a comparable or even higher corrosion resistance than of the stainless steels.
- The layers deposited by welding, followed by subsequent remelting on transverse direction (1T) and combined remelting (1C) showed the most favorable results in terms of corrosion resistance.
- The research on the AlCr0.7FeNiMo0.1 medium-entropy alloy, produced by this innovative method, highlights the outstanding performance of the alloy, as well as the economic benefits du to the low costs of the standard welding equipment and of the common filler metals. Besides, these filler materials include a minimal amount of Ni-Cr superalloy and exclude expensive elements such as cobalt (Co).

The investigation of the properties of the layers deposited by TIG welding revealed two great advantageous characteristics of the multi-element alloy AlCr0.7FeNiMo0.1: superior corrosion resistance relative to stainless steels and enhanced wear resistance in comparison to the coatings made with conventional materials in similar applications. From a sustainable and cost-effective perspective, the depositions produced with AlCr0.7FeNiMo0.1 medium-entropy alloy by this innovative patented process present a promising alternative for industrial applications in which the materials/surfaces with both high wear and corrosion resistance are demanded.

7.1.4. Modeling and simulation of the multi-element alloy deposition process, with or without remelting, and validation of the numerical model

The finite element analysis of the simulation of AlCr0.7FeNiMo0.1 medium-entropy multi-element alloy deposition by TIG welding has revealed significant findings, summarized as follows:

- The maximum temperature reached in the welding pool ranges from 1650 to 1800°C, being dependent on the welding technology applied. These values are in concordance with the results reported by other researchers whose studies focused on the simulation of ferrous alloys welding.
- For the welding variant without subsequent remelting, the maximum Von Mises equivalent stress reached approximately 700MPa in the multi-element alloy and between 300 and 350MPa in the S235 steel substrate. Given the tensile strength of these materials (1400-2100MPa for the alloy and 440-450MPa for the steel), it can be concluded that the multi-component structure obtained by this innovative method is adequate to perform well under operational conditions.
- In the scenario involving longitudinal remelting, the maximum Von Mises stress values reached 700MPa during deposition welding and 900MPa during remelting. Conversely, in the case of transverse remelting, applying lower heat input led to reduced equivalent Von Mises stress level (650MPa during deposition welding and up to 700MPa during the remelting phase). The highest Von Mises stress (930MPa), reached in the deposited material, was observed in the combined remelting variant, the explanation being the longest exposure to high-temperature.
- The model developed for simulation of the AlCr0.7FeNiMo0.1 alloy deposition on S235 steel substrate was experimentally validated by measuring the temperature with thermocouples and the stress level with strain gauges, using an original experimental stand designed and made in the Centre for Advanced Research in Welding (SUDAV).
- The comparative analysis of the experimental and numerical values of temperature and stress level revealed minor errors in the range of 4-6% which demonstrates the viability and accuracy of the numerical model that could be effectively applied to other materials and welding regimes.

7.2. Personal contributions

The results found by theoretical and experimental research can be considered significant contribution to the knowledge improvement in the development of advanced materials and welding process. This research is strongly characterized by interdisciplinary due to the integrated concepts and methods from industrial processes, materials science, heat transfer, and advanced mathematical data processing. Based on the complex and comprehensive research methodology, developed in the doctoral study program, significant and original contributions in terms of materials with special properties and methods to achieve them are briefly presented below:

- Based on detailed examination of 305 references, a complex and comprehensive review was conducted in order to assess the current state of research in terms of multi-element alloys development and fabrication methods. This analysis provided critical insights into the chemical and mechanical characterization of these materials, as well as the methods to achieve them, with the main objective of identifying new research directions, developing the research methodology, and defining the goals of the PhD thesis (Chap. 1, Chap. 2).

- Development of an original and economically viable procedure for performing depositions of AlCrFeNi multi-element alloys that was recently patented (invention patent no. 135988/29.03.2024). This novel process consists of melting and depositing on structural steel substrate a bundle of rods with distinct chemical compositions and diameters by TIG welding, with Ar inert shielding gas. The process allows the control of the alloy chemical composition by adjusting the rods configuration and type, taking into consideration the specific industrial requirements (wear resistance, corrosion resistance, oxidation resistance, and impact resistance (Chap. 3).
- New chemical composition recipes for performing medium-entropy multi-element alloys were developed, improving the knowledge level of these relatively unexplored alloys in the literature (Chap. 3, Subchap. 3.2).
- An analytical method for estimating the chemical composition of multi-element alloys produced by melting a bundle of rods with distinct chemical compositions and diameters was developed (Chap. 3, Subchap. 3.2.2).
- A comprehensive experimental program was developed to implement the original method for producing AlCrFeNi multi-element alloys by TIG welding. This program aimed to investigate the properties of these advanced materials and establish the foundation for technology transfer from research laboratory to several industrial sectors (Chap. 4).
- Four technologies for producing the AlCr0.7FeNiMo0.1 medium-entropy multi-element alloy by melting and depositing a bundle of three rods with distinct chemical compositions and identical diameters by TIG welding were designed and optimized to ensure high-quality multi-element alloy coatings (Chap. 4).
- Three technologies that include also the subsequent remelting process on transverse, longitudinal, and combined (transverse and longitudinal) directions were designed and optimized. The phase, applied to remelt the medium-entropy AlCr0.7FeNiMo0.1 alloy layers, was made by TIG welding without filler material and the aim was to ensure high-quality multi-element alloy coatings (Chap .4, Subchap. 4.1).
- Characterization of the AlCr0.7FeNiMo0.1 medium-entropy alloy layers, deposited by TIG welding, without subsequent remelting or followed by remelting on transverse, longitudinal, and combined directions, were investigated from chemical point of view. The study provided significant and valuable information in terms of diffusion of chemical elements, and identification of potential impurities and chemical heterogeneities (Chap 4, Subchap 4.2).
- Assessment of the wear resistance of the AlCr0.7FeNiMo0.1 medium-entropy alloy, produced by TIG deposition welding, with or witout subsequent remelting, aiming to evaluate the performance and to identify the industrial applications of the multi-component structures (AlCr0.7FeNiMo0.1 alloy layers deposited on S235 steel substrate) where the resistance to wear is a demand (Chap. 4, Subchap. 4.2).
- Assessment of the corrosion resistance of the AlCr0.7FeNiMo0.1 medium-entropy alloy, deposited using TIG welding, with or witout subsequent remelting, aiming to determine the performance and industrial applicability of these multi-component structures (S235 steel substrate cladded with AlCr0.7FeNiMo0.1 alloy) under corrosive conditions which are typical for the chemical industry and marine environment (Chap. 4, Subchap. 4.2).
- Development of an original finite element model useful to simulate the thermal and the mechanical effects associated with TIG deposition welding process, without or with subsequent remelting. This model allows the analysis of heat distribution, thermal cycles, equivalent Von Mises stress level, and displacements developed during the deposition of

AlCr0.7FeNiMo0.1 medium entropy alloys deposited by TIG welding on S235 steel substrate. (Chap. 5, Subchap. 5.3 and 5.4).

- Design and build an original experimental stand, including thermocouples and strain gauges, for measuring the temperature and the stress level in the multi-component structure made by AlCr0.7FeNiMo0.1 medium-entropy alloy and S235 steel substrate (Chap. 6, Subchap. 6.1.1).

7.3. Perspectives and future research directions

The research findings related to the application of the novel method to achieve depositions of AlCr0.7FeNiMo0.1 multi-element alloys by TIG welding, with or without subsequent remelting, as well as the assessment of the layers properties are promising and suggest new perspectives for advancement in the development of advanced materials and fabrication methods. Future research direction will focus on the following topics:

- Investigating the influence of the primary welding parameters on the participation coefficient of the substrate material in the formation of the welding pool, in order to more accurately estimate the chemical composition of the multi-element alloy, especially in the area of the fusion line.
- Investigation the influence of the rods positioning, in the bundle of rods and in relation to the electric arc, on the chemical homogeneity degree of the deposited alloy.
- Investigating the possibility of splice of rods bundle, using with wire with a similar or different chemical composition of the rods, and studying the influence on the chemical homogeneity and properties of the deposited multi-element alloy.
- Improving the analytical calculus method for estimating the chemical composition of the multi-element alloy, especially in the area of the fusion line, by introducing coefficients that take into consideration the chemical composition of the substrate material.
- Development of new multi-element alloy recipes, obtained by diversifying the rods, from the point of view of chemical composition, and by changing the number and diameters of the rods that are included in bundle of filler materials.
- Investigating the influence of heat treatment on the mechanical properties of multi-element alloy layers deposited by the original and innovative method presented in this work.
- Investigating the properties of the multi-component structure, performed by buttering method, in order to improve the metallurgically compatibility between the substrate material and the multi-element alloy.
- Investigating the reconfiguration of deposition welding and remelting paths, in order to significantly decrese the level of stress and strain developed in the multi-component structure by manufacturing process.

Selective references

[1] Krishna, S.A.; Noble, N.; Radhika, N.; Saleh, B. A Comprehensive Review on Advances in High Entropy Alloys: Fabrication and Surface Modification Methods, Properties, Applications, and Future Prospects. Journal of Manufacturing Processes 2024, 109, 583–606, doi:10.1016/j.jmapro.2023.12.039.

[2] Miracle, D.B. High Entropy Alloys as a Bold Step Forward in Alloy Development. Nat Commun 2019, 10, 1805, doi:10.1038/s41467-019-09700-1.

[3] Miracle, D.B.; Senkov, O.N. A Critical Review of High Entropy Alloys and Related Concepts. Acta Materialia 2017, 122, 448–511, doi:10.1016/j.actamat.2016.08.081.

[4] George, E.P.; Raabe, D.; Ritchie, R.O. High-Entropy Alloys. Nat Rev Mater 2019, 4, 515–534, doi:10.1038/s41578-019-0121-4.

[5] Ye, Y.F.; Wang, Q.; Lu, J.; Liu, C.T.; Yang, Y. High-Entropy Alloy: Challenges and Prospects. Materials Today 2016, 19, 349–362, doi:10.1016/j.mattod.2015.11.026.

[6] Gao, X.; Chen, R.; Liu, T.; Fang, H.; Qin, G.; Su, Y.; Guo, J. High-Entropy Alloys: A Review of Mechanical Properties and Deformation Mechanisms at Cryogenic Temperatures. J Mater Sci 2022, 57, 6573–6606, doi:10.1007/s10853-022-07066-2.

[7] Sharma, P.; Dwivedi, V.K.; Dwivedi, S.P. Development of High Entropy Alloys: A Review. Materials Today: Proceedings 2021, 43, 502–509, doi:10.1016/j.matpr.2020.12.023.

[8] Sarswat, P.; Smith, T.; Sarkar, S.; Murali, A.; Free, M. Design and Fabrication of New High Entropy Alloys for Evaluating Titanium Replacements in Additive Manufacturing. Materials 2020, 13, 3001, doi:10.3390/ma13133001.

[9] George, E.P.; Curtin, W.A.; Tasan, C.C. High Entropy Alloys: A Focused Review of Mechanical Properties and Deformation Mechanisms. Acta Materialia 2020, 188, 435–474, doi:10.1016/j.actamat.2019.12.015.

[10] Gopinath, V.M.; Arulvel, S. A Review on the Steels, Alloys/High Entropy Alloys, Composites and Coatings Used in High Temperature Wear Applications. Materials Today: Proceedings 2021, 43, 817–823, doi:10.1016/j.matpr.2020.06.495.

[11] King, D.J.M. Investigation of High-Entropy Alloys for Use in Advanced Nuclear Applications, University of Technology: Sydney, 2016.

[12] Zhang, Y.; Li, R. New Advances in High-Entropy Alloys. Entropy 2020, 22, 1158, doi:10.3390/e22101158.

[13] Menghani, J.; Vyas, A.; Patel, P.; Natu, H.; More, S. Wear, Erosion and Corrosion Behavior of Laser Cladded High Entropy Alloy Coatings – A Review. Materials Today: Proceedings 2021, 38, 2824–2829, doi:10.1016/j.matpr.2020.08.763.

[14] Scutelnicu, E.; Simion, G.; Rusu, C.C.; Gheonea, M.C.; Voiculescu, I.; Geanta, V. High Entropy Alloys Behaviour During Welding. Rev. Chim. 2001, 71, 219–233, doi:10.37358/RC.20.3.7991.

[15] Tsai, M.-H.; Yeh, J.-W. High-Entropy Alloys: A Critical Review. Materials Research Letters 2014, 2, 107–123, doi:10.1080/21663831.2014.912690.

[16] Li, W.; Xie, D.; Li, D.; Zhang, Y.; Gao, Y.; Liaw, P.K. Mechanical Behavior of High-Entropy Alloys. Progress in Materials Science 2021, 118, 100777, doi:10.1016/j.pmatsci.2021.100777.

[17] Liu, J.; Guo, X.; Lin, Q.; He, Z.; An, X.; Li, L.; Liaw, P.K.; Liao, X.; Yu, L.; Lin, J.; et al. Excellent Ductility and Serration Feature of Metastable CoCrFeNi High-Entropy Alloy at Extremely Low Temperatures. Sci. China Mater. 2019, 62, 853–863, doi:10.1007/s40843-018-9373-y.

[18] Zherebtsov, S.; Stepanov, N.; Ivanisenko, Y.; Shaysultanov, D.; Yurchenko, N.; Klimova, M.; Salishchev, G. Evolution of Microstructure and Mechanical Properties of a CoCrFeMnNi High-Entropy Alloy during High-Pressure Torsion at Room and Cryogenic Temperatures. Metals 2018, 8, 123, doi:10.3390/met8020123.

[19] Waseem, O.A.; Ryu, H.J. Combinatorial Development of the Low-Density High-Entropy Alloy Al10Cr20Mo20Nb20Ti20Zr10 Having Gigapascal Strength at 1000 °C. Journal of Alloys and Compounds 2020, 845, 155700, doi:10.1016/j.jallcom.2020.155700.

[20] Wang, W.-R.; Wang, W.-L.; Yeh, J.-W. Phases, Microstructure and Mechanical Properties of AlxCoCrFeNi High-Entropy Alloys at Elevated Temperatures. Journal of Alloys and Compounds 2014, 589, 143–152, doi:10.1016/j.jallcom.2013.11.084.

[21] Yeh, J. -W.; Chen, S. -K.; Lin, S. -J.; Gan, J. -Y.; Chin, T. -S.; Shun, T. -T.; Tsau, C. -H.; Chang, S. -Y. Nanostructured High-Entropy Alloys with Multiple Principal Elements: Novel Alloy Design Concepts and Outcomes. Adv Eng Mater 2004, 6, 299–303, doi:10.1002/adem.200300567.

[22] Cantor, B.; Chang, I.T.H.; Knight, P.; Vincent, A.J.B. Microstructural Development in Equiatomic Multicomponent Alloys. Materials Science and Engineering: A 2004, 375–377, 213–218, doi:10.1016/j.msea.2003.10.257.

[23] Senkov, O.N.; Senkova, S.V.; Woodward, C. Effect of Aluminum on the Microstructure and Properties of Two Refractory High-Entropy Alloys. Acta Materialia 2014, 68, 214–228, doi:10.1016/j.actamat.2014.01.029.

[24] Salishchev, G.A.; Tikhonovsky, M.A.; Shaysultanov, D.G.; Stepanov, N.D.; Kuznetsov, A.V.; Kolodiy, I.V.; Tortika, A.S.; Senkov, O.N. Effect of Mn and V on Structure and Mechanical Properties of High-Entropy Alloys Based on CoCrFeNi System. Journal of Alloys and Compounds 2014, 591, 11–21, doi:10.1016/j.jallcom.2013.12.210.

[25] Ng, C.; Guo, S.; Luan, J.; Wang, Q.; Lu, J.; Shi, S.; Liu, C.T. Phase Stability and Tensile Properties of Co-Free Al0.5CrCuFeNi2 High-Entropy Alloys. Journal of Alloys and Compounds 2014, 584, 530–537, doi:10.1016/j.jallcom.2013.09.105.

[26] Jiang, L.; Lu, Y.; Dong, Y.; Wang, T.; Cao, Z.; Li, T. Annealing Effects on the Microstructure and Properties of Bulk High-Entropy CoCrFeNiTi0.5 Alloy Casting Ingot. Intermetallics 2014, 44, 37–43, doi:10.1016/j.intermet.2013.08.016.

[27] Ji, W.; Fu, Z.; Wang, W.; Wang, H.; Zhang, J.; Wang, Y.; Zhang, F. Mechanical Alloying Synthesis and Spark Plasma Sintering Consolidation of CoCrFeNiAl High-Entropy Alloy. Journal of Alloys and Compounds 2014, 589, 61–66, doi:10.1016/j.jallcom.2013.11.146.

[28] Wang, Y.P.; Li, B.S.; Ren, M.X.; Yang, C.; Fu, H.Z. Microstructure and Compressive Properties of AlCrFeCoNi High Entropy Alloy. Materials Science and Engineering: A 2008, 491, 154–158, doi:10.1016/j.msea.2008.01.064.

[29] Jiang, Z.J.; He, J.Y.; Wang, H.Y.; Zhang, H.S.; Lu, Z.P.; Dai, L.H. Shock Compression Response of High Entropy Alloys. Materials Research Letters 2016, 4, 226–232, doi:10.1080/21663831.2016.1191554.

[30] Qiu, X.-W. Microstructure and Properties of AlCrFeNiCoCu High Entropy Alloy Prepared by Powder Metallurgy. Journal of Alloys and Compounds 2013, 555, 246–249, doi:10.1016/j.jallcom.2012.12.071.

[31] Dong, Y.; Lu, Y.; Kong, J.; Zhang, J.; Li, T. Microstructure and Mechanical Properties of Multi-Component AlCrFeNiMox High-Entropy Alloys. Journal of Alloys and Compounds 2013, 573, 96–101, doi:10.1016/j.jallcom.2013.03.253.

[32] Kuznetsov, A.V.; Shaysultanov, D.G.; Stepanov, N.D.; Salishchev, G.A.; Senkov, O.N. Tensile Properties of an AlCrCuNiFeCo High-Entropy Alloy in as-Cast and Wrought Conditions. Materials Science and Engineering: A 2012, 533, 107–118, doi:10.1016/j.msea.2011.11.045.

[33] Liu, L.; Zhu, J.B.; Zhang, C.; Li, J.C.; Jiang, Q. Microstructure and the Properties of FeCoCuNiSnx High Entropy Alloys. Materials Science and Engineering: A 2012, 548, 64–68, doi:10.1016/j.msea.2012.03.080.

[34] Daoud, H.M.; Manzoni, A.; Völkl, R.; Wanderka, N.; Glatzel, U. Microstructure and Tensile Behavior of Al8Co17Cr17Cu8Fe17Ni33 (at.%) High-Entropy Alloy. JOM 2013, 65, 1805–1814, doi:10.1007/s11837-013-0756-3.

[35] Zhang, H.; Meng, H.; Meng, F.; Tong, Y.; Liaw, P.K.; Yang, X.; Zhao, L.; Wang, H.; Gao, Y.; Chen, S. Magnificent Tensile Strength and Ductility Synergy in a NiCoCrAlTi High-Entropy Alloy at Elevated Temperature. Journal of Materials Research and Technology 2024, 28, 522–532, doi:10.1016/j.jmrt.2023.12.038.

[36] Carroll, R.; Lee, C.; Tsai, C.-W.; Yeh, J.-W.; Antonaglia, J.; Brinkman, B.A.W.; LeBlanc, M.; Xie, X.; Chen, S.; Liaw, P.K.; et al. Experiments and Model for Serration Statistics in Low-Entropy, Medium-Entropy and High-Entropy Alloys. Sci Rep 2015, 5, 16997, doi:10.1038/srep16997.

[37] Man, J.; Wu, B.; Duan, G.; Zhang, L.; Du, X.; Liu, Y.; Esling, C. Super-High Strength of a CoCrNiFe Based High Entropy Alloy. Journal of Materials Science & Technology 2024, 177, 79–84, doi:10.1016/j.jmst.2023.08.032.

[38] Cui, Y.; Shen, J.; Manladan, S.M.; Geng, K.; Hu, S. Wear Resistance of FeCoCrNiMnAlx High-Entropy Alloy Coatings at High Temperature. Applied Surface Science 2020, 512, 145736, doi:10.1016/j.apsusc.2020.145736.

[39] Poletti, M.G.; Fiore, G.; Gili, F.; Mangherini, D.; Battezzati, L. Development of a New High Entropy Alloy for Wear Resistance: FeCoCrNiW0.3 and FeCoCrNiW0.3+ 5 at.% of C. Materials & Design 2017, 115, 247–254, doi:10.1016/j.matdes.2016.11.027.

[40] Sun, Z.; Zhang, M.; Wang, G.; Yang, X.; Wang, S. Wear and Corrosion Resistance Analysis of FeCoNiTiAlx High-Entropy Alloy Coatings Prepared by Laser Cladding. Coatings 2021, 11, 155, doi:10.3390/coatings11020155.

[41] Löbel, M.; Lindner, T.; Mehner, T.; Lampke, T. Microstructure and Wear Resistance of AlCoCrFeNiTi High-Entropy Alloy Coatings Produced by HVOF. Coatings 2017, 7, 144, doi:10.3390/coatings7090144.

[42] Chen, M.; Shi, X.H.; Yang, H.; Liaw, P.K.; Gao, M.C.; Hawk, J.A.; Qiao, J. Wear Behavior of Al 0.6 CoCrFeNi High-Entropy Alloys: Effect of Environments. J. Mater. Res. 2018, 33, 3310–3320, doi:10.1557/jmr.2018.279.

[43] Thurston, K.V.S.; Gludovatz, B.; Hohenwarter, A.; Laplanche, G.; George, E.P.; Ritchie, R.O. Effect of Temperature on the Fatigue-Crack Growth Behavior of the High-Entropy Alloy CrMnFeCoNi. Intermetallics 2017, 88, 65–72, doi:10.1016/j.intermet.2017.05.009.

[44] Feng, R.; Rao, Y.; Liu, C.; Xie, X.; Yu, D.; Chen, Y.; Ghazisaeidi, M.; Ungar, T.; Wang, H.; An, K.; et al. Enhancing Fatigue Life by Ductile-Transformable Multicomponent B2 Precipitates in a High-Entropy Alloy. Nat Commun 2021, 12, 3588, doi:10.1038/s41467-021-23689-6.

[45] Chen, P.; Lee, C.; Wang, S.-Y.; Seifi, M.; Lewandowski, J.J.; Dahmen, K.A.; Jia, H.; Xie, X.; Chen, B.; Yeh, J.-W.; et al. Fatigue Behavior of High-Entropy Alloys: A Review. Sci. China Technol. Sci. 2018, 61, 168–178, doi:10.1007/s11431-017-9137-4.

[46] Li, W.; Chen, S.; Liaw, P.K. Discovery and Design of Fatigue-Resistant High-Entropy Alloys. Scripta Materialia 2020, 187, 68–75, doi:10.1016/j.scriptamat.2020.05.047.

[47] Seifi, M.; Li, D.; Yong, Z.; Liaw, P.K.; Lewandowski, J.J. Fracture Toughness and Fatigue Crack Growth Behavior of As-Cast High-Entropy Alloys. JOM 2015, 67, 2288–2295, doi:10.1007/s11837-015-1563-9.

[48] Hou, L.; Hui, J.; Yao, Y.; Chen, J.; Liu, J. Effects of Boron Content on Microstructure and Mechanical Properties of AlFeCoNiBx High Entropy Alloy Prepared by Vacuum Arc Melting. Vacuum 2019, 164, 212–218, doi:10.1016/j.vacuum.2019.03.019.

[49] Stepanov, N.D.; Yurchenko, N.Yu.; Zherebtsov, S.V.; Tikhonovsky, M.A.; Salishchev, G.A. Aging Behavior of the HfNbTaTiZr High Entropy Alloy. Materials Letters 2018, 211, 87–90, doi:10.1016/j.matlet.2017.09.094.

[50] Karati, A.; Guruvidyathri, K.; Hariharan, V.S.; Murty, B.S. Thermal Stability of AlCoFeMnNi High-Entropy Alloy. Scripta Materialia 2019, 162, 465–467, doi:10.1016/j.scriptamat.2018.12.017.

[51] Feng, J.; Song, K.; Liang, S.; Guo, X.; Jiang, Y. Electrical Wear of TiB2 Particle-Reinforced Cu and Cu–Cr Composites Prepared by Vacuum Arc Melting. Vacuum 2020, 175, 109295, doi:10.1016/j.vacuum.2020.109295.

[52] Güler, S.; Alkan, E.D.; Alkan, M. Vacuum Arc Melted and Heat Treated AlCoCrFeNiTiX Based High-Entropy Alloys: Thermodynamic and Microstructural Investigations. Journal of Alloys and Compounds 2022, 903, 163901, doi:10.1016/j.jallcom.2022.163901.

[53] Zhang, P.; Li, Y.; Chen, Z.; Zhang, J.; Shen, B. Oxidation Response of a Vacuum Arc Melted NbZrTiCrAl Refractory High Entropy Alloy at 800–1200 °C. Vacuum 2019, 162, 20–27, doi:10.1016/j.vacuum.2019.01.026.

[54] Geanta, V.; Voiculescu, I. Characterization and Testing of High-Entropy Alloys from AlCrFeCoNi System for Military Applications. In Engineering Steels and High Entropy-Alloys; Sharma, A., Duriagina, Z., Kumar, S., Eds.; IntechOpen, 2020 ISBN 978-1-78985-947-8.

[55] Onawale, O.T.; Cobbinah, P.V.; Nzeukou, R.A.; Matizamhuka, W.R. Synthesis Route, Microstructural Evolution, and Mechanical Property Relationship of High-Entropy Alloys (HEAs): A Review. Materials 2021, 14, 3065, doi:10.3390/ma14113065.

[56] Santodonato, L.J.; Zhang, Y.; Feygenson, M.; Parish, C.M.; Gao, M.C.; Weber, R.J.K.; Neuefeind, J.C.; Tang, Z.; Liaw, P.K. Deviation from High-Entropy Configurations in the Atomic Distributions of a Multi-Principal-Element Alloy. Nat Commun 2015, 6, 5964, doi:10.1038/ncomms6964.

[57] Jablonski, P.D.; Licavoli, J.J.; Gao, M.C.; Hawk, J.A. Manufacturing of High Entropy Alloys. JOM 2015, 67, 2278–2287, doi:10.1007/s11837-015-1540-3.

[58] Wang, C.; Ji, W.; Fu, Z. Mechanical Alloying and Spark Plasma Sintering of CoCrFeNiMnAl High-Entropy Alloy. Advanced Powder Technology 2014, 25, 1334–1338, doi:10.1016/j.apt.2014.03.014.

[59] Joseph, J.; Hodgson, P.; Jarvis, T.; Wu, X.; Stanford, N.; Fabijanic, D.M. Effect of Hot Isostatic Pressing on the Microstructure and Mechanical Properties of Additive Manufactured AlxCoCrFeNi High Entropy Alloys. Materials Science and Engineering: A 2018, 733, 59–70, doi:10.1016/j.msea.2018.07.036.

[60] Shen, Q.; Kong, X.; Chen, X. Fabrication of Bulk Al-Co-Cr-Fe-Ni High-Entropy Alloy Using Combined Cable Wire Arc Additive Manufacturing (CCW-AAM): Microstructure and Mechanical Properties. Journal of Materials Science & Technology 2021, 74, 136–142, doi:10.1016/j.jmst.2020.10.037.

[61] Ma, S.G.; Zhang, S.F.; Gao, M.C.; Liaw, P.K.; Zhang, Y. A Successful Synthesis of the CoCrFeNiAl0.3 Single-Crystal, High-Entropy Alloy by Bridgman Solidification. JOM 2013, 65, 1751–1758, doi:10.1007/s11837-013-0733-x.

[62] Zuo, T.; Yang, X.; Liaw, P.K.; Zhang, Y. Influence of Bridgman Solidification on Microstructures and Magnetic Behaviors of a Non-Equiatomic FeCoNiAlSi High-Entropy Alloy. Intermetallics 2015, 67, 171–176, doi:10.1016/j.intermet.2015.08.014.

[63] Ma, S.G.; Zhang, S.F.; Qiao, J.W.; Wang, Z.H.; Gao, M.C.; Jiao, Z.M.; Yang, H.J.; Zhang, Y. Superior High Tensile Elongation of a Single-Crystal CoCrFeNiAl0.3 High-Entropy Alloy by Bridgman Solidification. Intermetallics 2014, 54, 104–109, doi:10.1016/j.intermet.2014.05.018.

[64] Zuo, T.; Ren, S.; Liaw, P.K.; Zhang, Y. Processing Effects on the Magnetic and Mechanical Properties of FeCoNiAl0.2Si0.2 High Entropy Alloy. Int J Miner Metall Mater 2013, 20, 549–555, doi:10.1007/s12613-013-0764-x.

[65] Laurent-Brocq, M.; Akhatova, A.; Perrière, L.; Chebini, S.; Sauvage, X.; Leroy, E.; Champion, Y. Insights into the Phase Diagram of the CrMnFeCoNi High Entropy Alloy. Acta Materialia 2015, 88, 355–365, doi:10.1016/j.actamat.2015.01.068.

[66] Jiang, L.; Jiang, H.; Lu, Y.; Wang, T.; Cao, Z.; Li, T. Mechanical Properties Improvement of AlCrFeNi2Ti0.5 High Entropy Alloy through Annealing Design and Its Relationship with Its Particle-Reinforced Microstructures. Journal of Materials Science & Technology 2015, 31, 397–402, doi:10.1016/j.jmst.2014.09.011.

[67] Alijani, F.; Reihanian, M.; Gheisari, Kh. Study on Phase Formation in Magnetic FeCoNiMnV High Entropy Alloy Produced by Mechanical Alloying. Journal of Alloys and Compounds 2019, 773, 623–630, doi:10.1016/j.jallcom.2018.09.204.

[68] Salemi, F.; Abbasi, M.H.; Karimzadeh, F. Synthesis and Thermodynamic Analysis of Nanostructured CuNiCoZnAl High Entropy Alloy Produced by Mechanical Alloying. Journal of Alloys and Compounds 2016, 685, 278–286, doi:10.1016/j.jallcom.2016.05.274.

[69] Li, W.; Liu, P.; Liaw, P.K. Microstructures and Properties of High-Entropy Alloy Films and Coatings: A Review. Materials Research Letters 2018, 6, 199–229, doi:10.1080/21663831.2018.1434248.
[70] Li, J.; Huang, Y.; Meng, X.; Xie, Y. A Review on High Entropy Alloys Coatings: Fabrication Processes and Property Assessment. Adv. Eng. Mater. 2019, 21, 1900343, doi:10.1002/adem.201900343.
[71] Arif, Z.U.; Khalid, M.Y.; ur Rehman, E.; Ullah, S.; Atif, M.; Tariq, A. A Review on Laser Cladding of High-Entropy Alloys, Their Recent Trends and Potential Applications. Journal of Manufacturing Processes 2021, 68, 225–273, doi:10.1016/j.jmapro.2021.06.041.
[72] Duchaniya, R.K.; Pandel, U.; Rao, P. Coatings Based on High Entropy Alloys: An Overview. Materials Today: Proceedings 2021, 44, 4467–4473, doi:10.1016/j.matpr.2020.10.720.
[73] Sharma, A. High Entropy Alloy Coatings and Technology. Coatings 2021, 11, 372, doi:10.3390/coatings11040372.
[74] Meghwal, A.; Anupam, A.; Murty, B.S.; Berndt, C.C.; Kottada, R.S.; Ang, A.S.M. Thermal Spray High-Entropy Alloy Coatings: A Review. J Therm Spray Tech 2020, 29, 857–893, doi:10.1007/s11666-020-01047-0.
[75] Liao, W.-B.; Zhang, H.; Liu, Z.-Y.; Li, P.-F.; Huang, J.-J.; Yu, C.-Y.; Lu, Y. High Strength and Deformation Mechanisms of Al0.3CoCrFeNi High-Entropy Alloy Thin Films Fabricated by Magnetron Sputtering. Entropy 2019, 21, 146, doi:10.3390/e21020146.
[76] Liao, W.; Lan, S.; Gao, L.; Zhang, H.; Xu, S.; Song, J.; Wang, X.; Lu, Y. Nanocrystalline High-Entropy Alloy (CoCrFeNiAl0.3) Thin-Film Coating by Magnetron Sputtering. Thin Solid Films 2017, 638, 383–388, doi:10.1016/j.tsf.2017.08.006.
[77] Braic, M.; Braic, V.; Vladescu, A.; N. Zoita, C.; Balaceanu, M. Solid Solution or Amorphous Phase Formation in TiZr-Based Ternary to Quinternary Multi-Principal-Element Films. Progress in Natural Science: Materials International 2014, 24, 305–312, doi:10.1016/j.pnsc.2014.06.001.
[78] Shen, W.-J.; Tsai, M.-H.; Yeh, J.-W. Machining Performance of Sputter-Deposited (Al0.34Cr0.22Nb0.11Si0.11Ti0.22)50N50 High-Entropy Nitride Coatings. Coatings 2015, 5, 312–325, doi:10.3390/coatings5030312.
[79] An, Z.; Jia, H.; Wu, Y.; Rack, P.D.; Patchen, A.D.; Liu, Y.; Ren, Y.; Li, N.; Liaw, P.K. Solid-Solution CrCoCuFeNi High-Entropy Alloy Thin Films Synthesized by Sputter Deposition. Materials Research Letters 2015, 3, 203–209, doi:10.1080/21663831.2015.1048904.
[80] Jiang, Y.Q.; Li, J.; Juan, Y.F.; Lu, Z.J.; Jia, W.L. Evolution in Microstructure and Corrosion Behavior of AlCoCrxFeNi High-Entropy Alloy Coatings Fabricated by Laser Cladding. Journal of Alloys and Compounds 2019, 775, 1–14, doi:10.1016/j.jallcom.2018.10.091.
[81] Liu, J.; Liu, H.; Chen, P.; Hao, J. Microstructural Characterization and Corrosion Behaviour of AlCoCrFeNiTix High-Entropy Alloy Coatings Fabricated by Laser Cladding. Surface and Coatings Technology 2019, 361, 63–74, doi:10.1016/j.surfcoat.2019.01.044.
[82] Ji, X.; Duan, H.; Zhang, H.; Ma, J. Slurry Erosion Resistance of Laser Clad NiCoCrFeAl 3 High-Entropy Alloy Coatings. Tribology Transactions 2015, 58, 1119–1123, doi:10.1080/10402004.2015.1044148.
[83] Zhang, H.; Wu, W.; He, Y.; Li, M.; Guo, S. Formation of Core–Shell Structure in High Entropy Alloy Coating by Laser Cladding. Applied Surface Science 2016, 363, 543–547, doi:10.1016/j.apsusc.2015.12.059.
[84] Fereidouni, M.; Sarkari Khorrami, M.; Heydarzadeh Sohi, M. Liquid Phase Cladding of AlxCoCrFeNi High Entropy Alloys on AISI 304L Stainless Steel. Surface and Coatings Technology 2020, 402, 126331, doi:10.1016/j.surfcoat.2020.126331.
[85] Huo, W.; Shi, H.; Ren, X.; Zhang, J. Microstructure and Wear Behavior of CoCrFeMnNbNi High-Entropy Alloy Coating by TIG Cladding. Advances in Materials Science and Engineering 2015, 2015, 1–5, doi:10.1155/2015/647351.
[86] Shang, C.; Axinte, E.; Sun, J.; Li, X.; Li, P.; Du, J.; Qiao, P.; Wang, Y. CoCrFeNi(W1−xMox) High-Entropy Alloy Coatings with Excellent Mechanical Properties and Corrosion Resistance Prepared by Mechanical Alloying and Hot Pressing Sintering. Materials & Design 2017, 117, 193–202, doi:10.1016/j.matdes.2016.12.076.

[87] Tang, Y.; Wang, S.; Sun, B.; Wang, Y.; Qiao, Y. FABRICATION AND WEAR BEHAVIOR ANALYSIS ON AlCrFeNi HIGH ENTROPY ALLOY COATING UNDER DRY SLIDING AND OIL LUBRICATION TEST CONDITIONS. Surf. Rev. Lett. 2016, 23, 1650018, doi:10.1142/S0218625X16500189.

[88] Scutelnicu, E.; Simion, G.; Mircea, O.; Rusu, C.C.; Mistodie, L.R.; Gheonea, M.C.; Geanta, V.; Voiculescu, I. Procedeu de Realizare a Unei Depuneri Din Aliaj Multielement Tip AlCrFeNi Prin Topire Cu Arc Electric in Mediu de Gaz Protector Inert 2024.

[89] Ren, M.; Wang, G.; Li, B. Microstructure and Properties of AlCrFeNi Intermetallic for Electronic Packaging Shell. In Proceedings of the 2017 18th International Conference on Electronic Packaging Technology (ICEPT); IEEE: Harbin, August 2017; pp. 817–820.

[90] Yuan, J.; Yang, Y.; Duan, S.; Dong, Y.; Li, C.; Zhang, Z. Rapid Design, Microstructures, and Properties of Low-Cost Co-Free Al-Cr-Fe-Ni Eutectic Medium Entropy Alloys. Materials 2022, 16, 56, doi:10.3390/ma16010056.

[91] Silwal, B.; Walker, J.; West, D. Hot-Wire GTAW Cladding: Inconel 625 on 347 Stainless Steel. Int J Adv Manuf Technol 2019, 102, 3839–3848, doi:10.1007/s00170-019-03448-0.

[92] Xu, G.; Kutsuna, M.; Liu, Z.; Yamada, K. Comparison between Diode Laser and TIG Cladding of Co-Based Alloys on the SUS403 Stainless Steel. Surface and Coatings Technology 2006, 201, 1138–1144, doi:10.1016/j.surfcoat.2006.01.040.

[93] Shang, C.Y.; Wang, Y. AlCrFeNi High-Entropy Coating Fabricated by Mechanical Alloying and Hot Pressing Sintering. MSF 2017, 898, 628–637, doi:10.4028/www.scientific.net/MSF.898.628.

[94] Jumaev, E.; Abbas, M.A.; Mun, S.C.; Song, G.; Hong, S.-J.; Kim, K.B. Nano-Scale Structural Evolution of Quaternary AlCrFeNi Based High Entropy Alloys by the Addition of Specific Minor Elements and Its Effect on Mechanical Characteristics. Journal of Alloys and Compounds 2021, 868, 159217, doi:10.1016/j.jallcom.2021.159217.

[95] Dong, T.; Zheng, X.; Li, G.; Wang, H.; Liu, M.; Zhou, X.; Li, Y. Effect of Tungsten Inert Gas Remelting on Microstructure, Interface, and Wear Resistance of Fe-Based Coating. Journal of Engineering Materials and Technology 2018, 140, 041007, doi:10.1115/1.4040005.

[96] Zhu, L.; Cui, Y.; Cao, J.; Tian, R.; Cai, Y.; Xu, C.; Han, J.; Tian, Y. Effect of TIG Remelting on Microstructure, Corrosion and Wear Resistance of Coating on Surface of 4Cr5MoSiV1 (AISI H13). Surface and Coatings Technology 2021, 405, 126547, doi:10.1016/j.surfcoat.2020.126547.

[97] Tian, H.L.; Wei, S.C.; Chen, Y.X.; Tong, H.; Liu, Y.; Xu, B.S. Microstructure and Wear Resistance of an Arc-Sprayed Fe-Based Coating After Surface Remelting Treatment. Strength Mater 2014, 46, 229–234, doi:10.1007/s11223-014-9540-z.

[98] Ji, M.; Huang, L.; An, Q.; Bao, Y.; Cui, X.; Jiao, Y.; Geng, L. Microstructure Refinement and Strengthening Mechanisms of Network Structured TiBw/Ti6Al4V Composites by TIG Remelting. Materials Science and Engineering: A 2021, 804, 140755, doi:10.1016/j.msea.2021.140755.

[99] Chișiu, G.; Gheța, R.-A.; Stoica, A.-M.; Stoica, N.-A. Comparative Micro-Scale Abrasive Wear Testing of Thermally Sprayed and Hard Chromium Coatings. Lubricants 2023, 11, 350, doi:10.3390/lubricants11080350.

[100] Silva, F.J.G.; Martinho, R.P.; Baptista, A.P.M. Characterization of Laboratory and Industrial CrN/CrCN/Diamond-like Carbon Coatings. Thin Solid Films 2014, 550, 278–284, doi:10.1016/j.tsf.2013.11.042.

[101] Cozza, R.C. A Study on Friction Coefficient and Wear Coefficient of Coated Systems Submitted to Micro-Scale Abrasion Tests. Surface and Coatings Technology 2013, 215, 224–233, doi:10.1016/j.surfcoat.2012.06.088.

[102] Sadiq, K.; Sim, M.; Black, R.; Stack, M. Mapping the Micro-Abrasion Mechanisms of CoCrMo: Some Thoughts on Varying Ceramic Counterface Diameter on Transition Boundaries In Vitro. Lubricants 2020, 8, 71, doi:10.3390/lubricants8070071.

[103] Resendiz-Calderon, C.D.; Cázares-Ramírez, I.; Samperio-Galicia, D.L.; Farfan-Cabrera, L.I. Method for Conducting Micro-Abrasion Wear Testing of Materials in Oscillating Sliding. MethodsX 2022, 9, 101703, doi:10.1016/j.mex.2022.101703.
[104] Thakare, M.R.; Wharton, J.A.; Wood, R.J.K.; Menger, C. Effect of Abrasive Particle Size and the Influence of Microstructure on the Wear Mechanisms in Wear-Resistant Materials. Wear 2012, 276–277, 16–28, doi:10.1016/j.wear.2011.11.008.
[105] Navas, C.; Colaço, R.; De Damborenea, J.; Vilar, R. Abrasive Wear Behaviour of Laser Clad and Flame Sprayed-Melted NiCrBSi Coatings. Surface and Coatings Technology 2006, 200, 6854–6862, doi:10.1016/j.surfcoat.2005.10.032.
[106] Standard Practice for Calculation of Corrosion Rates and Related Information from Electrochemical Measurements.; ASTM G102-89(2010); West Conshohocken, PA, USA, 1999.
[107] 107. Electrochemical Impedance Spectroscopy (EIS) on Coated and Uncoated Metallic Specimens.; ISO 16773-1-4:2016; Geneva, Switzerland, 2016.
[108] Simion, G.; Bertapelle, M.; Mirza-Rosca, J.; Voiculescu, I.; Scutelnicu, E. The Influence of the Re-Melting on the Microstructure and Corrosion Resistance of New Welding Material. Microscopy and Microanalysis 2024, 30, ozae044.670, doi:10.1093/mam/ozae044.670.
[109] Stern, M.; Geaby, A.L. Electrochemical Polarization. J. Electrochem. Soc. 1957, 104, 56, doi:10.1149/1.2428496.
[110] Jones, D.A. Principles and Prevention of Corrosion; 2. int. ed.; Pearson Education: Harlow, 2014; ISBN 978-1-292-04255-8.
[111] Xu, Y.; Zhou, Q.; Liu, L.; Zhang, Q.; Song, S.; Huang, Y. Exploring the Corrosion Performances of Carbon Steel in Flowing Natural Sea Water and Synthetic Sea Waters. Corrosion Engineering, Science and Technology 2020, 55, 579–588, doi:10.1080/1478422X.2020.1765476.
[112] Onyeji, L.; Kale, G. Preliminary Investigation of the Corrosion Behavior of Proprietary Micro-Alloyed Steels in Aerated and Deaerated Brine Solutions. J. of Materi Eng and Perform 2017, 26, 5741–5752, doi:10.1007/s11665-017-3031-x.
[113] Saeed, A. Low Activation-Modified High Manganese-Nitrogen Austenitic Stainless Steel for Fast Reactor Pressure Vessel Cladding. NS 2018, 3, 45, doi:10.11648/j.ns.20180303.14.
[114] Nadliriyah, N.; Putri, A.L.; Triwikantoro, T. PANi/ZrO 2 -Composite Coating for Corrosion Protection in 3.5 M NaCl Solution. IOP Conf. Ser.: Mater. Sci. Eng. 2019, 496, 012059, doi:10.1088/1757-899X/496/1/012059.
[115] Moradi, M.; Ghoreishi, M.; Rahmani, A. Numerical and Experimental Study of Geometrical Dimensions on Laser-TIG Hybrid Welding of Stainless Steel 1.4418. Journal of Modern Processes in Manufacturing and Production, 2016, 5, 21–31.
[116] Ullah, R.; Lian, J.; Akmal, J.; Wu, J.; Niemi, E. Prediction and Validation of Melt Pool Dimensions and Geometric Distortions of Additively Manufactured AlSi10Mg. Int J Adv Manuf Technol 2023, 126, 3593–3613, doi:10.1007/s00170-023-11264-w.
[117] Suman, S.; Biswas, P. Microstructural, Strength and Residual Stress Studies on Single- and Double-Side Single-Pass Submerged Arc Welding of 9Cr–1Mo–V Steel Plate. J. Inst. Eng. India Ser. C 2022, 103, 1177–1191, doi:10.1007/s40032-022-00870-4.
[118] Ahmad, A.S.; Wu, Y.; Gong, H.; Liu, L. Numerical Simulation of Thermal and Residual Stress Field Induced by Three-Pass TIG Welding of Al 2219 Considering the Effect of Interpass Cooling. Int. J. Precis. Eng. Manuf. 2020, 21, 1501–1518, doi:10.1007/s12541-020-00357-1.
[119] Farias, R.M.; Teixeira, P.R.F.; Araújo, D.B. Thermo-Mechanical Analysis of the MIG/MAG Multi-Pass Welding Process on AISI 304L Stainless Steel Plates. J Braz. Soc. Mech. Sci. Eng. 2017, 39, 1245–1258, doi:10.1007/s40430-016-0574-y.
[120] Reda, R.; Magdy, M.; Rady, M. Ti–6Al–4V TIG Weld Analysis Using FEM Simulation and Experimental Characterization. Iran J Sci Technol Trans Mech Eng 2020, 44, 765–782, doi:10.1007/s40997-019-00287-y.

SCIENTIFIC ACTIVITY

Articles published in journals and indexed volumes Web of Scenice (Clarivate): 5

[1] Chaturvedi M., Subbiah A.V., **Simion G**. , Rusu C.C. Scutelnicu E., *Critical Review on Magnetically Impelled Arc Butt Welding:Challenges, Perspectives and Industrial Applications*, Materials **2023**, Vol. 16, 7054. https://doi.org/10.3390/ma16217054, FI(2023)=3.1, **revistă zona roşie**, **WOS: 001099516300001**.

[2] Voiculescu, I.; Geanta, V.; Stefanescu, E.V.; **Simion, G**.; Scutelnicu, E. *Effect of Diffusion on Dissimilar Welded Joint between Al0.8CoCrFeNi High-Entropy Alloy and S235JR Structural Steel*. Metals **2022**, Vol. 12, 548, doi:10.3390/met12040548, FI(2022)=2.9, **revistă zona galbenă, WOS:000786074200001**.

[3] Mitru, A.; Semenescu, A.; **Simion, G**.; Scutelnicu, E.; Voiculescu, I. *Study on the Weldability of Copper—304L Stainless Steel Dissimilar Joint Performed by Robotic Gas Tungsten Arc Welding*. Materials **2022**, Vol. 15, 5535, doi:10.3390/ma15165535, FI(2022)=3,4, **revistă zona galbenă**, **WOS:000845640800001**.

[4] **Simion G.**,Birsan D. , Voiculescu I., Scutelnicu E., *Simulation by FEM of TIG deposition welding of multicomponent alloy on carbon steel substrate*,The 5th International Conference *Modern Technologies in Manufacturing* - MTeM 2023, Cluj-Napoca, 18-21 oct. 2023, https://easychair.org/cfp/MTeM2023, în curs de indexare în WoS.

[5] **Simion G.**, Bertapelle M., Mirza-Rosca J., Voiculescu I., Scutelnicu E., *The Influence of the Re-Melting on the Microstructure and Corrosion Resistance of New Welding Material*, Microscopy and Microanalysis, Vol. 30, Suppl.(1), The Official M&M 2024 Proceedings, https://doi.org/10.1093/mam/ozae044.670, pag. 1363–1366, Cleveland, Ohio, USA, July 28 – August 1, 2024, în curs de indexare în WoS.

Articles published in BDI indexed journals, in accordance with the standards CNATDCU – C16: 4

[1] Georgescu B., **Simion G.**, *A Synthetic Approach to Cold Presure Welding on Cogged Surfaces*, Annals of "Dunarea de Jos" University of Galati, Fascicle XII, Welding Equipment and Technology (AWET), Vol. 34, Year XXXIV, **2023**, Elsevier-SCOPUS, pp. 57-64, DOI: 10.35219/awet.2023.06, **Elsevier-SCOPUS, ProQuest, DOAJ**.

[2] Birsan, D.C.; **Simion, G**. *Numerical Modelling of Thermo-Mechanical Effects Developed in Resistance Spot Welding of E304 Steel with Copper Interlayer*, Annals of "Dunarea de Jos" University of Galati, Fascicle XII, Welding Equipment and Technology (AWET), Vol. 33, Year XXXIII, **2022**, pp. 89-94, DOI:10.35219/awet.2022.07**, Elsevier-SCOPUS, ProQuest, DOAJ**.

[3] Birsan, D.C.; **Simion, G**.; Voiculescu, I.; Scutelnicu, E., *Numerical Model Developed for Thermo-Mecahnical Analysis in AlCrFeMnNiHf0.05–Armox 500 Steel Welded Joint*, Annals of "Dunarea de Jos" University of Galati, Fascicle XII Welding Equipement and Technology **2021**, Vol. 32, Year XXXII, pp. 37–46, doi:10.35219/awet.2021.05, **Elsevier-SCOPUS, ProQuest, DOAJ**.

[4] Scutelnicu E., **Simion G**., Rusu C. C., Gheonea M. C., Voiculescu I., Geanta V., *High Entropy Alloys Behaviour During Welding*, Revista de Chimie, 2020, Vol. 71, pag. 219-233, **Elsevier-SCOPUS**.

Articles published in recognized journals CNCSIS: 1

[1] **Simion G**., *Rusu* C. C., Scutelnicu E., Voiculescu I., Geantă V., *Stadiul actual al sudării aliajelor cu entropie ridicată (State of the Art of Welding High Entropy Alloys*, Revista SUDURA, Vol. 3, 2019, pag 5-15, ISSN: 1453 – 0384, https://asr.ro/revista-sudura-nr-3-2019/

Papers presented at international conferences: 8

[1] **Simion G.,** Scutelnicu E., Mirza Rosca J., Voiculescu I., *New Medium Entropy Alloy Deposition Achieved by TIG Cladding,* 13th International Conference on Materials Science & Engineering – BRAMAT 2024, 13th – 16th March 2024, Brasov, poster.

[2] **Simion G.**, Bertapelle M., Mirza-Rosca J., Voiculescu I., Scutelnicu E., *The Influence of the Re-Melting on the Microstructure and Corrosion Resistance of New Welding Material,* Microscopy and Microanalysis (M&M) 2024 Conference July 28 - August 1, 2024, Cleveland, USA, poster.

[3] **Simion G.,**Birsan D. , Voiculescu I., Scutelnicu E.*, Simulation by FEM of TIG Deposition Welding of Multicomponent Alloy on Carbon Steel Substrate*, The 5th International Conference *Modern Technologies in Manufacturing* - MTeM 2023, 18-21 oct 2023, Cluj-Napoca, Romania, https://www.utcluj.ro/media/documents/2023/Final-Program-MTeM_2023_v3.pdf

[4] **Simion G.,** Mircea O., Rusu C.C, Gheonea M.C., Birsan D.C., Voiculescu I., Scutelnicu E., *Numerical model developed for simulating multicomponent-alloy cladding on a steel substrate*, The 11th Edition of Scientific

Conference of Doctoral Schools, *Perspectives and Challenges in Doctoral Research*, 8th-9th June 2023, Galati, Romania.

[5] Mircea O., **Simion G**., Gheonea M.C., *Caracterizarea îmbinărilor din cupru și aluminiu sudate prin presiune la rece*, Conferința Internațională SUDURA 2023, 27-28 apr. 2023, Galați, https://asr.ro/documents/manifestari_stiintifice/ASR-Program%20Conferinta%20Sudura%202023%20Galati%2C%2027-28.04.2023.pdf

[6] **Simion G**., Mircea O., Gheonea M.C., Bîrsan D.C., Rusu C.C., Scutelnicu E., *Simularea comportării termo-mecanice a depunerii unui aliaj multicomponent pe un substrat din oțel carbon*, Conferința Internațională SUDURA 2023, 27-28 apr 2023, Galați, Romania, https://asr.ro/documents/manifestari_stiintifice/ASR-Program%20Conferinta%20Sudura%202023%20Galati%2C%2027-28.04.2023.pdf

[7] **Simion. G**, Scutelnicu E., *Overview on high entropy alloys: Characterisation and applicability*, The 9th Edition Scientific Conference of Doctoral Schools, *Perspectives and Challenges in Doctoral Research*, 10th-11th June 2021, Galati, Romania.

[8] **Simion G.,** Scutelnicu E*., High Entropy Alloy Cladding – a short Review*, 1st International Conference on Advanced Research in Engineering CARE 2020, Şcoala Doctorală "Acad. Radu Voinea", 30 Oct. 2020, Craiova, Romania.

Papers presented at other national scientific events: 7

[1] **Simion. G**., *Sisteme de protecție individuala și colectivă pe bază de aliaje cu entropie ridicată*, Conferința TECH-TALK(ING) *Smart Industry. Smart Technology. Smart People*, Prima Ediție, Universitatea ”Dunărea de Jos” din Galați,15 Decembrie, 2020, Galaţi, Romania.

[2] **Simion G**., Rusu C. C., Gheonea M. C, Voiculescu I., Geanta V., Scutelnicu E., *Proiectarea morfo-funcțională a sistemelor de protecție pentru domeniul militar*, Conferința ASR ”SUDURA 2020”, Educație, cercetare și inovare în domeniul sudării, 20–22 Oct. 2020, Ploiești, Romania.

[3] **Simion G.,** *Studiul configurației blindajelor militare realizate din aliaje cu entropie ridicată*, Sesiunea Națională de Comunicări Științifice Studențești ˝ANGHEL SALIGNY˝, ediția a XII-a, 2020, Secțiunea nr. 6: *Masterandul de Azi – Cercetătorul de Mâine*, Galati, Romania.

[4] **Simion G**., Scutelnicu E., *Caracterizarea aliajelor cu entropie ridicată utilizate la sistemele de protecție individuală și colectivă*, Workshop “*Tendințe actuale și perspective în dezvoltarea proceselor de sudare*”, organizat de *Centrul de Cercetări Avansate în Domeniul Sudării* (SUDAV) în colaborare cu Asociația de Sudură din România - Sucursala Galați (ASR) și LINDE GAZ România, 23 Mai 2019, Galați, Romania.

[5] **Simion G.**, Scutelnicu E., *Tehnici de sudare și brazare pentru îmbinarea aliajelor cu entropie ridicată,* Workshop *“Tendințe actuale și perspective în dezvoltarea proceselor de sudare*” organizat de *Centrul de Cercetări Avansate în Domeniul Sudării (SUDAV)* în colaborare cu Asociația de Sudură din România - Sucursala Galați (ASR) și LINDE GAZ România, 23 Mai 2019, Galați, Romania.

[6] **Simion G.**, *Stadiul actual al sudării și brazării aliajelor cu entropie ridicată*, *Sesiunea Națională de Comunicări Științifice Studențești ˝ANGHEL SALIGNY˝*, ediția a XI-a 2019, Secțiunea nr. 7: *Masterandul de Azi – Cercetătorul de Mâine*, Galaţi, Romania.

[7] **Simion G.,** *Studiul încălzirii la sudarea cap la cap prin presiune în stare solidă*, în *Sesiunea Națională de Comunicări Științifice Studențești ˝ANGHEL SALIGNY˝*, 17-18 mai 2018 Galați, Romania.

Patents granted: 1

[1] Scutelnicu E., **Simion G**., Mircea O., Rusu C.C., Mistodie L.R., Gheonea M.C., Geanta V, Voiculescu I., *Procedeu de realizare a unei depuneri din aliaj multi-element tip AlCrFeNi prin topire cu arc electric in mediu de gaz protector inert*, Brevet de invenție nr . 135988/29.03.2024.

Published books: 1

[1] Rusu C.C., **Simion G**., Scutelnicu E., *Caracterizarea îmbinărilor sudate Lucrări aplicative*, Editura Zigotto, Galați, 2022, ISBN 978-606-669-208-3, 120 pag.

Research projects: 2

[1] Proiect complex **PN-III-P1-1.2-PCCDI-2017-0875,** *Sisteme de protecție individuală și colectivă pentru domeniul militar pe bază de aliaje cu entropie ridicată – HEAPROTECT*, Contract: 20PCCDI / 2018, Autoritatea contractantă: Unitatea Executivă pentru Finanțarea Învățământului Superior, a Cercetării, Dezvoltării și Inovării (UEFISCDI), perioadă implementare 2018 – 2021, membru în echipa proiectului (asistent de cercetare).

[2] Grant cercetare *Sudarea subacvatică a subansamblurilor de aluminiu pentru industria navală și off-shore* (AQUA-WELD), contract de finanțare nr: RF 2472/31.05.2024 câştigat prin competiţie instituţională, membru în echipa proiectului (asistent de cercetare).

Projects financed by the EU: 1

[1] *STEM for Youngsters*, proiect Erasmus+ - STEM Education for Primary Schools, contract de finanțare nr. 2021-1-EL01-KA220-SCH-000023967, perioada de implementare 2022-2024, membru în echipa proiectului (formator)

Awards: 10

[1] **Medalia de aur INVENTICA 2024** pentru Brevetul nr. 135988/29.03.2024, *Procedeu de realizare a unei depuneri din aliaj multi-element tip AlCrFeNi prin topire cu arc electric în mediu de gaz protector inert*, autori: Scutelnicu E., **Simion G**., Mircea O., Rusu C.C., Mistodie L.R., Gheonea M.C., Geantă V., Voiculescu I., Expoziția Internațională de Invenții INVENTICA 2024, Iași, 03-05.07.2024, ediția a XXVIII.

[2] **Premiul Special al Universității Tehnice din Cluj-Napoca** pentru Brevetul nr. 135988/29.03.2024, *Procedeu de realizare a unei depuneri din aliaj multi-element tip AlCrFeNi prin topire cu arc electric în mediu de gaz protector inert*, autori: Scutelnicu E., **Simion G**., Mircea O., Rusu C.C., Mistodie L.R., Gheonea M.C., Geantă V., Voiculescu I., Expoziția Internațională de Invenții INVENTICA 2024, Iași, 03-05.07.2024, ediția a XXVIII.

[3] **Premiul Special al Universității Politehnica Timișoara** pentru brevetul nr. 135988/29.03.2024, *Procedeu de realizare a unei depuneri din aliaj multi-element tip AlCrFeNi prin topire cu arc electric în mediu de gaz protector inert*, autori: Scutelnicu E., **Simion G**., Mircea O., Rusu C.C., Mistodie L.R., Gheonea M.C., Geantă V., Voiculescu I., Expoziția Internațională de Invenții INVENTICA 2024, Iași, 03-05.07.2024, ediția a XXVIII.

[4] **Premiul pentru cea mai bună lucrare din secțiunea *Advanced Manufacturing Technologies*,** autori: **Simion G.,** Birsan D., Voiculescu I., Scutelnicu E., *Simulation by FEM of TIG deposition welding of multicomponent alloy on carbon steel substrate*, The 5th International Conference - MTeM 2023, Cluj-Napoca, 18-21 oct 2023.

[5] **Marele Premiu acordat de Forumul Inventatorilor din România**, pentru cererea de brevet no. A100210/21.04.2022, *Procedure for obtaining deposition of AlCrFeNi multi-element alloy by fusion with electric arc and inert shielding gas,* autori: Scutelnicu E., **Simion G**., Mircea O., Rusu C.C., Mistodie L.R., Gheonea M.C., Geantă V., Voiculescu I., Salonul de Inovare și Cercetare UGAL INVENT 2023, Galați.

[6] **Medalia de Aur și Trofeul UGAL INVENT 2023** pentru cererea de brevet no. A100210/21.04.2022, *Procedure for obtaining deposition of AlCrFeNi multi-element alloy by fusion with electric arc and inert shielding gas*, autori: Scutelnicu E., **Simion G**., Mircea O., Rusu C.C., Mistodie L.R., Gheonea M.C., Geantă V., Voiculescu I., Salonul de Inovare și Cercetare UGAL INVENT 2023, Galați.

[7] **GOLD MEDAL** pentru cererea de brevet no. A100210/21.04.2022, *Procedure for Obtaining Multi-element Alloys from the AlCrFeNi System* , autori: Scutelnicu E., **Simion G**., Mircea O., Rusu C.C., Mistodie L.R., Gheonea M.C., Geantă V., Voiculescu I., European Exhibition of Creativity and Innovation - EUROINVENT 2023, Iași.

[8] **Premiul I** pentru lucrarea *Numerical model developed for simulating multicomponent-alloy cladding on a steel substrate,* autori**: Simion G.,** Mircea O., Rusu C.C, Gheonea M.C., Birsan D.C., Voiculescu I., Scutelnicu E., The 11th Edition of Scientific Conference of Doctoral Schools, 8th-9th of June 2023 Galaţi.

[9] **Mențiune** pentru lucrarea *Overview on high entropy alloys: Characterisation and applicability***,** autori: **Simion. G**, Scutelnicu E., The 9th Edition of Scientific Conference of Doctoral Schools, Galaţi, 10th-11th June 2021.

[10] **Mențiune** pentru lucrarea **Simion G.**, *Stadiul actual al sudării și brazării aliajelor cu entropie ridicată*, Sesiunea Națională de Comunicări Științifice Studențești ″ANGHEL SALIGNY″, ediția a XI-a 2019, Secțiunea nr. 7: *Masterandul de Azi – Cercetătorul de Mâine*.

Papers presented during the doctoral training period: 3

[1] **Simion G.,** *Stadiul actual al studiilor privind straturile depuse prin sudare cu aliaje multicomponent*, 2021.

[2] **Simion G.,** *Investigații asupra proprietăților straturilor depuse prin sudare cu aliaje multicomponent,* 2022.

[3] **Simion G**., *Modelarea cu elemente finite a nivelului de tensiuni şi deformații din straturile depuse cu aliaje multicomponent,* 2023